NTNU
Norwegian University of
Science and Technology

Assessment of Downspout Disconnection by Modeling Infiltration Potential in Urban Areas

Mareike Anika Becker

Civil and Environmental Engineering
Submission date: June 2016
Supervisor: Tone Merete Muthanna, IVM

Norwegian University of Science and Technology
Department of Hydraulic and Environmental Engineering

Preface

This Master thesis is conducted at the Department of Hydraulic and Environmental Engineering at the Norwegian University of Science and Technology, NTNU Trondheim. This thesis investigates the effect of downspout disconnection as a measure for stormwater management. The topic of this thesis has its origin in a summer job I had in 2015 at Oslo municipality, and was partly based on desires from Oslo municipality. I decided to move forward with this topic because of my interest in stormwater management, and the ability to combine theory with practical investigations. The work in connection with this thesis includes literature search, data collection from the different sites at Ekeberg in Oslo and Elvegata in Trondheim, Establishment of a MATLAB-model, simulations and assessment of downspout disconnection as a measure.

I would like to thank my supervisor, Tone Merete Muthanna, for excellent guidance and constructive suggestions during my work with this thesis. I would also like to thank Bent C. Braskerud, Engineer at Oslo Municipality, for guidance and for the adaption of the opportunity to write this thesis. Lastly I would like to thank Oslo municipality and Trondheim municipality for the cooperation during the conduction of this project.

Abstract

Climate change, which leads to more intense precipitation, combined with an increase of impervious surface, due to an increase of urbanization, has resulted in an increasing amount of stormwater entering the sewer system. This increase will lead to heavier loads on the existing sewer system, which in most cases already are overloaded, resulting in more frequent surface flooding causing damage to buildings and infrastructure. To improve this situation, there has lately been an increase in focusing on a sustainable stormwater management, which is based on Sustainable urban drainage systems, SUDS.

One measure, which is considered used by multiple municipalities, is downspout disconnection. This measure is rarely used to day, and there is therefore little information about the effect of this measure. Usually the downspouts are connected to the sewer system and the surface water generated from the roof is therefore directly entering the sewer system. The runoff from the roof is usually generated very fast, and gives thus a great contribution to the amount of stormwater in the sewer system. This can easily be reduced by disconnecting the downspouts and lead the water to an appropriate infiltration surface. The effect of this measure is closely connected to the soils ability to infiltrate water, and it is therefore difficult to predict the reduction of stormwater without conducting field investigations.

To be able to investigate the effect of downspout disconnection, and as a tool for making it easier to see if an area is suited for this measure or not, it has therefore ben established a MATLAB-model, in this thesis, which computes the amount of infiltrated water and the amount of generated runoff at each site. The MATLAB- model calculates with both using the Green-Ampt infiltration model and the Philip infiltration model, and was used to calculate the amount of infiltration and runoff at eleven sites in Oslo and four sites in Trondheim. In Oslo, the results showed a variation in the amount of infiltrated water. The best conditions for downspout disconnection was seen at site B28, L34, R44, R5 and S75. At these sites it is suggested that the soil is capable to infiltrate the amount of generated stormwater without further measures. The sites in Trondheim showed all great conditions for infiltration, but because of the size of the infiltration area and the location, was site 3 and 4 preferred.

To be able to see how different soil parameters affects the amount of infiltration, some simulations where done by changing some of the soil parameters. These simulations showed that the amount

of infiltration is dependent on the soils saturated hydraulic conductivity, the initial soil moisture content and the wetting front capillary suction head. Because of this dependence, it is recommended that these parameters are measured at the site, and it is important that especially the K_{sar}- value is measured at multiple points at the site in order to obtain a representative value.

By comparing the soil types at the sites and the ratio between the size of the roof area and the size of the infiltration area, the following is suggested. If the soil at the site is sandy and the infiltration area is one to twice as big as the roof area, it can be assumed that the infiltration capacity is good enough to infiltrate the amount of generated stormwater. Silty soil covers however a rather large range of K_{sat}- values depending on the percentage of silt in the soil, and the K_{sat}- value of the site should therefore be measured. Dependent on the soils ability to infiltrate water, it may be enough that the infiltration area is one to twice as big as the roof area, but this should be considered especially if the soils saturated hydraulic conductivity is of the lower value. The same yield also for a soil with a very high clay content. Whether this soil has a large enough infiltration capacity or not is dependent on the percentage of silt and sand fraction in the soil. The calculations done in this thesis shows also that for a site with a very high clay content, and thus a low K_{sat}- value, it is recommended to use an infiltration area three times or more, as big as the size of the roof area.

The establishment of this model will help to develop downspout disconnection as a measure for stormwater managing, especially in residential areas. The results obtained in this thesis, shows that by disconnecting the downspouts from the sewer system, the reduction of amount of stormwater can be significant, where the soil properties are adequate. Downspout disconnection is therefore evaluated as a measure that should be considered in areas where stormwater management is a challenge.

Sammendrag

Klimaendringer, som fører til mer intens nedbør, kombinert med en økning i andelen tette flater i forbindelse med en økende grad av urbanisering, har ført til en økende mengde overflateavrenning. Dette fører til at ledningsnettet, som allerede er svært belastet og noen steder er i veldig dårlig stand, blir ytterligere belastet. Den økende mengden overflateavrenning kan dermed føre til overbelastning på ledningsnettet, som igjen kan resultere i store oversvømmelser og skader på bygninger og infrastruktur. Videre har dette ført til et større behov for å håndtere overvannet på en sikker og miljøhensiktsmessig måte som er både framtidsrettet og bærekraftig. Nyere tids overvannshåndtering viser derfor en tendens til økt bruk av åpne, lokale og naturlige løsninger, som med en samlebetegnelse kalles LOD, lokal overvannsdisponering (eng. SUDS). I forbindelse med fokuset på å håndtere overvannet mer lokalt, har Norsk Vann utarbeidet den såkalte 3-trinnsstrategien, og det er det første leddet i denne strategien som blir diskutert i denne oppgaven. Dette trinnet går ut på å fange opp og infiltrere overvannet fra nedbørshendelser som har en mindre nedbørsmengde enn et visst antall millimeter. Et tiltak som kan bli brukt i trinn 1 er frakobling av taknedløp.

Overflatevann fra taket ledes som regel rett inn på det kommunale ledningsnettet. I områder med mange tak og tette flater, bidrar dette til å generere en rask avrenning og gir et stort bidrag til mengden overvann i avløpssystemet. Dersom ledningsnettet i området allerede er høyt belastet og underdimensjonert, kan dette føre til tilbakeslag og kjelleroversvømmelser. For å redusere mengden vann i avløpssystemet, kan takrennene kobles fra ledningsnettet og føres ut på plenen slik at vannet kan infiltrere i grunnen. Mange kommuner støtter dette tiltaket, men det finnes lite informasjon om effekten av å koble fra takrennene fra det kommunale ledningsnettet. Siden virkningen av dette tiltaket er nært knyttet til jordens evne til å infiltrere vann, er det vanskelig å kunne forutsi effekten på forhånd uten å hå gjennomført feltundersøkelser. En risiko ved å koble fra takrennene, er at jorden har så liten infiltrasjonskapasitet at vannet renner av på overflaten, og renner videre ned i nærmeste kum. Dersom dette er tilfellet har vannet kanskje blitt forsinket, men mengden vann i avløpssystemet har ikke blitt redusert betraktelig. For å undersøke effekten av å koble fra takrennene, og som et verktøy for å lettere kunne vurdere om et område egner seg for dette tiltaket, har det i denne oppgaven blitt laget en MATLAB- modell som beregner mengden infiltrasjon for hvert område.

Denne MATLAB-modellen består av to script og et tilhørende Excel-ark for inputparametre. Hver av de to scriptene beregner mengden infiltrasjon og avrenning, basert på hver sin infiltrasjonsmodell. For å kunne sammenlikne resultatene fra to ulike infiltrasjonsmodeller, og for å kunne se hvordan det vil påvirke resultatene, ble det derfor bestemt å bruke både Green-Ampt infiltrasjonsmodell og Philip infiltrasjonsmodell. Dette ble også gjort for at brukeren kan velge den modellen som man er mest komfortabel med, eller som man har de passende inputparametrene til. Denne MATLAB- modellen ble så brukt til å beregne mengden infiltrasjon og mengden overflateavrenning i to case- områder; et boligområde på Ekeberg i Oslo, og et sentrumsområde i Elvegata i Trondheim. Basert på en gitt regnhendelse, størrelsesforholdet mellom takarealet og infiltrasjonsarealet og basert på jordens egenskaper til å infiltrere vann, ble mengden infiltrasjon og mengden overflateavrenning beregnet for disse to områdene. I Oslo ble det gjennomført beregninger for 11 hager i det utvalgte området, mens det i Trondheim ble beregnet for fire offentlige gressplener langs Elvegata. På begge stedene ble beregningene gjort ved bruk av både Green-Ampts modell og Philips modell. Disse beregningene utgjør det som i oppgave blir kalt referanse simulering. For å kunne se hvordan de forskjellige jordparameterne påvirker jordens evne til å infiltrere vann, ble det gjort simuleringer hvor disse ble endret, og resultatene ble så sammenliknet med resultatene fra referanse simuleringen.

Referanse simuleringene viste at det til dels er gode forhold for frakobling av taknedløp. I Trondheim ble mengden infiltrasjon beregnet til å være 100% på alle de fire forskjellige stedene, både beregnet med Green-Ampts modell og Philips modell. Dette tyder på at disse stedene er egnet til infiltrasjon, likevel foretrekkes sted tre og fire som egnede steder på grunn av deres størrelse på infiltrasjonsområdet og deres plassering. I Oslo var resultatene litt mer varierende. I forhold til at det ble brukt en veldig kraftig regnhendelse i simuleringene, har de fleste stedene i Oslo en ganske høy andel infiltrasjon. Av stedene i Oslo kan hagene B28, L34 og R44 trekkes fram. Disse tre stedene har tilnærmet 100% infiltrasjon ved bruk av Green-Ampt modellen, og det er derfor foreslått at disse stedene klarer å håndtere regnvannet uten videre tiltak. Stedene R5 og S75 har noe lavere andel infiltrasjon, men på grunn av deres store hagearealer, vil disse også trolig klare å håndtere alt regnvannet. Ved de andre stedene bør det vurderes om infiltrasjonskapasiteten er høy nok, eller om frakobling av taknedløp bør kombineres med andre tiltak som for eksempel en infiltrasjonsgrøft eller et regnbed.

Simuleringene viste at mengden infiltrasjon påvirkes av flere faktorer. To av disse er jordens mettede hydrauliske konduktivitet og jordens fuktinnhold. Simuleringene viste at mengden infiltrasjon påvirkes i høy grad av jordens mettede hydrauliske konduktivitet, og siden denne verdien kan variere stort i urban jord, bør denne verdien bli målt i felt. På grunn av store lokale variasjoner i urban jord, blir det også anbefalt at jordens mettede hydrauliske konduktivitet måles flere steder i samme hage for å finne en representabel verdi til bruk i beregningene. En annen faktor som også påvirker andelen infiltrasjon er jordens fuktinnhold under regnhendelsen. Resultatene viste at mengden infiltrasjon synker med økende fuktinnhold i jorden. Siden denne verdien ikke er konstant, men avhengig av jordtype og regnmengde og varighet mellom regnhendelser, bør fuktinnholdet i jorden vurderes når det dimensjoneres for frakobling av taknedløp. Infiltrasjonsområdet bør også kunne infiltrere mesteparten av regnvannet, også når jorden er tilnærmet mettet for å sikre en sikker overvannshåndtering.

Ved å sammenlikne de forskjellige jordtypene og forholdet mellom takarealet og infiltrasjonsarealet, er følgende foreslått. Dersom jorden inneholder mye sand og infiltrasjonsarealet er ett til to ganger større enn takarealet, kan det antas at infiltrasjonskapasiteten er tilstrekkelig til å håndtere avrenningen fra taket. Siltig jord dekker et større spekter med varierende verdier for mettet hydraulisk konduktivitet, avhengig av innholdet av de forskjellige kornfraksjonene. Ved siltig jord bør derfor infiltrasjonskapasiteten bli beregnet basert på jordparameterne. Avhengig av jordens evne til å infiltrere vann, kan det hende at et infiltrasjonsområde som er to ganger større holder for å infiltrere den genererte avrenningen fra taket. Det samme gjelder også for jord med høyt leirinnhold. Infiltrasjonskapasiteten til leirholdig jord er avhengig av andelen sand og silt i jorden. Kalkuleringene gjort i denne oppgaven viser at dersom et område har et veldig høyt innhold av leire, og dermed en lav K_{sat}- verdi, bør infiltrasjonsområdet trolig være tre ganger, eller mer, større enn takarealet.

Etableringen av denne modellen vil være til hjelp for å utvikle frakobling av taknedløp som et tiltak for å håndtere overvann, spesielt i boligområder. Gjennom resultatene fra denne oppgaven, ser man at ved å koble fra takrennene fra det kommunale ledningsnettet, kan mengden overvann reduseres betraktelig der jordforholdene er tilstrekkelig. Frakobling av taknedløp er derfor et tiltak som bør vurderes i områder hvor overvannshåndtering er en utfordring.

Table of Content

List of Figures XIII
List of Tables XV
1. Introduction 1
2. Urban Hydrology 3
2.1 The Impact of Urbanization 3
2.2 Effect of climate change 7
3. Stormwater management 11
3.1 Sustainable Urban Drainage Systems (SUDS) 11
3.2 Downspout disconnection 12
4. The process of infiltration 15
4.1 Soil properties 15
4.2 Infiltration and water movement 19
5. Infiltration models 23
5.1 Richards Equation: 23
5.2Philip model: 26
5.3 Horton Equation: 28
5.4 Green-Ampt model 30
6. Modeling Method 35
6.1 Model limitations and choice of infiltration models 35
6.2 Choice of model language 36
6.3 Corresponding Excel-sheet for input parameters 36
6.4 Matlab-script 37
6.4.1 Green- Ampt infiltration model: 38
6.4.2 Philip infiltration model: 42
6.5 Input parameters 46
6.5.1 Saturated hydraulic conductivity 46
6.5.2 Porosity 47
6.5.3 Bubbling-pressure, pore-size distribution index, and wetting front capillary pressure head 47
6.5.4 Initial soil moisture content 49
6.5.5 K_p 49
6.6 Case study: Trondheim and Oslo 49

6.6.1 Choice of location and description of the sites 49
6.6.2 Computation of K_{sat}- values 51
6.6.3 Computation of Porosity 53
6.6.4 Computation of Bubbling-pressure, pore-size distribution index, and wetting front capillary pressure head 54
6.6.5 Computation of soil moisture content 56
6.6.6 Size of roof area and infiltration area 57
6.6.7 Rainfall event 58
7. Results and discussion 61
7.1 Amount of infiltrated water and amount of generated runoff 61
7.2 Differences between Green-Ampt infiltration model and Philip infiltration model 67
7.3 The impact of change in soil moisture content 68
7.4 The impact of change in saturated hydraulic conductivity 74
7.5 The effect of soil suction on the amount of infiltration 78
7.6 Impact of the ratio between the roof area and the infiltration area 80
7.7 Comparison of places with the same soil type 82
7.8 Downspout disconnection as a measure for stormwater managing 85
8. Concluding Remarks 89
9. References 91
10. Appendix 93
Appendix 1: MATLAB-Code 93
MATLAB-code for the Green- Ampt infiltration model 93
MATLAB- code for the Philip infiltration model 95
Appendix 2: Input parameters used for the reference simulation 98
Appendix 3: Obtained graphs form the calculations 100
Results: Reference simulation 100
Results: Initial soil moisture content equal to the field capacity 116
Results: Initial soil moisture content equal to the porosity 123
Results: Different K_{sat}- values 130
Results: Change in size of infiltration area 136
Appendix 4: Excel input sheet 139
Appendix 5: Example m-table 140
Appendix 6: Values for Bulk density 141

Appendix 7: Soil samples 142

List of Figures

Figure 2.1 Impact of urbanization on infiltration and runoff.(County, 1999b).....4

Figure 2.2 Effect of urbanization on runoff hydrograph. The solid line shows the hydrograph before urbanization, and the dotted line shows the hydrograph after urbanization.(Pazwash, 2011) 5

Figure 3.1 Three-part strategy. The numbers used is just an example and has to be adjusted for each area.(Lindholm et al., 2008).....12

Figure 3.2 Downspout disconnection. The picture to the left shows how the downspout can be disconnected from the sewer system. The water is then led through a pipe to an appropriate infiltration surface were the water can infiltrate, like shown in the picture to the right. (Photo: Bent C. Braskerud).....13

Figure 4.1 Example of a moisture-characteristic curve.(Dingman, 2008) 18

Figure 4.2 Moisture zones during infiltration.(Chow et al., 1988) 20

Figure 4.3 Decrease of infiltration capacity over time. (Miyazaki et al., 1993) 21

Figure 5.1 Definition sketch used for deriving the Richards Equation. (Dingman, 2008) 24

Figure 5.2 The figure to the left shows infiltration into a column of soil for the Green-Ampt model, while the figure to the right shows the distribution of moisture content of the soil (Chow et al., 1988).....30

Figure 6.1 Flow chart describing the calculations for the Green-Ampt infiltration model.....41

Figure 6.2 Flow chart describing the calculations for the Philip infiltration model. 45

Figure 6.3 Map showing the investigated sites in Oslo.(maps.google.no).....50

Figure 6.4 Map showing the investigated sites in Trondheim.(maps.google.no) 51

Figure 6.5 Set up for measuring saturated hydraulic conductivity with MPD.(photo: Mareike Becker) 52

Figure 6.6 Rainfall event measured 5. august 2015 at Blindern gauging station in Oslo. 59

Figure 6.7 Rainfall event measured 27. August 2015 at Risvollan gauging station in Trondheim. 59

Figure 7.1 Shows the graph obtained for site S10. The red line represents the amount of generated runoff, while the green line represents the amount of infiltrated water. The graph to the left shows the result obtained by using the Green-Ampt model, while the graph to the right shows the result obtained by using the Philip model. The x-axis shows the duration of the rainfall and the y-axis shows the amount of water in cm/h.....64

Figure 7.2 Shows the graph obtained for site R44. The red line represents the amount of generated runoff, while the green line represents the amount of infiltrated water. The graph to the left shows the result obtained by using the Green-Ampt model, while the graph to the right shows the result obtained by using the Philip model. The x-axis shows the duration of the rainfall and the y-axis shows the amount of water in cm/h. 65

Figure 7.3 Shows an example of the development of the infiltration capacity over time. This graph is obtained for site S10 by using the Green-Ampt model. 67

Figure 7.4 Shows the differences in result when using different initial soil moisture content. The graph to the upper left shows the result when the initial soil moisture content is equal to the field capacity. The graph to the upper right shows the result for the reference simulation (with the measured initial soil moisture content), and the last graph shows the result with an initial soil moisture content equal to the porosity. All of the three situations are calculated for site S10 by using the Green-Amp model. The red line represents the amount of generated runoff, while the green line represents the amount of infiltrated water. 71

Figure 7.5 Shows the differences in initial infiltration capacity when using different initial soil moisture content. The graph to the upper left shows the result when the initial soil moisture content is equal to the field capacity. The graph to the upper right shows the result for the reference simulation (with the measured initial soil moisture content), and the last graph shows the development of the infiltration capacity with an initial soil moisture content equal to the porosity. All of the three situations are calculated for site R44 by using the Green-Amp model. 72

Figure 7.6 Differences in the infiltration capacity when changing the K_{sat}- values. The y-axis represents the infiltration capacity with the unit cm/h, and the x-axis represents the time duration of the rainfall event. The graph to the left shows the development of the infiltration capacity over time for K_{sat} equal to 12.94 cm/h, and the graph to the right shows the development of the infiltration capacity over time for K_{sat} equal to 88.82 cm/h. The graph in the middle shows the development of the infiltration capacity over time obtained with the reference simulation, meaning a K_{sat} equal to 46cm/h. 77

Figure 7.7 The results obtained with the different soil types found at site S75. The graph to the left shows the results for the loamy soil, and the graph to the right shows the result for the Sandy loam soil. Both graphs are calculated by using the Green- Ampt model. The red line represents the amount of generated runoff, while the green line represents the amount of infiltrated water. 84

List of Tables

Table 6.1 Input parameters for Green-Ampt infiltration model and Philip infiltration model. 46

Table 6.2 Measured K_{sat} range and computed average values and Median values for the investigated sites in Oslo. 53

Table 6.3 Measured K_{sat} range and computed average values and Median values for the different soil types investigated in Trondheim. 53

Table 6.4 Bulk density and calculated porosity for the different soil types. 54

Table 6.5 Computed Bubbling pressure, particle-size distribution index and wetting front capillary pressure head for the investigated sites in Oslo. 55

Table 6.6 Computed Bubbling pressure, particle-size distribution index and wetting front capillary pressure head for the different soil types investigated in Trondheim. 56

Table 6.7 Computed initial soil moisture content for the investigated sites in Oslo, and for the different soil types investigated in Trondheim. 56

Table 6.8 Roof area, size of infiltration area and number of downspouts used in calculations for the different sites in Oslo and Trondheim. 58

Table 7.1 The amount of infiltrated water and the amount of generated runoff for each site by using both Green-Ampt model and Philip model. The table shows the results obtained for the reference simulation. 62

Table 7.2 The different values used for the calculations done with the different soil moisture contents, and the sites which the computations were conducted for. 69

Table 7.3 The results obtained for the investigated sites for all of the different values of initial soil moisture content used in the simulations. The table is showing the results by using both the Green-Ampt model and the Philip model. 70

Table 7.4 The different sites used in the simulation and the different K_{sat}-values used in the different calculations. 75

Table 7.5 Results for the different sites obtained by changing the K_{sat}- value, for both Green-Amp model and Philip model. 75

Table 7.6 The percentage change in size of the infiltration area and percentage change in amount of infiltrated water compared to the reference simulation. Both for Green-Ampt model and Philip model. 82

1. Introduction

Stormwater, or surface runoff, is the portion of rainfall that doesn't infiltrate into the ground or evaporates, but runs off from urban surfaces like roofs, walls and other impervious surfaces. The combination of climate change, leading to more often and more intense precipitation, and urbanization, leading to an increase of impervious surface, is resulting in an increase of stormwater entering the sewer system. This increase will lead to heavier loads on the existing sewer systems, which in most cases already are overloaded. The capacity of the sewer system will therefore exceed more often, resulting in more frequent surface flooding which can cause damage to buildings and infrastructure. To improve this situation there has lately been an increase in focusing on a sustainable stormwater management, which based on a detaining and reduction of the runoff by using more open, local and natural solutions. Bothe Oslo municipality and Trondheim municipality has made strategies for stormwater management which focuses on exactly this way of managing stormwater.

One measure which is considered used by multiple municipalities, but there is little information about, is downspout disconnection. The effect of downspout disconnection is dependent on sufficient infiltration capacity in the soil, and is therefore difficult to estimate. A too low infiltration capacity can lead to a low amount of infiltrated water, and resulting in water flowing at the surface to the nearest gully, and the amount of stormwater in the sewer system is not significantly reduced. Since this measure is rarely used, there is little information about the amount of reduction of stormwater that can be obtained. Because of its dependence on the soils ability to infiltrate water, the effect of downspout disconnection will therefore probably vary from site to site, and it will therefore be difficult to predict the reduction of stormwater without conducting field investigations.

In this thesis, it has therefore ben established a MATLAB- model which calculates the amount of infiltrated water and the amount of generated runoff at a site, based on a given rainfall event and some soil properties. The established model is based on both the Green-Ampt infiltration model and the Philip infiltration model, and two locations, one in Oslo and one in Trondheim, has been investigated by using this model to evaluate downspout disconnection as a measure for stormwater management.

2. Urban Hydrology

2.1 The Impact of Urbanization

Urbanization is often defined as the growth of cities and towns, and leads often to alterations in the natural process of storm water runoff (Ødegaard et al., 2014). Urban development has a great impact on the relationship between the different processes of the hydrological cycle in the area. Therefore, in order to understand the problems in urban drainage, the effect urbanization has on the hydrological cycle has to be understood. The hydrological cycle represents the constant circulation of water among the different reservoirs on earth, and can be used to describe the global system, as well as for smaller areas usually defined as watersheds (Brattli, 2009). The quantitative amount of water in the different reservoirs can be described by the hydrological water balance, as presented by Dingman (2008).

$$P + G_{in} - (Q + ET + G_{out}) = \Delta S \tag{2.1}$$

Where P is precipitation, G_{in} is groundwater inflow, Q is stream outflow, ET is evapotranspiration, G_{out} is groundwater outflow and ΔS is the change in all forms of storage over a time period.

In nature, rain is falling on undisturbed land, such as forest, and will partly infiltrate in to the ground and recharge the groundwater, partly return to the atmosphere through evapotranspiration, and partly be retained by the surface. Only a small amount will be generated as surface runoff. The ratio between the amount of water that evaporates, infiltrates and generates as surface runoff is dependent on the surface characteristic in the area, and varies also with time. The amount generated as surface runoff will for example increase with time as the soil gets more and more saturated during the rain event (Butler and Davies, 2010).

As cities are constructed, vegetation is replaced by impervious surface to maximize the available area for infrastructure. This process is one of the most radical interventions of the water cycle, and leads to a significant change in the runoff characteristic of the area. By replacing natural vegetation with impervious surface, such as roads, parking areas and building roofs, and by channelizing rivers, urbanization not only results in less evaporation, less infiltration, and faster runoff, but leads also to a diminishing capacity of the soil to store water (Pazwash, 2011). Figure 2.1 shows how the hydrological water balance changes due to urbanization. Since less water is infiltrating in urban areas, more runoff will be generated during a rain event. In areas with natural ground cover and

areas with undeveloped conditions, surface runoff can range from 10-30 % of the total annual precipitation. If the ground cover in the area is changed with 75-100 % impervious surface, the amount of surface runoff will increase significantly. The change of the grounds physical conditions can result in an increase of surface runoff to over 50% of the overall precipitation, depending on the degree of development and which solutions used to drain the area (County, 1999b).

Additionally to urbanization, will the traditional drainage system containing of inlets, pipes, and drainage channels, turning overland flow to concentrated runoff by collecting and transporting runoff from developments. The smoother surfaces will increase the velocity of the water, resulting in a shorter time of concentration, and thereby increasing total runoff volume and peak flow rates (Pazwash, 2011).

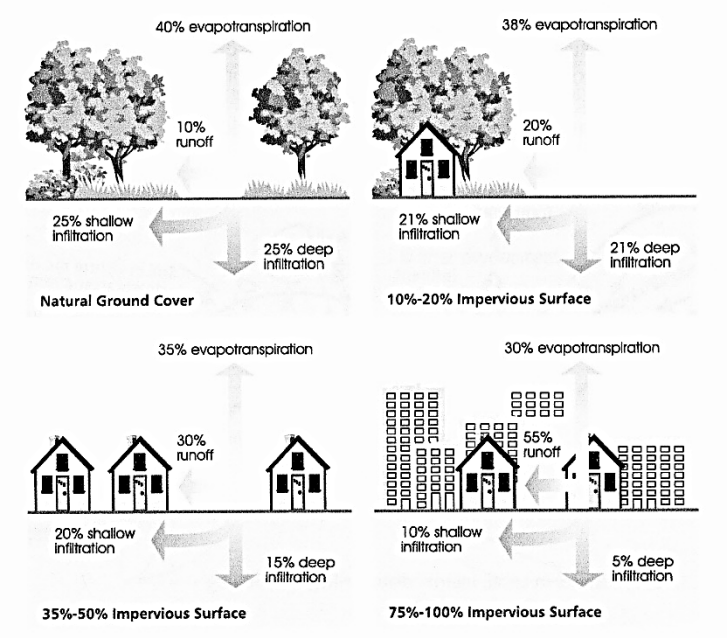

Figure 2.1 Impact of urbanization on infiltration and runoff.(County, 1999b)

Figure 2.2 shows that due to urbanization the peaks on the hydrograph will occur sooner and be significantly greater than before urbanization (Pazwash, 2011).

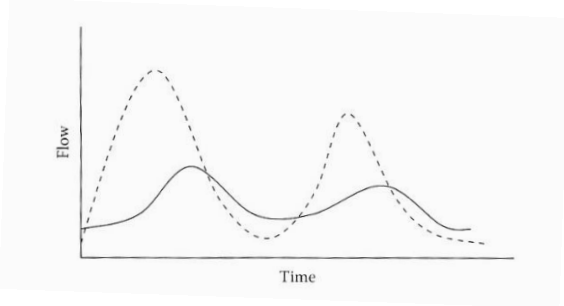

Figure 2.2 Effect of urbanization on runoff hydrograph. The solid line shows the hydrograph before urbanization, and the dotted line shows the hydrograph after urbanization.(Pazwash, 2011)

These figures show how urbanization increases the peak and volume of runoff, shortens the time of concentration and reduces the amount of infiltration.

The decrease of infiltration also leads to another important effect of urbanization, reduction of ground water recharge. In a natural state, infiltration and lateral inflow will over time balance the groundwater outflow. This will create a constant water table with some variations linked to the frequency and intensity of rainfall events. If the infiltration is reduced due to impervious surface, the groundwater outflow will be greater than the inflow, resulting in a lowering of the water table. This can cause damage to infrastructure and houses due to soil settling (Ødegaard et al., 2014).

Reduction of natural infiltration in urban areas is not only due to increase of impervious surface, but also a result of other factors. Reduction of natural infiltration can also, according to Pitt et al. (2002), be a result of urban activities. Construction work or other urban activities like car driving or pedestrians, leads to a compaction of the soil and disturbance of the soil structure, and reduces the soils infiltration capacity. Removal of the upper layer of the soil, and thereby exposing underlying soil which typically has a lower infiltration capacity, is also reducing the natural infiltration (Pitt et al., 2002). From this it can be understood that urban activities change the properties of the soil, and urban soil has therefore a different behavior than natural soil.

Phillip (2016) (siting (Bockheim, 1974)) defines urban soil as:

> "A soil material having a non-agricultural, man-made surface layer more than 50 cm thick, that has been produced by mixing, filling, or by contamination of land surface in urban and suburban areas."

This means that urban soil is soil where a part of the profile has been disturbed, or the entire profile consist of fill. Unlike for natural soil where wind, ice, water, gravity and heat are the main active agents, humans are the primary agent of the disturbance for urban soil. The mixing, filling and contamination that follows urban activities creates a soil material that is different from its natural counterpart, and thus characterized differently.

According to Phillip (2016), urban soil is characterized as a soil with:

- Great vertical and spatial variability
- Modified soil structure leading to compaction
- Presence of a surface crust
- Modified soil reaction
- Restricted aeration and water drainage
- Interrupted nutrient cycling and modified soil organism activity
- Presence of anthropic materials and other contaminants
- Modified soil temperature regimes

Although the soils infiltration capacity is dependent on several factors, like soil type and water content, a study done by Pitt et al. (2002), showed that compaction of the soil is the most critical factor for reduction of the soils infiltration capacity, and has a negative influence.

Soil compaction can be explained by the concept of stress-strain phenomena, by considering the soil as an elastic material. Dependent on the soil strength, the soil will react elastically up to a certain limit of stress under loading and unloading forces on the soil. Any incremental force creating stress beyond that limit will result in a plastic deformation (Horn et al., 1995). The soils reaction to stress is closely related to soil type, and is closely dependent on soil properties such as water content, amount of organic matter, particle size distribution, plasticity index and clay mineralogy (Soane et al., 1980). In case of compaction, a microscopically rearrangement of the soils particles happens, which moves the soil grains closer to each other, and thus changes the properties of the soil (Nawaz et al., 2013). This rearrangement, which results in soil compaction, affects the physical properties, and thus the soils infiltration capacity. Compaction of the soil increases the strength and bulk density of the soil, decreases the porosity of the soil and reduces the distribution of pore sizes within the soil (Gregory et al., 2006). Modification of the pore volume

and pore structure of the soil, reduces both size and number of macro pores and changes shape and continuity of the pores (Soane et al., 1980). By reducing the size of the pores, the way that water and air move through the soil changes and thus affecting the infiltration rate. Because of the change in soil properties, soil compaction has a great impact on the hydraulic properties of the soil. The compaction influences properties such as soil water retention, soil water diffusivity, unsaturated hydraulic conductivity and saturated hydraulic conductivity, which all are properties governing infiltration rate of the soil (Gregory et al., 2006).

Because of the compaction of the soil, it has to be expected that soil in urban areas behaves different than natural soil. This difference in behavior was shown in a project paper written by the current author. In this paper it was shown that the measured saturated hydraulic conductivity varied significantly from place to place, also for samples of same soil type. By comparing the measured values for saturated hydraulic conductivity with standardized values for saturated hydraulic conductivity for the different soil types, it showed that the majority of the measured values was lower than the standardized values. This shows the effect of urbanization and the importance of thorough field work when planning for infiltration devices.

2.2 Effect of climate change

Together with urbanization and densification of cities, climate change is becoming a great challenge in the field of urban drainage (Butler and Davies, 2010). Climate change involves that the "average weather" changes character over time, e.g. more or less precipitation, higher or lower temperature, more or less wind etc. The global climate has changed significantly since the first measurements was taken in 1860, and it seems that the climate in average is getting warmer (Ødegaard et al., 2014). To explain climate change, a great variety of hypotheses have been proposed, ranging from explaining the mechanisms behind the change with natural causes to changes due to human impact (Tarbuck et al., 2011). One accepted theory argues that the rise in air temperature is caused by the significant increase in the concentration of greenhouse gases in the atmosphere, which has resulted in that the global average surface-air temperature has increased with approximately 0.6 degrees over the 20. Century (Butler and Davies, 2010).

The climate in Norway varies greatly with season and also geographically. The spring is normally the time with less precipitation, and the time with the most precipitation is found in the second half of the year. The eastern parts of Norway have normally the greatest rainfalls in august, while the

coastline of Norway has the greatest rainfalls in the autumn (Ødegaard et al., 2014). These variations are also reflected in the changes of the climate. A study done by RegClim (2005), predicts that the annual average temperature in Norway will increase by between 2.5 and 3.3 °C within year 2100, dependent of region, with the greatest temperature increase in north and in the inland of Norway (RegClim, 2005). The warm surface will lead to increased evapotranspiration, and thereby increase the amount of vapor in the atmosphere (Dingman, 2008). When the air becomes warmer, it can contain more moisture than cold air, leading to consequently more precipitation. RegClim (2005) predicted that the annual rainfall in Norway will increase by between 5-20%, dependent on region with the greatest increase in the southwestern parts and northern parts of Norway. The precipitation will increase the most in the autumn, and will have an increase greater than 20 % in the western, middle and northern parts of Norway. In the eastern parts of Norway, the precipitation during autumn and winter will increase with between 15-20%. In the eastern and southern parts of Norway the precipitation in the summer will decrease by up to 15 %. It is also expected that extreme rainfalls will occur more often in Norway (RegClim, 2005).

The climate change will also result in a rise of the sea level. It is expected that the sea level will rise between 15-25 cm in certain places within the year 2050 and up to 70 cm within the year 2100. The sea level rise will result in a lower hydraulic capacity in the sewer system, which consequently increases the risk for flood damages and combined sewer overflows (Lindholm et al., 2008).

Climate change will alter the ratio between the different processes in the hydrological cycle, and will change the urban drainage. The climate changes which are most relevant for urban drainage, are the increase of precipitation, and hence runoff, and the increase of storm intensities (Butler and Davies, 2010). As the amount of rain days per year increases, the soil will be saturated more often and hence it is more likely that also the runoff coefficient will increase as well (Ødegaard et al., 2014). This increase in amount of surface runoff, due to more precipitation, combined with the enlargement of impervious surfaces will lead to heavier loads on the existing sewer systems which in most cases already are overloaded. The capacity of the sewer systems will be exceeded more often, resulting in more frequent surface flooding and property damage (Butler and Davies, 2010). Lindholm et al. (2008) investigated the impacts that climate change will lead to for the next 50 years for some cities, and found that the effect of climate change can cause twice as many houses than today to be flood damaged. The additional volume of water in the sewer system will also lead

to more frequent combined sewer overflows (CSO) spills. The same study found that the combined sewer overflows will increase with between 50-100% in relation to the current climate. The higher frequency of combined sewer overflows and storm water overflows will also result in poorer water quality in the rivers. Due to less precipitation in the summer, there will be a greater build-up of surface pollutants resulting in a more polluted first flush(Butler and Davies, 2010).

As we can see, the increase in precipitation and storm intensities will give challenges for the existing sewer system, and it is therefore important to understand and plan for a changing climate. Upgrading the existing sewer network in response to potential climate change is expensive and time consuming, and therefore unlikely (Butler and Davies, 2010). In order to relive the sewer system for the increased amount of runoff, it will be important to handle the water on the surface before it is flowing into the sewer system. This can be done by leading the water through suitable streets and roads to appropriate infiltration surface, like the green infrastructure in the city, e.g. football fields etc. This will decrease the pressure on the sewer system, but it will also require good spatial planning (Ødegaard et al., 2014).

3. Stormwater management

3.1 Sustainable Urban Drainage Systems (SUDS)

Stormwater (surface runoff) is the portion of rainfall that doesn't infiltrate into the ground or evaporates, but runs off from urban surface like roofs, walls or other impervious surfaces. Since stormwater is in contact with the surface, the quantity and quality of the stormwater is closely related to the nature and characteristics of both the rainfall and the catchment. Stormwater management is a major concern to the drainage engineer, and it is important to secure safe and efficient drainage to maintain public health and safety, and to protect the receiving water environment (Butler and Davies, 2010). Managing stormwater can be done either locally or by leading it to sewer pipes. In many years, stormwater was seen as a problem, and the most common and traditionally method was therefore based on leading the stormwater away as quickly as possible in a closed pipe system. Due to the increased urbanization it appears that the existing pipe system don't have the capacity to handle the increasing amount of stormwater. Recently, it is therefore become more normal to treat stormwater as a resource, and focus on a more open and natural managing of the stormwater. This way of managing stormwater is referred to as sustainable urban drainage systems (SUDS)(Ødegaard et al., 2014). The primary goal for SUDS is to recreate the site hydrology of the areal equal to before it was developed. This is done by using site design techniques which are based on storing, infiltrating, evaporating and detaining runoff. This will drain the area in a more natural way and as far as possible maintain the natural water balance in the area, and thus preserve the hydrological cycle by reducing surface runoff and ensure sufficient groundwater recharge (County, 1999a). Good stormwater management involves methods adapted to the local conditions and needs. The solutions should be sustainable and add quality to the surroundings by using the stormwater to create recreation and positive elements in the community. A provident and sustainable stormwater management is based on keeping the stormwater in the area by diminishing and reducing the amount of surface runoff and to prevent water contamination (Lindholm et al., 2008). By managing runoff from "everyday rain" as close as possible to the source by using natural materials like plants, soil and gravel, which can easily be integrated in the area, SUDS reduces the speed and peak volume of urban runoff, resulting in a reduced likelihood for flooding and erosion. The reduction of surface runoff is also reducing the amount of water collected in the storm sewer, resulting in the possibility to use a smaller dimension on the storm sewer pipes, and a reduction of combined sewer overflow spills (Butler and Davies, 2010). Another benefit is the improved water

quality. Because of the reduction of erosion, the water quality in the natural watersheds that receives the runoff will improve. SUDS themselves will also improve the quality of runoff through filtration and biological action (Butler and Davies, 2010). SUDS promotes therefore a multifunctional landscape where processes like collection, infiltration and reuse of stormwater is incorporated to ensure reduction of the runoff volume, improve runoff quality and to create recreation and positive elements in the community.

To secure safe and efficient drainage, Norsk Vann has compiled a strategy for managing stormwater known as the three-steps strategy. Figure 3.1 shows the principle behind the strategy, which is based on infiltration, delaying, attenuation and ensuring safe flood paths. The strategy involves that smaller, everyday rainfalls up to a certain amount of millimeters shall be intercepted and infiltrated. When the rainfall is of a greater volume, it will be generated surface runoff. The amount of water that does not infiltrate shall then be lead to open drainage systems which delays and attenuates the water. Some rainfalls have such large water volumes that the normal systems can't handle the generated runoff alone. For these cases it should be established secure flood paths that can direct the water safely away from buildings and infrastructure (Lindholm et al., 2008).

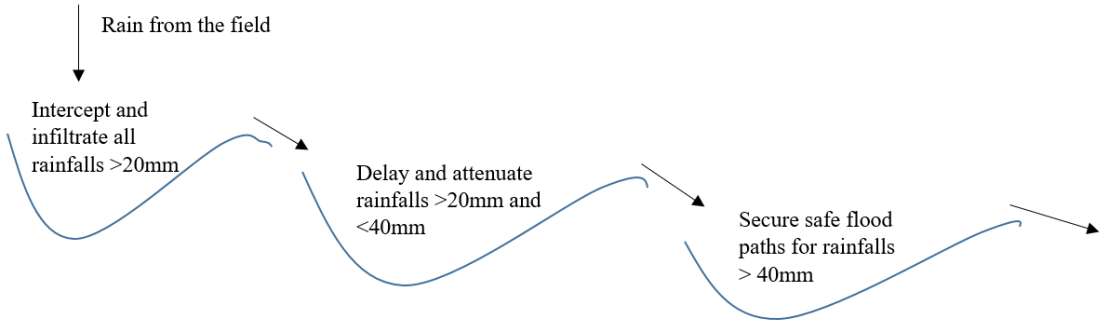

Figure 3.1 Three-part strategy. The numbers used is just an example and has to be adjusted for each area.(Lindholm et al., 2008)

In this work measures for step one in the three-part strategy will be discussed.

3.2 Downspout disconnection

As described in the previously section, surface runoff has to be managed on the surface in order to reduce the increasing pressure on the existing sewer system. One measure to reduce the amount of water in the sewer pipes is to disconnect downspouts. Runoff from the roof is usually lead directly to the sewer system by downspouts. In areas with many roofs and impervious surfaces, is the runoff

generated very fast, and thus gives a great contribution to the amount of stormwater in the sewer system. To reduce this amount of stormwater, the roof areas can easily be disconnected from the traditional sewer system, and the runoff generated from the roof areas can instead be lead to an appropriate infiltration surface. However, it is important that the water is transported far enough from the foundation of the house before infiltrating into the ground, to prevent damage due to moisture. When leading the water to an infiltration surface, it is important that the excessed water, water that does not manage to infiltrate, is dealt with by leading it to for example a raingarden with an overflow connected to the sewer system. This is important to avoid erosion or that the water flows to the neighbor and damages buildings or infrastructure. To ensure a safe management of stormwater by infiltration, the infiltration area should be 1-2 times greater than the roof area (Lindholm et al., 2008).

Figure 3.2 Downspout disconnection. The picture to the left shows how the downspout can be disconnected from the sewer system. The water is then led through a pipe to an appropriate infiltration surface were the water can infiltrate, like shown in the picture to the right. (Photo: Bent C. Braskerud)

The effect of downspout disconnection is closely related to the infiltration capacity of the soil. In the following chapter the process of infiltration is therefore described.

4. The process of infiltration

Infiltration is the process by which water arriving at the soil surface, due to rainfall, snowmelt and irrigation, enters the soil. This process is closely related to the process of soil water movement, which describes the movement of water flowing from one point to another within the soil (Rawls et al., 1992). Since the rate of infiltration is controlled by the rate of water movement in the soil, infiltration and soil movement has to be seen as one process. Infiltration cannot continue indefinitely unless percolation removes infiltrated water from the surface soil (Pazwash, 2011). Because infiltration involves unsaturated flow in porous medium, and since water movement within the soil is strongly dependent on the physical properties of the soil, we have to understand the material and the hydraulic properties of the soil (Dingman, 2008). The following paragraphs will therefore describe soil properties affecting the process of infiltration.

4.1 Soil properties

Soil is a porous medium comprising soil particles and voids that may be filled with water or air. The fact that soil is a porous medium and not a solid matter, makes it possible for water to move within the soil (Tarboton, 2003). The free flow of water in the soil is closely related to the soils porosity. A soils porosity, designated as n, is defined as the portion of pore space in a volume of soil

$$n = \frac{V_a + V_w}{V_s} \tag{4.1}$$

where V_s is the total volume of the soil sample and V_a and V_w are the volumes of the air and liquid water of the soil, respectively (Dingman, 2008). The soils porosity is closely linked to the soils size fractions, particle size, particle shape, degree of compaction and orientation of the grains. The particle size distribution is important for the porosity because it affects the volume between the grains. If a soil is poorly sorted, the smaller grains will fill the spaces between the larger grains and the porosity will decrease. On the other hand, if the soil is well sorted the porosity will be higher, there is more room for water entering the soil, and there will be a higher infiltration rate. It is common to distinguish between total porosity and effective porosity, n_{eff}. Total porosity includes all pores, also pores that are closed or little permeable for liquid or gas. Effective porosity includes only the volume of the drainable pores (Brattli, 2009). Some of the water in the soil is adhesive attached to the soil particles and being retained in disconnected pores and thus cannot be drained. This amount of water is called the residual moisture content or in some cases the irreducible

moisture content θ_r. The effective porosity is therefore the same as the volume of water that can flow free through the soil, and is defined as n_{eff}=n-θ_r (Tarboton, 2003).

The pores can be partly or totally filled with air or water. The volume occupied by water is defined by the ratio of water volume to soil volume, and is called volumetric water content, θ.

$$\theta = \frac{V_w}{V_s} \tag{4.2}$$

The soils water content can vary in both time and space, and has a theoretical range from zero to saturation. If the soil water content is equal to zero, the soil is completely dry, while if the water content is equal to the porosity the soil is saturated. The water content is therefore also sometimes characterized by the degree of saturation, S=θ/n (Dingman, 2008).

Flow through porous medium is described by Darcy's law. Darcy found that the rate of flow was proportional to the cross sectional area, A, and to head loss, Δh, and invers proportional to the length of flow path, Δl (Rawls et al., 1992). The volumetric discharge or flow rate through a cross sectional area can be described by equation 4.3, known as Darcy's equation or Darcy's law.

$$Q = -K * A * \frac{\Delta h}{\Delta l} \quad , \left(\frac{m^3}{s}\right) \tag{4.3}$$

K, the proportionality constant, is called the hydraulic conductivity. The rate at which water is able to move through a porous medium under a unit potential- energy gradient is described by the hydraulic conductivity of the soil. This rate is closely related to the size of the pathways available for water transmission, as well as the fluid properties of viscosity and density (Dingman, 2008).

Darcy's law can also be rewritten to describe the specific discharge, q, representing the per unit area flow through the cross section

$$q_x = -K * \frac{d\left(z + \frac{p}{\gamma_w}\right)}{dx} = -K * \left(\frac{dz}{dx} + \frac{d(p/\gamma_w)}{dx}\right) , \left(\frac{L}{T}\right) \tag{4.4}$$

where z is elevation above an arbitrary datum (L); p is the water pressure (F/L^2); γ is the weight density of water (F/L^3); K is the hydraulic conductivity (L/T).

The two terms, dz/dx and $d(p/\gamma_w)/dx$, are the two spatial gradients of mechanical potential energy, which causes flow. The first describes the gradient of gravitational potential energy per unit weight

of flowing water, and the lateral describes the gradient of pressure potential energy per unit weight of flowing water. Because we only consider infiltration in the vertical (z) direction, q can be expressed by equation 4.5.

$$q = -K * \frac{d\left(z + \frac{p}{\gamma_w}\right)}{dz} = -K * \left(1 + \frac{d\left(\frac{p}{\gamma_w}\right)}{dz}\right) \tag{4.5}$$

As an effect of only considering the vertical direction, the magnitude of the gravitational potential energy gradient will always equal unity. Since the weight density of water, γ_w, is constant, the term describing the gradient of pressure potential energy can be expressed by the pressure head, ψ, defined as

$$\psi = \frac{P}{\gamma_w} \tag{4.6}$$

The unsaturated flow through porous media is dependent on the soils water content, θ, and thus are both the pressure head and the hydraulic conductivity for a given soil a function of the soil-water content. We can hence write Darcy's law for vertical unsaturated flow as

$$q = -K(\theta) * \left(1 + \frac{d\psi(\theta)}{dz}\right) \tag{4.7}$$

The pressure is measured relative to atmospheric pressure. At the water table the pressure in the pores of a porous medium is exactly atmospheric. In the saturated zones of the soil the pressure head is positive, while it is negative in the unsaturated zones. The negative pressure head in the unsaturated soil is often called tension or suction, and ψ is thus called tension head, matric potential or matric suction. In the unsaturated soil the water is held to the mineral grains by surface-tension forces. Across each pore channel there is a concave meniscus ranging from grain to grain. The size of the radii of curvature of each meniscus describes the surface tension on each individual, microscopic air-water interface. A decrease in the radii of curvature of the meniscus, increases the surface tension. This means that for a given soil, the surface tension increases with decreasing water content in the soil (Dingman, 2008). The curves describing the relation between pressure head and water content for a given soil is referred to as a moisture-characteristic curve. This curve shows that when the water content equals the soils porosity, the pressure head is zero. At a point of the curve the water content changes little as the tension increases up to a point of inflection. This distinct point is called the air-entry tension or bubbling-pressure, ψ_a, and describes the tension at which significant volumes of air begins to appear in the soil. In the lower part of the vadose zone,

the entire zone of negative water pressure above the water table, the soil is saturated as a result of capillary forces (see section 4.2), and is thus known as the capillary fringe. At the top of this zone, the pores are partly filled with air, and the pressure head at this point is thus equal to the air-entry tension. The absolute value of the air-entry tension head is therefore equal to the height of the capillary fringe (Dingman, 2008).

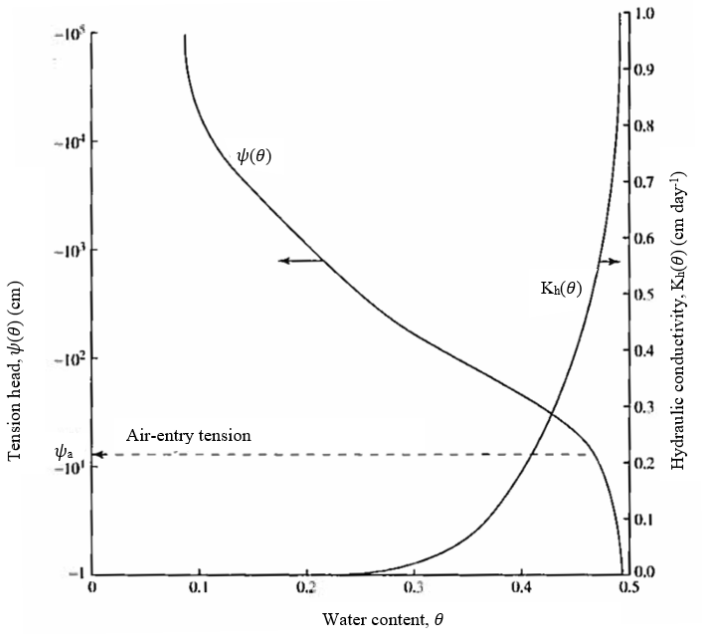

Figure 4.1 Example of a moisture-characteristic curve.(Dingman, 2008)

The moisture-characteristic curves are related to the size distribution and structure of the pore space of the soil, and are thus unique for each soil. For practical use it is convenient to mathematically represent the characteristic functions. It will here be used the Clapp and Hornberger simplification of Brooks and Corey functions.

$$|\psi(\theta)| = |\psi_a| * \left(\frac{n}{\theta}\right)^b \tag{4.8}$$

$$K(\theta) = K_{sat} * \left(\frac{\theta}{n}\right)^c \tag{4.9}$$

K_{sat} is the saturated hydraulic conductivity and b and c are fitting parameters. The pore size distribution determines the relationship between suction and moisture content, and is described by the pore size distribution index, b. The parameter c is referred to as the pore disconnectedness

index, representing the relationship between the hydraulic conductivity and the changes in how disconnected and tortuous flow paths become as moisture content is reduced (Dingman, 2008).

It can be seen from the moisture- characteristic curves that as the moisture drains from the soil under gravitational processes, both the hydraulic conductivity and drainage rate are reduced. The drainage rate declines exponentially and after some days it is negligible. The point where the water content in the soil can be held against the force of gravity, and further drainage is negligible, is defined as a soils field capacity, designated θ_{fc}. To be able to define a point where the drainage rate is negligible, it is common to define the field capacity as the water content corresponding to a pressure head of -340 cm (Dingman, 2008).

By rearranging equation 4.8, the filed capacity can be expressed by

$$\theta_{fc} = n * \left(\frac{|\psi_a|}{|-340|} \right)^{\lambda} \tag{4.10}$$

The pressure force in equation 4.7 will in the earliest stages of vertical infiltration be much greater than the gravity force. The rate which the water will be drawn into an unsaturated soil under these conditions, without gravity forces, is described by the soils sorptivity, S_p (Dingman, 2008).

4.2 Infiltration and water movement

As described above, infiltration is the process of water entering the soil due to gravity forces and capillary suction in the soil (Tarboton, 2003). During the rainfall, the upper layer of the soil will get saturated due to infiltration of ponded water standing on the surface or by water flowing over the surface. The moisture content in the soil will then, be spread gradually, due to downward water movement, through the soil profile, creating four moisture zones illustrated in figure 4.2. Near the surface the soil will be saturated, and the pores are thus completely filled with water. The water from the saturated soil will move downwards to a transmission zone. This zone is characterized by an unsaturated flow and a relatively uniform moisture content. The next zone is the wetting zone where the moisture content decreases with the depth, ending in a significantly change in the moisture content creating sharp discontinuity between the wet soil above and the dry soil below, which is called the wetting front (Chow et al., 1988).

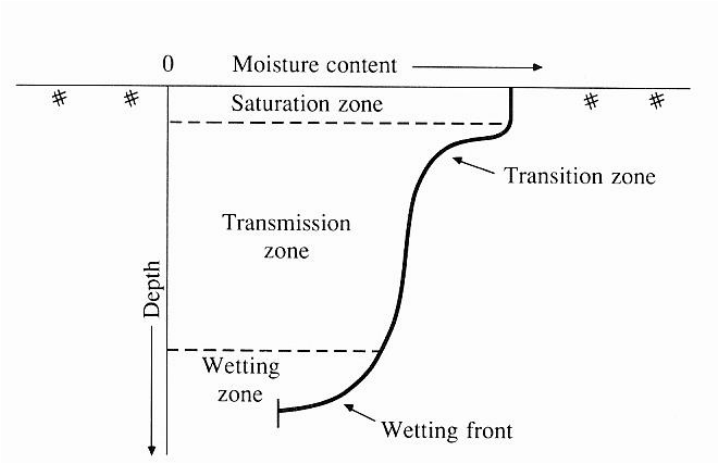

Figure 4.2 Moisture zones during infiltration.(Chow et al., 1988)

The downward movement of water in the soil profile is mainly due to the two forces, gravity and capillary suction (matric potential). Dependent on the moisture content in the soil, will either the gravity potential or the matric potential dominate. If the water content in the soil is greater than the irreducible moisture content, the gravity potential will be the dominating force, but if the soil is very dry the matric potential can be many magnitudes higher than the gravity potential.

In the saturated part of the soil, the gravity force will dominate. When soil is saturated, the larger pores are filled with water creating a network of interconnected and continuous conductors in the porous material. This network moves the water rapidly through the soil, and as the water amount in the soil increases, more pores will be filled with water, and the velocity of the flow increases. As the moisture content in the soil decreases, downward the soil profile, both the amount and size of the conductors decreases. The water between the soil grains decreases and hence the radius of the curvature of the meniscus decreases. This results in a higher water tension, and the water is held more closely to the soil grains. This means that when the soil is dry the continuous filled conductors are gone, and the soils capacity to lead the water is reduced. The major force moving the water in unsaturated soil is therefore capillary suction (or matric potential). Capillary suction in the soil can be illustrated with the capillary rise theory. When a thin tube is placed in water with a free surface, the hydrogen bonds in the water molecules will be attracted to the surface of the tube. This will create a surface tension between the water molecules and the surface of the tube, which will draw the molecules that are in contact with the tube upwards. Because of the strong intermolecular hydrogen bounds, the rest of the water volume in the tube will also be drawn

upwards. Under this process it is formed a curved surface, a meniscus, on the water surface. This means that the pressure on the concave side of the water film is greater than the pressure on the convex side. To compensate for this pressure difference, the water will rise in the tube to a water column height equal to the pressure difference. The area between the pores can be seen as capillary tubes, where the water has tension inversely proportional to the curvature of the menisci (Brattli, 2009).

The rate at which infiltration occurs is called the infiltration rate, often designated f, and depends on the moisture content and distribution in the soil, and soil properties (Tarboton, 2003). The maximum rate a soil, under given conditions, can absorb rain as it falls is called the infiltration capacity, designated f_c. Infiltration capacity describes the maximum infiltration rate under ponded conditions, and the infiltration rate of a soil can thus vary from zero up to the infiltration capacity (Horton, 1941). The infiltration capacity is higher for a dry soil than for a wet soil. As figure 4.4 shows, the infiltration capacity decreases with time, due to the changes of the soil during a rainfall. At the beginning of infiltration, the wetting front will be near the surface, resulting in a high infiltration capacity due to the high matric head gradient at the wetting front. As the rain continues, the soil profile gets more and more saturated, which moves the wetting front further down in the soil profile, and thus reduces the capillary force in the upper layer (Horton, 1941). Another factor reducing the infiltration capacity, is the reduction of pore size. The force from raindrops falling at the soil will break up soil aggregates, creating fine soil particles, which will be spread over the surface and washed into pores, causing clogging and reduction of water entering the soil. In soil containing colloids, the clay will swell, resulting in reduction of the pore space available for water movement (Tarboton, 2003). The infiltration capacity will therefore first decrease rapidly, then approaching an asymptotic line until a certain constant minimum infiltration capacity is reached (Horton, 1941).

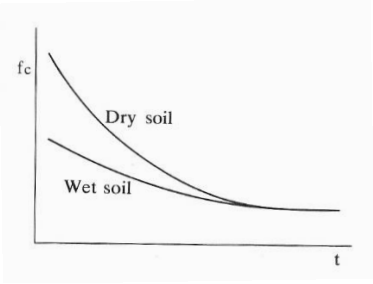

Figure 4.3 Decrease of infiltration capacity over time. (Miyazaki et al., 1993)

5. Infiltration models

To be able to estimate the amount of infiltration, a number of equation or models have been developed through the past century. These infiltration models are usually based on a simplified concept, which are predicting the infiltration rate or cumulative infiltration volume by assuming that surface ponding begins when the surface water input rate exceeds the soil surface infiltration rate, f<w. Based on which assumptions the different models are derived from, the infiltration models can either be characterized as empirical models, theoretical- based models or physical-based models. Physical- based models reflect the process of infiltration as close as possible by specifying appropriate boundary conditions, and requires therefore detailed input data. One physical-based model used for describing water flow in soils is the Richards equation. Solving physical- based models like the Richards equation is extremely difficult, and there has therefore been developed approximations to the physical-based models, called theoretical- based models (Rawls et al., 1992). These models are derived from ideal physical models, and are thus based on a physical basis. Theoretical-based models see the soil as a bundle of capillary tubes which infiltrates water into the whole porous media. The different infiltration parameters usually have a physical meaning, and can be found from soil physical properties like hydraulic conductivity, porosity, soil water pressure head and soil water content. Green-Ampt model and Philip equation are examples of theoretical- based models derived from Richards equation (Ghorbani Dashtaki et al., 2009). Empirical models have normally a simpler form than theoretical- based models. The equation describing infiltration in empirical models are derived by curve fitting of real measurements of cumulative infiltration and infiltration rate, by using fitting parameters relating to the types of soil, and corresponding soil properties like bulk density, initial water content and non-uniformity of soils (Miyazaki et al., 1993). Empirical models are also derived under the assumption of a constant water content available on the surface soil, and do not give information about the water content distribution in the soil. One of the most known empirical model describing infiltration is the Horton equation (Ghorbani Dashtaki et al., 2009).

5.1 Richards Equation:

Richards (1931) equation is the foundation for many infiltration models, and describes the vertical movement of water through unsaturated soil. To express the process of infiltration mathematically,

Richard combined the principle of physical conservation of mass, expressed through the continuity equation, with quantification of unsaturated flow through soil, expressed by Darcy's equation. Richards equation can therefore be derived by first deriving the continuity equation, and then substitute it in Darcy's equation (Tarboton, 2003).

The continuity equation can be derived by considering a rectangular parallelepiped of an unsaturated porous medium, as shown in figure 5.1. In this derivation, the flow occurs only vertically, designated as the z'- direction. The conservation of water mass for this volume element during a small time increment Δt is

$$\rho_w * q_{z'} * \Delta x * \Delta y * \Delta t - \rho_w * \left(q_{z'} + \frac{\partial q_{z'}}{\partial z'} * \Delta z\right) * \Delta x * \Delta y * \Delta t = \rho_w * \frac{\partial \theta}{\partial t} * \Delta t * \Delta x * \Delta y * \Delta z \quad (5.1)$$

where ρ_w is the mass density of water, $q_{z'}$ is the volumetric flow rate in the z'-direction at the top of the element, and θ is the water content of the soil.

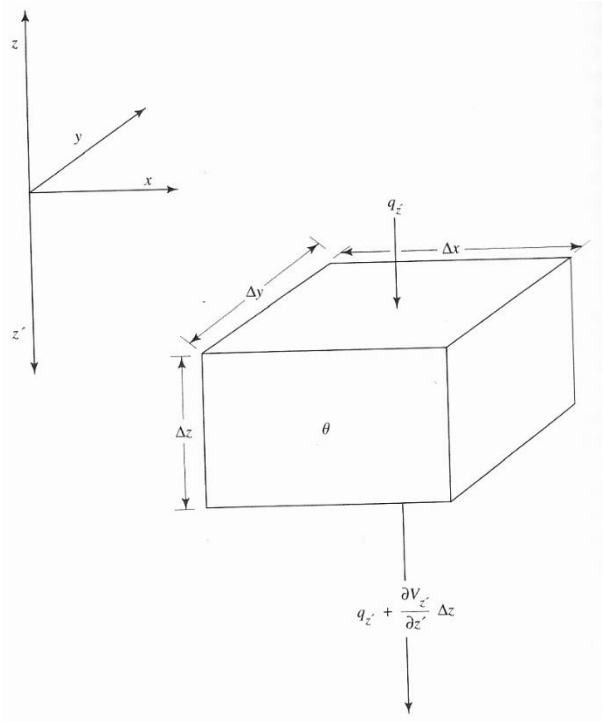

Figure 5.1 Definition sketch used for deriving the Richards Equation. (Dingman, 2008)

Assuming a constant density, and dividing by Δx *Δy* Δz* Δt, equation 5.1 can be simplified, and yields the continuity equation for this situation

$$-\frac{\partial q_{z'}}{\partial z'} = \frac{\partial \theta}{\partial t} \tag{5.2}$$

Darcy's law for unsaturated flow in the z'- direction is

$$q_{z'} = -K_h(\theta) * \frac{\partial\big(z + \psi(\theta)\big)}{\partial z'} = -K_h(\theta) * \frac{\partial z}{\partial z'} - K_h(\theta) * \frac{\partial \psi(\theta)}{\partial z'} \tag{5.3}$$

But since $\frac{\partial z}{\partial z'} = -1$ we have

$$q_{z'} = K_h(\theta) - K_h(\theta) * \frac{\partial \psi(\theta)}{\partial z'} \tag{5.4}$$

Taking the derivative of this expression with respect to the z'- direction, yields

$$\frac{\partial q_{z'}}{\partial z'} = \frac{\partial K_h(\theta)}{\partial z'} - \frac{\partial}{\partial z'}\left(K_h(\theta) * \frac{\partial \psi(\theta)}{\partial z'}\right) \tag{5.5}$$

Substituting equation 5.3 into equation 5.2 gives the basic equation for vertical unsaturated porous-media flow:

$$-\frac{\partial K_h(\theta)}{\partial z'} + \frac{\partial}{\partial z'}\left(K_h(\theta) * \frac{\partial \psi(\theta)}{\partial z'}\right) = \frac{\partial \theta}{\partial t} \tag{5.6}$$

Known as the Richards equation (Dingman, 2008).

Richards equation can also be expressed in form of diffusivity

$$-\frac{\partial K_h(\theta)}{\partial z'} + \frac{\partial}{\partial z'}\left(D_h(\theta) * \frac{\partial(\theta)}{\partial z}\right) = \frac{\partial \theta}{\partial t} \tag{5.7}$$

where $D = K\left(\frac{\partial \psi}{\partial \theta}\right)$

Because Richards equation contains the soil moisture characteristic relationship, considering the relation between moisture content and pressure head, (ψ), and the relation between hydraulic conductivity and pressure head or moisture content, K(ψ) or K(θ), the equation is difficult to compute mathematically. Numerical solutions of Richards equation are very complex, and would require detailed soil data. As a result of this, it has been developed infiltration models which includes an approximation of the Richards equation. Some of these infiltration models will be discussed in the next paragraphs (Tarboton, 2003).

5.2Philip model:

The first and best known attempt to develop approximate analytical solution to the Richards equation, was developed by Philip (1957). By assuming that the soils hydraulic conductivity, K, and soil water diffusivity, D, can vary with the moisture content θ, Philip solved Richards equation under less restricted conditions. He used the Boltzmann transformation $B(\theta) = zt^{-\frac{1}{2}}$ to convert equation 5.7 into an ordinary differential equation and formulated an infinite-series solution (Chow et al., 1988). Equation 5.8 shows the Philip equation, and describes infiltration into an infinite deep soil, with a uniform initial water content, and a ponded surface.

$$f(t) = \frac{S_p}{2} * t^{-\frac{1}{2}} + A_2 + A_3 * t^{\frac{1}{2}} + A_4 * t + \cdots + A_n^{\frac{n}{2}-1} \tag{5.8}$$

Usually the solution is approximated by only using the two first terms of this series, where A_2 is a parameter with dimension of hydraulic conductivity, designated K_p, resulting in

$$f(t) = \frac{S_p}{2} t^{-\frac{1}{2}} + K_p \tag{5.9}$$

were S_p is the sorptivity, which describes the soil suction potential (Dingman, 2008). The first term of equation 5.9 represents the effect of soil suction, and the second term represents the effect of gravity head.

The cumulative infiltration is given by integrating equation 5.9 over time, expressed in equation 5.10.

$$F(t) = S_p t^{\frac{1}{2}} + K_p t \tag{5.10}$$

(Chow et al., 1988)

Philip equation can be rewritten in terms of cumulative infiltrated depth, F, by eliminating t between equation 5.9 and equation 5.10.

$$f_c(F) = K_p + \frac{K_p S_p}{\sqrt{S_p^2 + 4K_p F} - S_p} \tag{5.11}$$

(Tarboton, 2003)

The different parameters in equation 5.9 and equation 5.10 can be found from experimental infiltration data using regression data, but they can also be estimated from soil data by using the following approximations. Rawls et al. (1992) suggested that the soils sorptivity, S_p, is given by

$$S_p = \sqrt{2(n-\theta_i)K_{sat}|\psi_f|} \tag{5.12}$$

where ψ_f is the matric potential describing the suction head at the wetting front; n is the total porosity which can be estimated if the soils bulk density is known; θ_i is the initial moisture content which can be estimated from water-retention data according to the degree of wetness; and K_{sat} is the saturated hydraulic conductivity. The parameter K_p in equation 5.9 is, according to Rawls et al. (1992), ranging from $0.33K_{sat}$ to K_{sat}, with K_{sat} being recommended value. However, Dingman (2008) reports that using K_p ranging between $1/3K_{sat}$ and $2/3K_{sat}$ fits measured values better for short time periods.

Before ponding, cumulative infiltration is F=wt, given a surface water input rate of w. Ponding starts when the soils infiltration capacity is equal or less than the water input rate, f_c=w. An equation describing cumulative infiltration at ponding is obtained by setting f_c=w in equation 5.11.

Philip cumulative infiltration at ponding is therefore given by

$$F_p = \frac{S_p^2\left(w-\frac{K_p}{2}\right)}{2\left(w-K_p\right)^2} \tag{5.13}$$

The time to ponding is given by F_p/w, and is then given by

$$t_p = \frac{S_p^2\left(w-\frac{K_p}{2}\right)}{2w\left(w-K_p\right)^2} \tag{5.14}$$

To solve for the infiltration that occurs after ponding, the time period, t_0, where infiltration occurs under ponded conditions, has to be calculated. ts describes the time at the end of the time step, where it is still ponding.

$$t_0 = t_s - \frac{1}{4K_p^2}\left(\sqrt{S_p^2+4K_pF_s}-S_p\right)^2 \tag{5.15}$$

Philip infiltration under ponded conditions can thus be obtained from

$$F = S_p(t - t_0)^{\frac{1}{2}} + K_p(t - t_o) \quad (5.16)$$

(Tarboton, 2003)

5.3 Horton Equation:

A well-known empirical relationship describing infiltration is the Horton Equation(Horton, 1941). He observed that the initial infiltration capacity decreases over time until it reaches a constant rate. The reduction of infiltration capacity as rain continues are due to exhausting processes in the soil. Horton defined an exhausting process as one "process at which the rate of performing work is proportional to the amount of work remaining to be performed" (Horton, 1941). In case of a soil surface the rate of performing work is df/dt, and since the work is decreasing df/dt is negative. The work remaining to be performed can be expressed by (f-f_c) and is the changing of the infiltration capacity, f, at a given time t to its constant value f_c. By introducing a factor of proportionality, K_f, the equation gives

$$-\frac{df}{dt} = K_f(f - f_c) \quad (5.17)$$

The following derivation follows the derivation of Horton equation described in (Horton, 1941).

Equation 5.17 can be written as

$$-\frac{df}{f - f_c} = K_f dt \quad (5.18)$$

But

$$\frac{df}{f - f_c} = d\ln(f - f_c) \quad (5.19)$$

Integrating equation 5.18 and changing signs, yields

$$\ln(f - f_c) = -K_f t + constant \quad (5.20)$$

When t equals zero, the infiltration capacity is equal to the initial infiltration capacity yielding that the constant is equal to ln (f_0-f_c) and

$$\ln\frac{f - f_c}{f_0 - f_c} = -K_f t \quad (5.21)$$

or

$$\frac{f - f_c}{f_0 - f_c} = e^{-K_f t} \tag{5.22}$$

Which can be written as

$$f = f_c + (f_0 - f_c)e^{-K_f t} \tag{5.23}$$

Equation 5.23 is known as the Horton equation, where f is the infiltration capacity, f_0 is the initial infiltration capacity at the beginning of the rainfall or at a chosen moment, f_c is the final constant infiltration capacity and K_f is known as a decay constant, a constant which governs the time required under given conditions for infiltration capacity to change from its initial value f_0 to nearly its constant value f_c (Horton, 1941).

Integrating equation 5.23 gives cumulative infiltration:

$$F(t) = f_c t + \left[\frac{(f_0 - f_c)\left(1 - e^{-K_f t}\right)}{K_f}\right] \tag{5.24}$$

This equation is only valid for rain intensity greater than infiltration capacity.

To be able to solve equation 5.23 and equation 5.24, the parameters f_c, f_0 and K_f has to be known. These can be found by measuring the infiltration rate over an extended period of time. Reported values of the parameters for the different soil types can be found in literature. However, since the infiltration capacity depends on the initial moisture content, amount of organic matter in the soil, vegetative cover and season, the reported values of the parameters can vary widely from researcher to researcher (Pazwash, 2011).

In later times, Eagleson (1970) showed that Horton's Equation also can be derived from Richards' equation. This can be done by assuming that K and D are constants independent of the moisture content of the soil. Under this assumption Richards' equation is reduced to

$$\frac{\partial \theta}{\partial t} = D\left(\frac{\partial^2 \theta}{\partial z^2}\right) \tag{5.25}$$

Equation 5.25 shows the standard form of a diffusion equation, and can thus be solved to express the moisture content as a function of time and depth. By solving for the rate of moisture diffusion at the soil surface, Horton equation can be derived (Chow et al., 1988).

5.4 Green-Ampt model

Green and Ampt (1911) used a simplified picture of infiltration, shown in figure5.2, to develop a more approximate physical model for modeling the process of infiltration (Chow et al., 1988).

Green-Ampt considered a vertical block of soil, of unit horizontal cross-sectional area, and locked at a control volume around the wet soil between the surface and depth L. If the water -input rate is greater than the saturated hydraulic conductivity, water ponds on the surface to a depth of H_0 over the ground. Before infiltration the moisture content is designated θ_i, throughout its entire depth, but as the infiltration begins the moisture content in the upper layer of the soil will increase from θ_i to the porosity, n. This interference between saturated and unsaturated soil is called the wetting front, and is seen as a sharp boundary dividing soil with moisture content equal to θ_i below, from saturated soil with moisture content equal to n above, see figure 5.2. The difference in moisture content between the saturated and unsaturated soil creates a sharp moisture gradient resulting in a high infiltration rate. As the infiltration continues over time, the wetting front moves downward and eventually reaches the groundwater table (Pazwash, 2011).

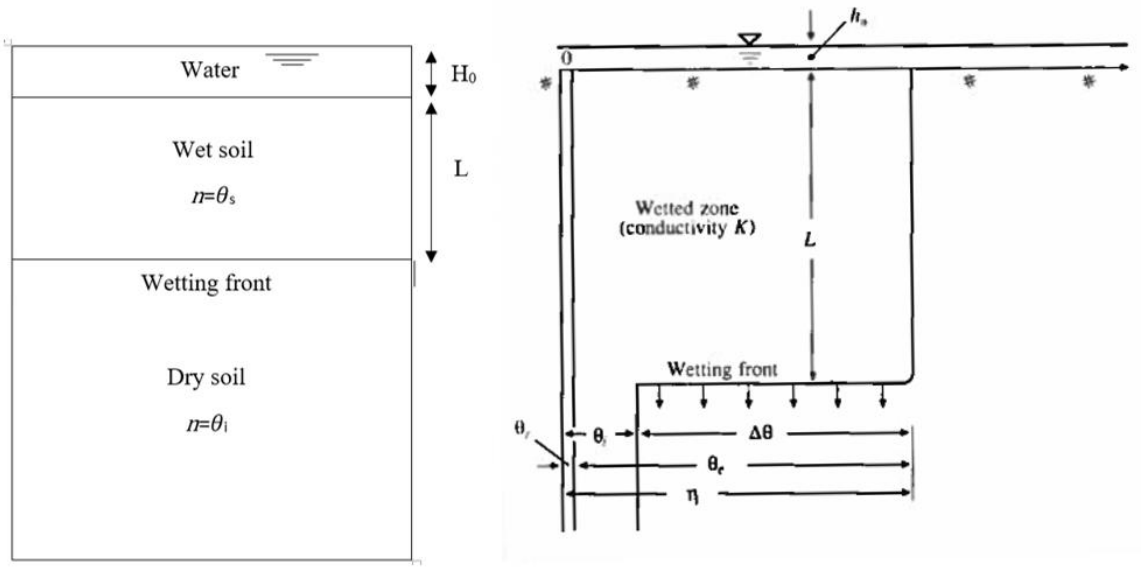

Figure 5.2 The figure to the left shows infiltration into a column of soil for the Green-Ampt model, while the figure to the right shows the distribution of moisture content of the soil (Chow et al., 1988).

As a result of infiltration, the increase in stored water within the soil in the control volume is L(n-θ_i), and is by definition equal to the cumulative depth of water infiltrated into the soil. (Chow et al., 1988)

$$F(t) = L(n - \theta_i) = L\Delta\theta, \quad where\ \Delta\theta = n - \theta_i \tag{5.26}$$

Like Richards equation, Green-Ampt model is based on Darcy's Law and the principle of conservation of mas (Dingman, 2008). In the described case above, the Darcy flux, q, is constant throughout the depth, and is equal to -f, where f is the infiltration rate. The following derivation follows the derivation of Green Ampt infiltration equation as described in Chow et al. (1988). By defining two points, point one located at the ground surface and point two located right after the wetting front at the dry side, Darcy's Law can be approximated by

$$f = K * \left[\frac{h_1 - h_2}{z_1 - z_2}\right] \tag{5.27}$$

At the surface, the head h_1 is equal to the depth of the ponded water, H_0. The head at the dry side of the wetting front, h_2, is equal to ($-\psi_f$-L), where ψ_f is the wetting front capillary pressure head and L is the length of the wet soil. The difference in z-direction, z_1-z_2, is equal to L. Darcy's Law for this system can thus be written as

$$f = K\left(\frac{H_0 - (-\psi_f - L)}{L}\right) \tag{5.28}$$

Since H_0 is negligible compared to ψ_f and L, equation 5.28 is approximately equal to

$$f = K\left(\frac{\psi_f + L}{L}\right) \tag{5.29}$$

From equation 5.26, we have that L=F/$\Delta\theta$. Substituting this into equation 5.29 gives

$$f = K\left(\frac{\psi_f \Delta\theta + F}{F}\right) \tag{5.30}$$

Since the infiltration rate is the change in cumulative infiltration over time, f=dF/dt, equation 5.30 can be written as differential equation with one unknown, F.

$$\frac{dF}{dt} = K\left(\frac{\psi_f \Delta\theta + F}{F}\right) \tag{5.31}$$

To solve for F, equation 5.31 is cross-multiplied to obtain

$$\left(\frac{F}{F + \psi_f \Delta\theta}\right) dF = Kdt \tag{5.32}$$

Splitting the left side into two parts

$$\left(\left(\frac{F+\psi_f\Delta\theta}{F+\psi_f\Delta\theta}\right)-\left(\frac{\psi_f\Delta\theta}{F+\psi\Delta\theta}\right)\right)dF = Kdt \tag{5.33}$$

And integrate

$$\int_0^{F(t)}\left(1-\left(\frac{\psi_f\Delta\theta}{F+\psi_f\Delta\theta}\right)\right)dF = \int_0^t Kdt \tag{5.34}$$

To obtain

$$F(t)-\psi_f\Delta\theta * \ln\left(1+\frac{F(t)}{\psi_f\Delta\theta}\right) = Kt \tag{5.35}$$

Which is the Green-Ampt equation for cumulative infiltration (Chow et al., 1988). Once F is found, the infiltration rate, f, can be obtained from equation 5.30.

$$f(t) = K\left(1+\frac{\psi\Delta\theta}{F(t)}\right) = K_{sat}\left(1+\frac{P}{F(t)}\right), \qquad where\ P = |\psi_f|\Delta\theta \tag{5.36}$$

As we can see from the equation, the reduction in infiltration capacity is expressed as a function of infiltrated depth, $f_c(F)$.

Prior to ponding the cumulative infiltration, F, is equal to the surface water input rate, w, multiplied with a time step t, F=wt. Ponding starts when the infiltration capacity is equal or less then the water input rate, w. By setting f_c=w in equation 5.36, and solving for F, the cumulative infiltration at ponding is obtained.

$$F_p = \frac{K_{sat}|\psi_f|\Delta\theta}{w-K_{sat}} \tag{5.37}$$

The time to ponding is then computed by

$$t_p = \frac{F_p}{w} = \frac{K_{sat}|\psi_f|\Delta\theta}{w(w-K_{sat})} \tag{5.38}$$

By recognizing that the infiltration rate is the derivative of cumulative infiltration, and is limited by the infiltration capacity, the infiltration occurring after ponding can be solved with the Green-Ampt infiltration model.

$$f(t) = \frac{dF}{dt} = f_c(t) \tag{5.39}$$

Using equation 5.36, the following differential equation is obtained.

$$\frac{dF}{dt} = K_{sat}\left(1 + \frac{P}{F}\right) \tag{5.40}$$

To derive an expression for Green-Ampt infiltration under ponded conditions, equation 5.40 has to be integrated using separation of variables, from any initial cumulative infiltration depth F_s at time t_s to a final cumulative infiltration depth F at time t.

$$t - t_s = \frac{F - F_s}{K_{sat}} + \frac{P}{K_{sat}} \ln\left(\frac{F_s + P}{F + P}\right) \tag{5.41}$$

Equation 5.41 cannot be solved explicit for F, but by setting t_s equal to t_p and F_s equal to F_p, it can be solved numerically for F, and gives thus the cumulative infiltration as a function of time (Tarboton, 2003).

6. Modeling Method

6.1 Model limitations and choice of infiltration models

In order to investigate the effect of downspout disconnection, a modelling program was developed to calculate the amount of infiltration and runoff. Because of the complexity of the infiltration process, the model is based on some assumptions and simplifications. When modeling a process in nature, assumptions and simplifications has to be made in order to decrease the complexity and the resources needed for running the model. However, the question has to be raised whether or not the simplifications are acceptable in relation to the accuracy to the field conditions. This will be an evaluation of the desired accuracy in relation to available input data and the purpose of the model. The idea behind the model, established in this thesis, was to develop a model requiring few input parameters to calculate an estimation of generated runoff and amount of infiltrated water, given a known rain event. The results from the model will indicate where the soil conditions allow for downspout disconnection, and where the soil conditions are too poor in regard to be able to infiltrate the amount of generated surface water. The model can be considered as a tool for the first step in evaluating if an area is suited for implementation of SUDS, or not. The model can indicate if SUDS can be considered for managing stormwater, if the area needs further modifications before implementing SUDS, or if the area is not suited at all. However, there will still be need for further investigations before decision making. In order to make this model as easy as possible for the user, it has been made some assumptions and simplifications.

Given a known rain event, the size of the roof, the size of the infiltration area and some soil properties, the model will calculate the amount of infiltrated water and the amount of surface runoff generated. The rain volume falling at the roof and the rain volume falling directly onto the infiltration area constitutes the amount of water that has to be infiltrated. It is assumed that the amount of water is distributed evenly over the infiltration area. In reality, the soil closest to the downspout will be saturated first, and the infiltrated water will move both vertically and horizontally. The developed model does not include overland flow nor horizontal infiltration, and calculates therefore only vertical infiltration of the soil, and can thus be seen rather as an at point infiltration model.

During the development of the model it had to be decided which infiltration equation it would be based on, i.e. Horton, Philip or Green Ampt. Because of the available input parameters, it was

decided to proceed with both the Green Ampt infiltration equation and the Philip equation. The reason behind choosing two infiltration equations, was to investigate whether there would be significant differences in the results, depending on which infiltration equation chosen. Horton infiltration equation was not chosen, because of the lack of required input parameters. The input parameters would then have been based on standardized values from tables, and since we are looking at infiltration into urban soil, and because it was found in Becker (2015) that urban soil do not always behave quite as the soil texture classification would indicate, it would be wrong to use values for natural soil.

6.2 Choice of model language

When establishing a numerically model, there has to be selected an appropriate software and program language which fits the required calculations. There are many different program languages which are widely used within numerical modeling like C++ and Java, but in this thesis the program language MATLAB is used. MATLAB was chosen primarily because of prior experience with the programming language, and since MATLAB is widely used within civil engineering and thus a widely used programming language at NTNU (Norwegian University of Science and Technology). MATLAB is a powerful mathematical and graphical software package including numerical, graphical and programming capabilities. Built- in functions and a complete set of programming constructs allows the user to customize programs to their own specifications (Attaway, 2011).

6.3 Corresponding Excel-sheet for input parameters

The corresponding excel file to the MATLAB code includes three sheets for calculating the different input parameters. The first sheet named “calculations” can be used to calculate the Bubbling-pressure, pore-size distribution index and Wetting front capillary pressure head for both Green Ampt equation and Philip equation. The first column contains the name of the sample, and the following four columns contains the amount of clay, silt, sand and gravel, respectively, in the sample. The porosity for each sample is given in column number seven. Based on the given amount of clay and sand, and the porosity, the bubbling-pressure, pore-size distribution index and wetting front capillary pressure head is calculated, and given in column eight, nine and ten. The layout of this sheet is shown in Appendix 4.

The following two sheets of the excel file, contains input parameters for the Green Ampt and Philip infiltration equation, respectively. These two sheets are based on the same layout, and are shown

in Appendix 4. Required input information for both Green Ampt equation and Philip equation has been divided into six categories; *Input parameters, calculated input parameters, Rainfall data, calculated rainfall data, input data* and *calculated input data*. The parameters in the category called *computed input parameters* are calculated based on the parameters in the category called *input parameters*. This also applies for the other categories. The categories *input parameters* and *calculated input parameters* contains parameters describing the soils properties and ability to infiltrate water, such as saturated hydraulic conductivity, porosity and sorptivity. The categories *Rainfall data* and *computed rainfall data* contains information about the modeled rainfall event. The duration of the rain event, often expressed in minutes, and incremental rainfall, expressed in millimeters, are found from registered statistics from measuring stations. By converting the unit for the duration and incremental rainfall from respectively minutes to hours and from millimeters to centimeters, the required unit for further calculations is obtained. Finally, after calculating the time step Δt, the Rainfall intensity can be computed. The last to groups, *input data* and *calculated input data*, contains information about the size of the roof and the size of the infiltration area. Since the amount of water modeled for is based on the volume of water generated from the roof in addition to the amount of water falling directly onto the infiltration area, an adjusted rainfall intensity has to be calculated. The water volume from the roof can be calculated by multiplying the area of the roof by the rainfall intensity.

$$V = A * w \quad , \left[\frac{cm^3}{h}\right] \tag{6.1}$$

Where V is the water volume generated from the roof, A is the area of the roof and w is the rainfall intensity. The adjusted rainfall intensity, w', for the infiltration area can then be calculated by dividing the water volume generated from the roof by the area of the infiltration area, plus the rainfall intensity for the rain falling directly onto the infiltration area.

$$w' = \left(\frac{V}{A_{infiltration\ area}}\right) + w \ , \left[\frac{cm}{h}\right] \tag{6.2}$$

6.4 Matlab-script

The scripts calculating the infiltration and runoff by using Green-Ampt and Philip infiltration model are based on the procedure described in Tarboton (2003).

6.4.1 Green- Ampt infiltration model:

The model established in this thesis is based on spreadsheet calculations and is storing the calculations and results for each time step in a table. The MATLAB-script can be divided into three parts; one reading step, one calculation step, and one graphical step. First, the script reads the corresponding excel-sheet for input parameters. Input parameters used for calculating infiltration and runoff with the Green-Ampt model are; saturated hydraulic conductivity, porosity, wetting front capillary pressure head, bubbling-pressure, pore size distribution index, initial soil moisture content and a P parameter, in addition to a given rainfall event. How to find these input parameters is described in section 6.5. The input parameters obtained from the excel-sheet are then stored as variables or constants, used in further calculations. Before starting the calculations, a table named m is created, with a size based on the number of time steps. The first four columns of the table m contain values obtained from the corresponding excel- sheet. The first column contains the time steps, column two contains the measured incremental rainfall during each time step, the third column contains the rainfall intensity for each time step, and column four contains Δt.

The calculation follows the flowchart represented in figure 6.1. Governed by a for-loop, the calculations run through the flowchart for each time step. Initially, both the first time step, t_1, and the cumulative infiltration, F_t, is set to zero. By knowing the cumulative infiltration for the current time step, the corresponding infiltration capacity can be calculated using equation 6.3, as shown in box A.

$$f_c = K_{sat} * \left(1 + \frac{P}{F}\right) \tag{6.3}$$

At t_1=0, the infiltration capacity is equal to infinity. The infiltration capacity is then compared with the rainfall intensity. If the infiltration capacity is smaller than the rain intensity, ponding starts at the beginning of this time interval. We are therefore moving from box A to box B of the flowchart. In situations where ponding occurs at the beginning of the time interval, the time to ponding is equal to the time, and hence is the cumulative infiltration at ponding equal to the cumulative infiltration at the beginning of this time interval, F_p=F_t. The cumulative infiltration at the end of the time interval, can be calculated by solving equation 6.4 for F.

$$t - t_s = \frac{F - F_p}{K_{sat}} + \frac{P}{K_{sat}} * \ln\left(\frac{F_p + P}{F + P}\right) \tag{6.4}$$

The amount of infiltration and runoff for this time interval is then calculated in box F.

If the infiltration capacity calculated in box A is greater than the rainfall intensity, we move to box C of the flowchart. There is no ponding at the beginning of the time interval, but we have to investigate if there is developed ponding during the time interval. In box C the tentative cumulative infiltration and the corresponding tentative infiltration capacity at the end of the time interval is calculated. The tentative cumulated infiltration at the end of the time interval is computed by

$$F' = F_t + w\Delta t \tag{6.5}$$

Where F_t is the cumulative infiltration at the beginning of the time interval, w is the rainfall intensity and Δt is the time step. The corresponding tentative infiltration capacity at the end of the time interval is computed by

$$f_c' = K_{sat} * \left(1 + \frac{P}{F'}\right) \tag{6.6}$$

f_c' is then compared with the rain intensity to investigate if there is occurring ponding at the end of the time interval. If the tentative infiltration capacity at the end of the time interval is greater than the rain intensity, there is no ponding at the end of the time interval, and we move to box E of the flowchart. Then $F_{t+\Delta t}$ is equal to F' of this current time interval.

If f_c' is smaller than the rain intensity at the end of the time interval, ponding occurs during this time interval, and we move to box D of the flowchart. The cumulative infiltration at ponding is given by equation 6.7

$$F_p = K_{sat} * \frac{P}{w - K_{sat}} \tag{6.7}$$

The partial time interval required for ponding is

$$\Delta t' = \frac{F_p - F_t}{w_t} \tag{6.8}$$

Time to when ponding start is hence

$$t_s = t + \Delta t' \tag{6.9}$$

Cumulative infiltration at the end of the time interval can then be calculated by solving equation 6.4 for F.

When finished computing either box B, box D or box E, we move to box F to calculate the amount of infiltration and generated runoff. The amount of infiltration can be calculated by

$$f_t = F_{t+\Delta t} - F_t \tag{6.10}$$

Runoff generated can be calculated by

$$r_t = w\Delta t - f_t \tag{6.11}$$

From box F we move to box G for calculating increment time t=t+Δt, and are moving to the beginning in box A. This entire sequence is then repeated until the amount of infiltration and runoff are computed for each time step.

When finishing the computations for all of the time steps, the script prints the table m and corresponding diagrams showing the infiltration capacity over time and the change in infiltration and generated runoff over time. Examples showing table m and the corresponding graphs are seen in the appendix.

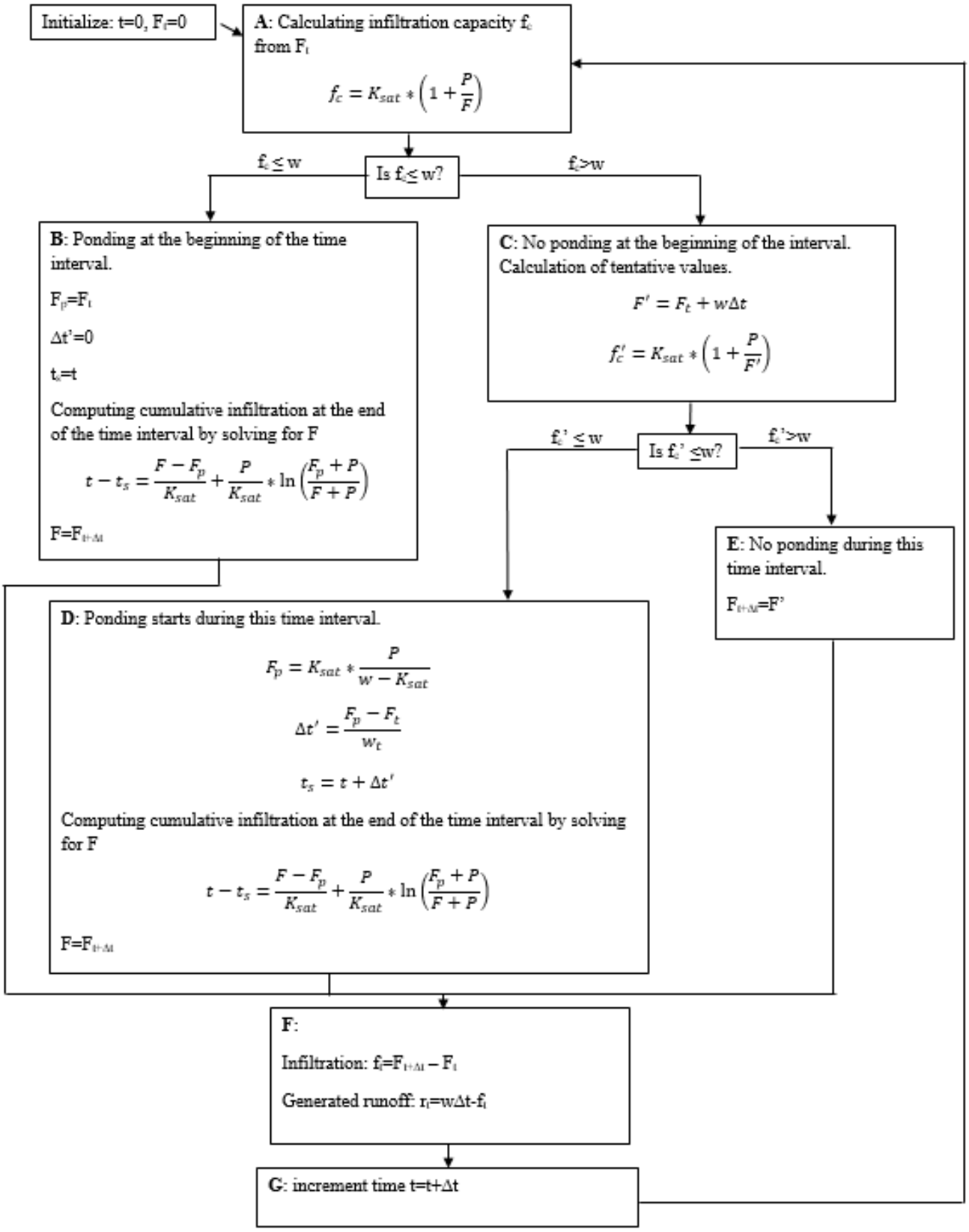

Figure 6.1 Flow chart describing the calculations for the Green-Ampt infiltration model.

6.4.2 Philip infiltration model:

As for the script calculating the Green Ampt infiltration model, the script calculating the Philip infiltration model reads the corresponding excel-sheet for input parameters. The input parameters used for calculating infiltration and runoff with the Philip infiltration model are; saturated hydraulic conductivity, porosity, wetting front capillary pressure head, bubbling- pressure, pore-size distribution index, initial soil moisture content, sorptivity and a parameter K_p in addition to a given rainfall event. How to find these input parameters is described in section 6.5. This script is constructed in the same way as for the Green Ampt infiltration model, and stores the input parameters as variables or constants before establishing the table named m. The computing method is also the same as for the Green Ampt infiltration model, but with other equations.

The calculations follow the flowchart represented in figure 6.2. Governed by a for-loop, the calculations run through the flowchart for each time step. Like for the Green-Ampt infiltration model, initially, both the time, t_1, and the cumulative infiltration, F_t, is set to zero. By knowing the cumulative infiltration for the current time step, the corresponding infiltration capacity can be calculated using equation 6.12, as shown in box A.

$$f_c = K_p + \frac{K_p S_p}{\sqrt{S_p^2 + 4K_p F} - S_p} \tag{6.12}$$

At t_1=0, the infiltration capacity is equal to infinity. The infiltration capacity is then compared with the rainfall intensity. If the infiltration capacity is smaller than the rain intensity, ponding starts at the beginning of this time interval. We are therefore moving from box A to box B of the flowchart. In the situations where ponding occurs at the beginning of the time interval, partial time interval required for ponding is equal to zero. Hence the time until ponding starts is equal to t. The cumulative infiltration is then computed by first calculating t_0 by equation 6.13

$$t_0 = t_s - \frac{1}{4K_p^2}\left(\sqrt{S_p^2 + 4K_p F} - S_p\right)^2 \tag{6.13}$$

Then solving equation 6.14 for F

$$F = S_p(t - t_0)^{\frac{1}{2}} + K_p(t - t_0) \tag{6.14}$$

The amount of infiltration and runoff for this time interval is then calculated in box F.

If the infiltration capacity calculated in box A is greater than the rainfall intensity, we move to box C of the flowchart. There is no ponding at the beginning of the time interval, but we have to investigate if there is developed ponding during the time interval. In box C the tentative cumulative infiltration and the corresponding tentative infiltration capacity at the end of the time interval is calculated. The tentative cumulated infiltration at the end of the time interval is computed by

$$F' = F_t + w\Delta t \tag{6.15}$$

where F_t is the cumulative infiltration at the beginning of the time interval, w is the rainfall intensity and Δt is the time step. The corresponding tentative infiltration capacity at the end of the time interval is computed by

$$f_c' = K_p + \frac{K_p S_p}{\sqrt{S_p^2 + 4K_p F'} - S_p} \tag{6.16}$$

f_c' is then compared with the rain intensity to investigate if there is occurring ponding at the end of the time interval. If the infiltration capacity at the end of the time interval is greater than the rain intensity, there is no ponding at the end of the time interval, and we move to box E of the flowchart. Then $F_{t+\Delta t}$ is equal to F' of this current time interval.

If f_c' is smaller than the rain intensity, ponding occurs during this time interval, and we move to box D of the flowchart. The cumulative infiltration at ponding is given by equation 6.17

$$F_p = \frac{S_p^2\left(w - \frac{K_p}{2}\right)}{2\left(w - K_p\right)^2} \tag{6.17}$$

The partial time interval required for ponding is

$$\Delta t' = \frac{F_p - F_t}{w_t} \tag{6.18}$$

The time until ponding start is hence

$$t_s = t + \Delta t' \tag{6.19}$$

Cumulative infiltration at the end of the time interval can then be calculated by first solving equation 6.13 for t_0, and then solving equation 6.14 for F.

When finished computing either box B, box D or box E, we move to box F for calculating amount of infiltration and generated runoff. Amount of infiltration can be calculated by

$$f_t = F_{t+\Delta t} - F_t \tag{6.10}$$

Runoff generated can be calculated by

$$r_t = w\Delta t - f_t \tag{6.11}$$

From box F we move to box G for calculating increment time t=t+Δt, and are starting at the beginning again in box A. This is then repeated until the amount of infiltration and runoff are computed for each time step.

When finishing the computations for all of the time steps, the script prints the table m and corresponding diagrams showing the infiltration capacity over time and the change in infiltration and generated runoff over time. Examples showing table m and the corresponding graphs are seen in the appendix.

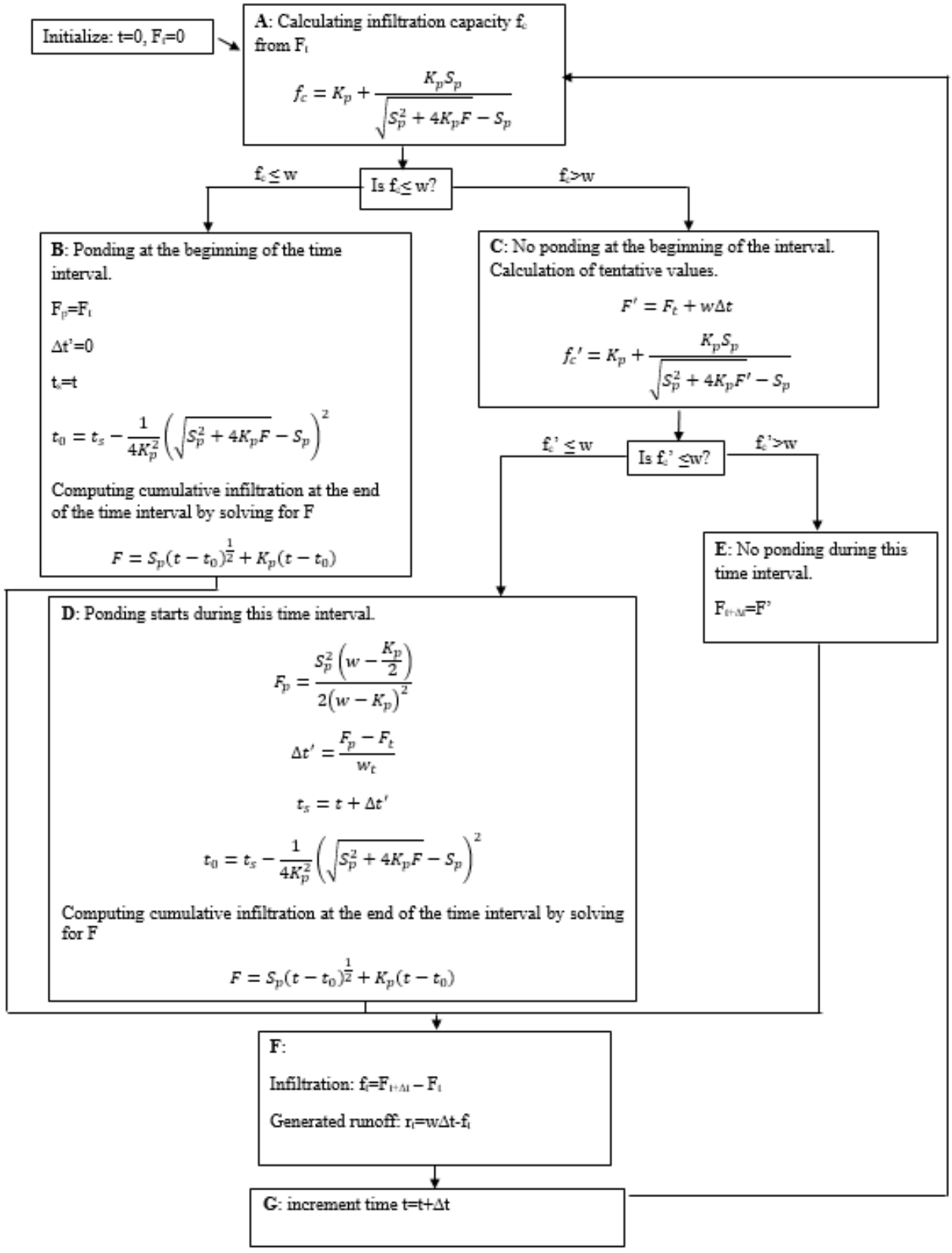

Figure 6.2 Flow chart describing the calculations for the Philip infiltration model.

6.5 Input parameters

The different input parameters for the two infiltration models are shown in table 6.1.

Input parameters for Green-Ampt model			**Input parameters for Philip model**		
Symbol	*Name*	*Unit*	*Symbol*	*Name*	*Unit*
K_{sat}	Saturated hydraulic conductivity	cm/h	K_{sat}	Saturated hydraulic conductivity	cm/h
n	Porosity	-	n	Porosity	-
ψ_f	Wetting front capillary pressure head	cm	ψ_f	Wetting front capillary pressure head	cm
ψ_a	Bubbling-pressure	cm	ψ_a	Bubbling-pressure	cm
b	Pore-size distribution index	-	λ	Pore-size distribution index	-
θ_i	Initial soil moisture content	-	θ_i	Initial soil moisture content	-
P	Parameter $(P = \lvert\psi_f\rvert(n - \Delta\theta))$	cm	S_p	Sorptivity $S_p = \sqrt{2(n-\theta_i)K_{sat}\lvert\psi_f\rvert}$	$cmh^{-1/2}$
			K_p	$1/3*K_{sat}$	cm/h

Table 6.1 Input parameters for Green-Ampt infiltration model and Philip infiltration model.

The following sections will describe how to find the different Input parameters both for Green-Ampt infiltration model and Philip infiltration model.

6.5.1 Saturated hydraulic conductivity

Saturated hydraulic conductivity (K_{sat}) describes a soils ability to lead water through a soil profile, and can be measured by using a Modified Philip-Dunne infiltrometer (MPD). MPD is a modification and adjustment of the original Philip-Dunne borehole infiltrometer (PM) (Philip, 1993). Unlike for the PD, where the infiltrometer is placed in a borehole, the MPD is knocked 5 cm into the soil, resulting in an incorporation of the surface soil. By including the surface soil, the MPD also includes the impact of sediment accumulation and the effect of surface soil compaction (Ahmed et al., 2011). The equipment used for this method is quite simple. The infiltrometer consist of a column with an internal diameter of 10cm and a height of 50 cm. A measuring tape is attached to the outside of the column in order to read the water level, and the infiltration rate can thus be calculated based on the ratio between the change in time and change in water height in the column. This method is easy to use, inexpensive and quick and gives accurate estimates. This makes this

method well suited for calculating saturated hydraulic conductivity in the field (Ahmed et al., 2011).

The value for the saturated hydraulic conductivity can vary even at the same location. This is due to processes like soil compaction, loss of soil structure, alternately freezing and thawing and clogging of pore volume. Because of these variations in K_{sat}- values, it is important to carry out several measurements using the MPD on site to be able to estimate the correct infiltration rate. The different soil layers further down in the soil profile, determines in which extent K_{sat} is influenced by the surface soil. Since the MPD only measures the saturated hydraulic conductivity in the upper 50 cm of the soil, the method will not be able to describe if there are some limited conditions further down into the soil profile (Ahmed et al., 2011).

6.5.2 Porosity

The porosity, n, can be calculated by (Dingman, 2008)

$$n = 1 - \frac{\rho_b}{\rho_m} \tag{6.20}$$

where ρ_b is the bulk density (g/cm^3) and ρ_m is the particle density (g/ cm^3), normally assumed to be equal to 2.65 g/ cm^3. The bulk density is defined as the dry density of the soil, and describes the ratio between the weight of dry soil and the bulk volume of the soil, where the bulk volume includes the volume of air, liquid water and mineral components of the soil. The bulk density can be calculated by

$$\rho_b = \frac{M_m}{V_a + V_w + V_m} \tag{6.21}$$

where M_m is the mass and V_a, V_w and V_m are the volumes of air, liquid water and mineral components of the soil, respectively (Dingman, 2008). Both the porosity and bulk density can also be determined by using average values for the different soil types form the literature (Rawls et al., 1992).

6.5.3 Bubbling-pressure, pore-size distribution index, and wetting front capillary pressure head

The wetting front capillary pressure head, ψ_f, can be calculated by using equation 6.22 (Brakensiek, 1977)

$$\psi_f = \frac{2+3\lambda}{1+3\lambda} * \frac{\psi_a}{2} \tag{6.22}$$

where ψ_a is the Brooks-Corey bubbling pressure, and λ is the Brooks-Corey pore-size distribution index. By describing the relationship between the matric potential head and the water content of the soil, Brooks and Corey (1964) derived an equation for estimating the Green-Ampt parameters. The Brooks and Corey equation is written as

$$S_e = \left(\frac{\psi_a}{\psi}\right)^{\lambda}, where\ S_e = \frac{\theta - \theta_r}{n - \theta_r} \tag{6.23}$$

where S_e is the effective saturation; θ is the soil water content cm^3/cm^3; θ_r is the residual saturation cm^3/cm^3; n is the total porosity cm^3/cm^3; ψ_a is the bubbling pressure cm; ψ is capillary pressure cm; and λ is the pore-size distribution index (Brooks and Corey, 1964). To solve equation 6.22, there has been developed several approaches to relate the different parameters to soil properties. One of these approaches where developed by Rawls and Brakensiek (1985), where they used regression analysis to relate the water- retention parameters to soil properties (Rawls et al., 1992). Equation 6.24 and 6.25 shows the regression equations developed by Rawls and Brakensiek for calculating the different Brooks and Corey parameters.

Brooks-Corey bubbling pressure Equation (6.24)

$$\begin{aligned}\psi_a = \exp[&5.3396738 + 0.1845038(c) - 2.48394546(n) - 0.00213853(c)^2 - 0.04356349(s)(n) \\ &- 0.61745089(c)(n) + 0.00143598(s)^2(n)^2 - 0.00855375(c^2)(n^2) \\ &- 0.00001282(s^2)(c) + 0.00895359(c^2)(n) - 0.00072472(s^2)(n) \\ &+ 0.0000054(c^2)(s) + 0.50028060(n^2)(c)]\end{aligned}$$

Brooks-Corey pore size distribution index Equation (6.25)

$$b = \exp[-0.7842831 + 0.0177544(s) - 1.062498(n) - 0.00005304(s^2) - 0.00273493(c^2) + 1.11134946(n^2) - 0.03088295(s)(n) + 0.00026587(s^2)(n^2) - 0.00610522(c^2)(n^2) - 0.00000235(s^2)(c) + 0.00798746(c^2)(n) - 0.00674491(n^2)(c)]$$

c is percent clay (5<%<60); s is percent sand (5<%<70); and n is the porosity (volume fraction). Equation 6.22, 6.24 and 6.25 can also be used for calculating the parameters used in Philip infiltration equation.

6.5.4 Initial soil moisture content

The initial soil moisture content, θ_i, should be measured (Rawls et al., 1992). This can either be done directly in the field or in the laboratory. Methods like Neutron moisture meters, and Gamma-ray scanners can be used for measuring moisture content in the field (for more detailed description of the different methods for measuring in the field it is referred to (Dingman, 2008)). In the laboratory, the soils water content is determined by first drying a soil sample of known volume, and then weighing the sample a second time. The water content of the soil sample can then be calculated by

$$\theta = \frac{M_{swet} - M_{sdry}}{\rho_w * V_s} \tag{6.26}$$

Where M_{swet} and M_{sdry} are the weights of the sample before and after drying, ρ_w is the density of water, and V_s is the volume of the sample.

6.5.5 K_p

K_p is often assumed to be equal to the saturated hydraulic conductivity K_{sat}, but Sharma et al. (1980) (siting (Brutsaert, 1976)) suggests that for short time periods, values ranging between $K_{sat}/3$ and $2K_{sat}/3$ will have a better fit with measurements. Sharma et al. (1980) also states that the K_p-value usually is closer to $K_{sat}/3$, and this value will therefore be used in further calculations in this project.

6.6 Case study: Trondheim and Oslo

6.6.1 Choice of location and description of the sites

Oslo Municipality have mapped out an area at Ekeberg in Oslo, which is characterized by several challenges related to both stormwater management and capacity in the existing sewer system. The sewer pipes in the area are very old and under dimensioned for today's capacity requirements, and can therefore result in basement flooding of the houses in the area. In that regard, the municipality has carried out a concept selection evaluation, (Norwegian: konseptvalgutredning (KVU)), for this area, with the goal of analyzing all needs, and identifying concepts that provides sustainable solutions in term of both stormwater management, drinking water -and sewer system, and for combined sewer overflows. According to the KVU, at least one of the concepts for solving the challenges connected to stormwater management must be based on sustainable urban drainage

systems (SUDS). As a result of this will downspout disconnection and disconnection of green areas be considered as a measure.

Filed investigations and geological maps shows that the area is characterized by soil with high clay content. Field investigations also showed that there is much visible rock in the area, which can contribute to a reduction of the infiltration rate. Drainage maps and observations made during heavy rainfalls show that large amounts of surface water are generated. The major stormwater volumes generated during a storm, combined with the steep terrain in the area, allows the water to get great speed, causing great damage to the pavement and properties in the area.

To be able to consider the effect of downspout disconnection, it is important to know the infiltration capacity of the area. As a part of this investigation, several infiltration measurements were carried out in a residential area of Ekeberg. Figure 6.3 shows a map of the area. The red stars in the map marks the addresses where the infiltration rate was measured. These addresses where selected randomly from a list over addresses where we had received permission to carry out the infiltration test in their private garden.

Figure 6.3 Map showing the investigated sites in Oslo.(maps.google.no)

Since the area in Oslo is characterized by soil with a high clay content, it was desired to investigate an area in Trondheim where there was sandy soil, so that it can be made a comparison of the different soil types. After conversations with the municipality of Trondheim, Elvegata was chosen as a suitable location. Trondheim municipality is interested in creating measures in this street that promotes infiltration, to relive the overflows with discharge into the river Nidelva. It is therefore a

great interest of the municipality to investigate the infiltration capacity of this area. The measurements were carried out at four different places, owned by the municipality, along the street named Elvegata. Figure 6.4 shows the selected places.

Figure 6.4 Map showing the investigated sites in Trondheim.(maps.google.no)

6.6.2 Computation of K_{sat}- values

Saturated hydraulic conductivity was measured by using the modified Philip-Dunne infiltrometer, and the measurements were carried out as described in (Braskerud et al. (2013)). Briefly told, the method involves registering the change in water level, over time, of a cylinder which is knocked into the soil and filled with water. By knowing the change of water level over time and some soil properties, the saturated hydraulic conductivity can be computed. For more information regarding the measuring method or the computation of the K_{sat}-value, it is referred to Becker (2015). Since the infiltration capacity is investigated in conjunction with disconnecting of downspouts, the saturated hydraulic conductivity was measured at five points along a line from the point where the downspout will lead the water onto the grass. The five columns were placed with increasing distance between each other dependent on the size of the available grass area. Figure 6.5 shows how the measurements of saturated hydraulic conductivity were carried out.

Figure 6.5 Set up for measuring saturated hydraulic conductivity with MPD.(photo: Mareike Becker)

Because of the differences between the location in Oslo and Trondheim, the process of calculating a representative K_{sat}- value for each site is slightly different. The infiltration capacity was calculated for each of the eleven gardens investigated in Oslo. For each of the eleven sites, an average value and a median value was computed based on the five K_{sat}-values measured in each garden. The range in measured K_{sat}-values and the computed average value and median value for each site is shown in table 6.2. Due to small differences between the average value and the median value, and because the median value was based on few measurements, it was decided that the average value is more representative and will thus be used in further calculations.

Site	**Soil texture**	**K_{sat} range (cm/h)**	**Average value**	**Median**
B20A	Loam	5.60-16.92	12.10	14.66
B28A+B	Silt clay loam	10.35-19.10	15.30	17.83
B30	Sandy loam	0.55-18.28	10.46	11.12
B65	Loam	0.00-42.50	15.15	9.05
E14	Loam	0.05-30.90	15.23	14.99
L34	Sandy loam	12.78-59.93	35.00	33.64
R5	Loam	0.00-20.02	6.34	4.82
R29	Sandy loam	8.96-27.13	18.42	18.79
R44	Loamy sand	12.94-88.82	46.00	23.33
S10	Loam	0.00-6.14	2.46	0.00

S75 (column a)	Sandy loam	29.96	29.96	29.96
S75 (column b,c,d,e)	Loam	8.71-27.91	18.76	19.22

Table 6.2 Measured K_{sat} range and computed average values and Median values for the investigated sites in Oslo.

The chosen location in Trondheim is not a typical residential area, which made it difficult to measure the infiltration capacity from the downspout. It was therefore thought that the water from the streets was collected and led to the infiltration area. The calculations from the measurements taken in Trondheim is therefore focusing on the impact of the different soil textures, and the measured K_{sat}- values were thus sorted by soil type. An average value and a median value for each soil type was computed, and is shown in table 6.3. Due to large variations in the measured K_{sat}-value, and the amount of values, it was decided that the median value was more representative, and is therefore used in further calculations.

Soil texture	**K_{sat} range (cm/h)**	**Average value**	**Median**
Loamy sand	8.59-92.74	31.20	15.11
Sandy loam	3.18-145.00	54.20	46.20

Table 6.3 Measured K_{sat} range and computed average values and Median values for the different soil types investigated in Trondheim.

Table 6.2 and 6.3 shows a great variation in measured K_{sat}- values for the different sites, both in Oslo and Trondheim. As we can see, all of the different soil types has a large range of measured K_{sat} -values, and there is not a clear distinction between the values for the different soil types. This variation in K_{sat} -values are most probably due to the effect of urbanization. To represent the whole range of measured K_{sat}- values, and to see how the saturated hydraulic conductivity affects the calculations of infiltration capacity, it was chosen to also run the calculations with the smallest measured value for K_{sat} and the largest measured value for K_{sat}, for some of the sites at each location.

6.6.3 Computation of Porosity

The soil samples taken at each location, both Oslo and Trondheim, can be divided into four soil textures; Loam, Silt clay loam, sandy loam and loamy sand. Table 6.4 shows values for bulk density and porosity for the different soil textures used in further calculations. The bulk density was not

measured in the field, and it was therefore used tables of average values for the different soil textures from the literature to find values for bulk density. When calculating porosity, the highest value for bulk density was used. A high bulk density will give a lower porosity, which was desirable in order to easier see the effect of compression of the soil. The porosity of each soil texture was then computed by using equation 6.20.

Soil texture	Bulk density	Porosity
Loam	1.45-1.6	0.40
Silt clay loam	1.4-1.45	0.45
Sandy loam	1.55-1.75	0.34
Loamy sand	> 1.75 (1.8)	0.32

Table 6.4 Bulk density and calculated porosity for the different soil types.

6.6.4 Computation of Bubbling-pressure, pore-size distribution index, and wetting front capillary pressure head

Bubbling- pressure and pore-size distribution index was calculated by using equation 6.24 and 6.25. To be able to compute these values, the amount of sand and clay and the porosity of the soil has to be known. A soil sample was taken at each site, and investigated in the lab to find the particle size distribution. The particle size distribution curve for each sample was then used to characterize the sample by using a texture triangle. For more details about finding the particle size distribution and values it is referred to Becker (2015) and appendix 7. Equation 6.24 and 6.25 can only be applied on soil samples with a sand content between 5-70% and a clay content between 5-60%. The soil samples taken in Trondheim was characterized either as loamy sand or sandy loam, and the clay content was measured to be zero for all of the samples. The reason for why the clay content was not measureable could be that the soil samples taken was too small for the smallest soil particles to be registered in the test. The clay content for the soil samples taken in Trondheim was therefore adjusted to be 5%. The samples taken in Oslo was characterized either as loam, silt clay loam, sandy loam or loamy sand. Two of the soil samples taken in Oslo, had a higher sand content then 70%, and was therefore adjusted to be 70%.

Five soil samples were taken at each site, one at each column. But in Oslo, the five soil samples were mixed together, resulting in one soil sample for each site. The bubbling- pressure, pore-size

distribution index and wetting front capillary pressure head was therefore calculated for each site, and is shown in table 6.5.

Site	Bubbling pressure, ψ_a	Particle size distribution index, λ	Wetting front capillary pressure head, ψ_f
B20A	36.29	0.29	27.81
B28AB	63.18	0.26	49.38
B30	24.39	0.41	17.68
B65	40.20	0.32	30.57
E14	51.82	0.32	39.20
L34	17.79	0.43	12.76
R5	30.93	0.30	23.55
R29	24.90	0.41	18.06
R44	19.69	0.48	13.85
S10	27.43	0.32	20.74
S75(a)	16.42	0.45	11.71
S75(bcde)	51.11	0.31	38.73

Table 6.5 Computed Bubbling pressure, particle-size distribution index and wetting front capillary pressure head for the investigated sites in Oslo.

In Trondheim the five soil samples taken at each column for each site was held apart, and the bubbling- pressure, pore-size distribution index and wetting front capillary pressure head was calculated for each of the five soil samples taken at each site. To find a representative value for the different parameters, an average value for each soil type was computed and used in further calculations. The computed values are shown in table 6.6. An excel-sheet sowing the calculations can be seen in the electronic appendix.

Soil texture	Bubbling pressure, ψ_a	Particle size distribution index, λ	Wetting front soil suction head, ψ_f
Loamy sand	25.28	0.50	17.67
Sandy loam	34.99	0.47	24.78

Table 6.6 Computed Bubbling pressure, particle-size distribution index and wetting front capillary pressure head for the different soil types investigated in Trondheim.

6.6.5 Computation of soil moisture content

The initial soil moisture content was computed as described in section 6.5.4, for each soil sample taken at the two different locations. In Oslo the moisture content for each site was calculated, while in Trondheim an average value for each soil type was calculated. Table 6.7 summarizes the values used for further calculations.

Oslo		*Trondheim*	
Site	**Initial soil moisture content**	**Soil texture**	**Initial soil moisture content**
B20A	0.33	Sandy loam	0.3
B28AB	0.33	Loamy sand	0.22
B30	0.26		
B65	0.31		
E14	0.33		
L34	0.31		
R5	0.31		
R29	0.28		
R44	0.30		
S10	0.32		
S75(a)	0.19		
S75(bcde)	0.30		

Table 6.7 Computed initial soil moisture content for the investigated sites in Oslo, and for the different soil types investigated in Trondheim.

If the initial soil moisture content has not been measured in the field, one way to estimate a value to use in the calculations could be to look at the amount of rainfall days during a year. According to eklima.no there is 113 days with precipitation, more than 1mm, during a year in Oslo. In Trondheim it is 146 days and in Bergen it is 184 days. That means that there is 30% rain days in Oslo, 40% rain days in Trondheim and 50% rain days in Bergen. Based on the soil type and the number of rain days, it can be estimated a factor representing how fast the soil is drained after a rainfall and thus the moisture content of the soil. This factor can then be multiplied by the porosity

to yield the initial soil moisture content. For example, is it found that the soil has a moisture content of 70% relative to the porosity. This factor is then multiplied by the porosity to obtain a value for the initial soil moisture content that can be used in the calculations instead of a measured value.

6.6.6 Size of roof area and infiltration area

To be able to calculate the infiltration capacity and thus the amount of infiltration and runoff, the area of the roof and the size of the infiltration area has to be known. In the calculations done for the measurements taken in Oslo, the size of the roofs was measured roughly by using Norgeskart (from www.norgeskart.no).In connection with the investigations made for the work done in Becker (2015), the number of downspouts was registered for each house. Assuming that the roof area is equally distributed to all of the downspouts, the area that each downspout is connected to can thus be calculated. The size of the infiltration area is dependent on the size of the garden, the distance from the downspout to the neighbor or to the street etc. The infiltration area for each garden was approximated by using pictures and maps of the area, and can therefore be somewhat inaccurate. Table 6.8 summarizes the areas used for further calculations done for Oslo.

The procedure to find the infiltration area and the roof area was slightly different for the locations in Trondheim. Since there were no roofs connected directly to the infiltration area, the adjoining street area was used to get an approximation of the area generating surface water connected to the infiltration area. The area of the adjoining streets, as well as the size of the infiltration area was measured at each site. Table 6.8 summarizes the areas used for calculations done for Trondheim.

Oslo				*Trondheim*		
Site	**Size of infiltration area**	**Roof area**	**Number of downspouts**	**Site**	**Size of infiltration area**	**Size of area generating surface water**
B20A	5	152	6	1	51 m^2	17m^2
B28AB	7	142	6	2	80m^2	64m^2
B30	5	85	3	3	94m^2	63m^2
B65	7	179	6	4	123m^2	47.5m^2
E14	7	251	4			
L34	7	127	4			
R5	10	64	4			

R29	4	129	4			
R44	7	104	3			
S10	10	74	4			
S75(a)	10	227	3			
S75(bcde)	10	227	3			

Table 6.8 Roof area, size of infiltration area and number of downspouts used in calculations for the different sites in Oslo and Trondheim.

6.6.7 Rainfall event

The rainfall events used for the computations are obtained from eklima.no, a web portal which gives free access to climate statistics measured at the different gauging stages in Norway. The rainfall event used for the computations done for Oslo was measured at Blindern gauging station in Oslo on 05. august 2015, and is presented in figure 6.6. The rainfall event used for the calculations done for Trondheim was measured at Risvollan gauging station in Trondheim on 27. august 2015, and is presented in figure 6.7. Both the rain event measured in Oslo and Trondheim are quite heavy, and will therefore most likely show the maximum capacity of the infiltration areas. The established MATLAB-script requires a constant rainfall, and the rainfall event was therefore divided into intervals of five minutes each. Each interval shows the average amount of rain falling during the interval of five minutes.

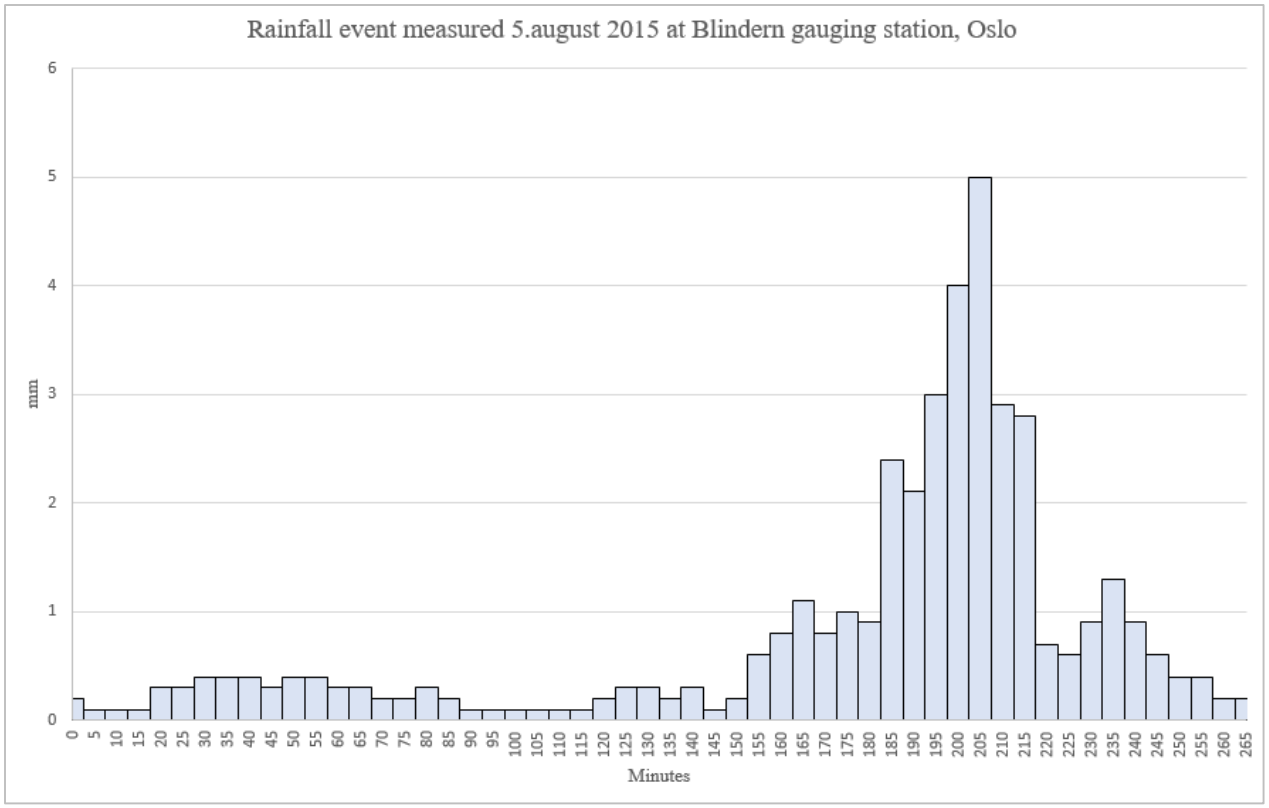

Figure 6.6 Rainfall event measured 5. august 2015 at Blindern gauging station in Oslo.

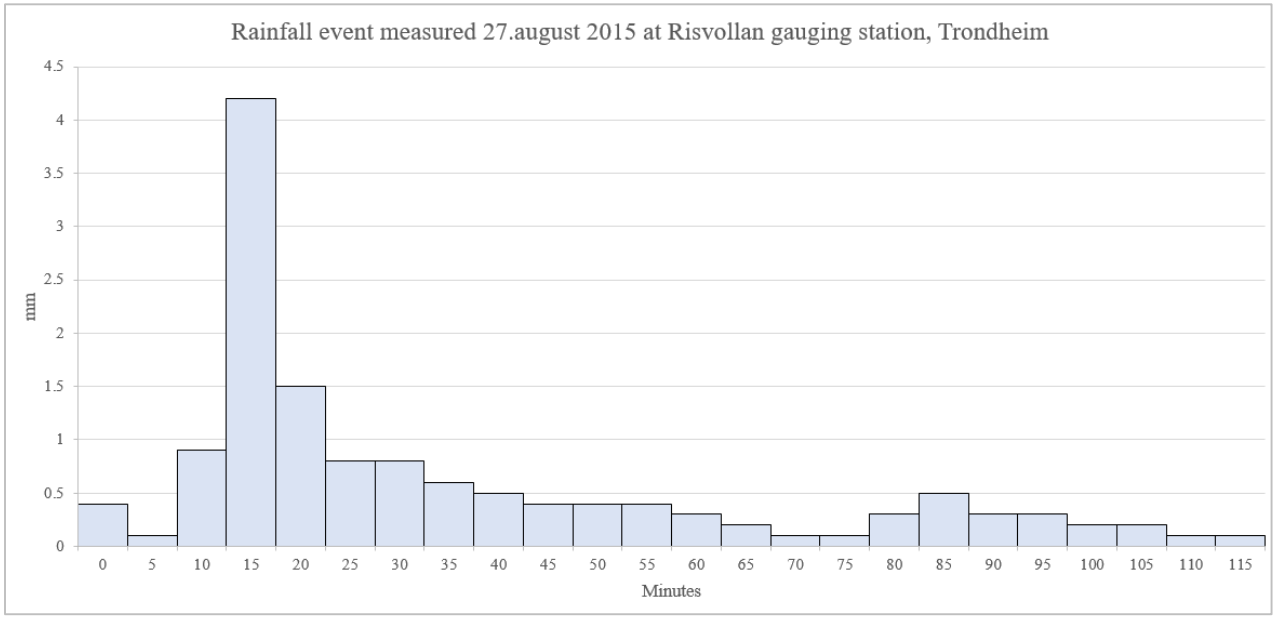

Figure 6.7 Rainfall event measured 27. August 2015 at Risvollan gauging station in Trondheim.

7. Results and discussion

In this section a series of results from different simulations will be presented and discussed in order to show how the model computes the amount of infiltrated water and the amount of generated runoff, and to be able to see how some of the different parameters affects the results. The model has been calibrated by using input parameters based on field data, but since there is no field data available about measured infiltration, the model cannot be verified. The discussion will therefore not include whether the results corresponds with reality, but will be a discussion of the results obtained with the different simulations. In order to see how specific parameters will affect the amount of infiltration, only one parameter at the time has been changed in the different simulations. Finally, the disadvantages and advantages of the established MATLAB- model will be discussed as well as downspout disconnection as a measure for managing stormwater.

7.1 Amount of infiltrated water and amount of generated runoff

The amount of infiltration and runoff generated during the simulated rainfall was computed for each of the eleven sites in Oslo and the four sites in Trondheim, with both using the Green-Ampt infiltration model and Philip infiltration model. Each site had its own set of input parameter values obtained from field investigations and computations as described in section x, which was used for the calculation of infiltration and runoff generated at each site. A table summarizing the used input parameter values at each site can be seen in Appendix 2. The simulations conducted with these input parameter values can be seen as a reference simulation, and forms the foundation of the discussion in this thesis. To be able to see how the different input parameters affects the computed amount of infiltrated water and the amount of generated runoff at each site, it was conducted simulations where some of the input parameters were changed, and the results was then compared with the results obtained with the reference simulation.

Since both the size of the roof area and the size of the available infiltration area varies from site to site, the adjusted rainfall intensity used in the calculations will also vary from site to site, and the amount of water desired infiltrated on each site is thus not equally. However, to easier be able to compare the different sites, the percentage amount of water infiltrating and the amount of generated runoff was calculated for each site. This was done by exporting the m-table (se section 6.4) generated for each calculation to excel. A file containing all of the generated m-tables can be found in the electronic Appendix. The m-table representing the calculations for each site was then used

to sum up the amount of infiltrated water and the amount of generated runoff during the rainfall event. Table 7.1 summarizes the computed values for each site both in Oslo and Trondheim, by both using the Green- Ampt infiltration model and the Philip infiltration model. To be able to compere the amount of infiltrated water and the amount of generated runoff at sites characterized with the same soil type, the soil texture at each site was also included in the table.

		Green-Ampt model		*Philip model*	
Site	**Soil texture**	**Infiltration %**	**Runoff %**	**Infiltration %**	**Runoff %**
Oslo					
B20A	Loam	78.92	21.08	62.83	37.17
B28AB	Silt clay loam	98.59	1.41	92.41	7.59
B30	Sandy loam	70.61	29.39	54.69	45.31
B65	Loam	92.27	7.73	75.86	24.14
E14	Loam	70.76	29.24	56.04	43.96
L34	Sandy loam	100.00	0.00	83.79	16.21
R5	Loam	90.21	9.79	76.99	23.01
R29	Sandy loam	76.41	23.59	57.29	42.71
R44	Loamy sand	100.00	0.00	88.31	11.69
S10	Loam	61.31	38.69	50.31	49.69
S75(a)	Sandy loam	93.46	6.54	67.55	32.45
S75(bcde)	Loam	83.48	16.52	72.57	27.43
Trondheim					
1	Loamy sand	100.00	0.00	100.00	0.00
2	Loamy sand	100.00	0.00	100.00	0.00
2	Sandy loam	100.00	0.00	100.00	0.00
3	Sandy loam	100.00	0.00	100.00	0.00
3	Loamy sand	100.00	0.00	100.00	0.00
4	Loamy sand	100.00	0.00	100.00	0.00

Table 7.1 The amount of infiltrated water and the amount of generated runoff for each site by using both Green-Ampt model and Philip model. The table shows the results obtained for the reference simulation.

The numbers in this table are percentage infiltration and runoff, based on the amount of water desired to infiltrate at each site. This amount of water is not equal for each site because of the differences in the ratio between the size of the roof area and the size of the infiltration area. Therefore, the amount of infiltrated water and the amount of generated runoff at each site cannot be compared directly.

The sites in Oslo where therefore divided into four groups according to the ratio between the size of the roof area and the size of the infiltration area at each site. Group one includes site R5 and S10, which has the smallest differences between the size of the roof area and the infiltration area. in this group the roof area is between 1.5-2 times greater than the corresponding infiltration area. In group two, the roof area is between 3.3-4.5 times greater than the corresponding infiltration area, and includes site B28, B65 and L34. Group three includes site B20, B30 and R44, where the ratio between the roof area and the infiltration area differs from 5-5.6. The last group, group four, includes the sites with the biggest difference in ratio between the roof area and the infiltration area. In this group site E14, R29 and S75 are found, where the roof area is between 7.5- 9 times greater than the corresponding infiltration area. When studying the sites in these four different groups, it is seen that even when the amount of desired infiltrated water is approximately equal, the amount of infiltrated water and the amount of generated runoff varies widely between the different sites in each group. The process of infiltration is complex and is dependent on many different factors, as will be shown in later sections. Therefore, even when two sites have the same amount of water to be infiltrated, the amount of infiltrated water and the amount of generated runoff will not necessarily be equal.

However, the results summarized in table 7.1, shows that the amount of infiltrated water compared to the amount of generated water at each site is quite high, both for the measurements done in Oslo and Trondheim. In Oslo the amount of infiltrated water relative to the amount of water desired to be infiltrated at each site varies from 69% to 100% by using the Green-Ampt model, and from 50% to 88% by using the Philip model. The differences in the results obtained by using the two different infiltration models will be discussed in a later section.

To discuss some examples, site R44 and S10 can be highlighted. Site R44 is the place with the highest amount of infiltrated water relative to the amount of water desired to be infiltrated at this site, while S10 has the lowest amount of infiltrated water relative to the amount of water desired to be infiltrated. Figure 7.1 and 7.2 shows the amount of infiltration and runoff for both of these sites, using both Green-Ampt model and Philip model. The red line represents the amount of generated runoff during the simulated rainfall, while the green line represents the amount of infiltrated water. The y-axis is the amount of water with the unit cm/h, and the x-axis shows the duration of the rainfall event.

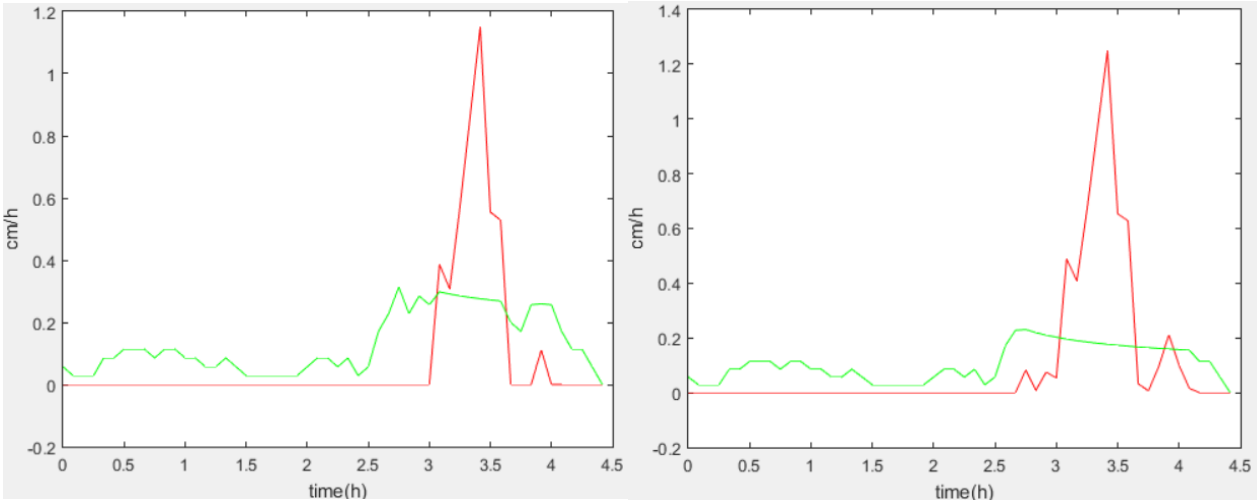

Figure 7.1 Shows the graph obtained for site S10. The red line represents the amount of generated runoff, while the green line represents the amount of infiltrated water. The graph to the left shows the result obtained by using the Green-Ampt model, while the graph to the right shows the result obtained by using the Philip model. The x-axis shows the duration of the rainfall and the y-axis shows the amount of water in cm/h.

Site S10 is the place with the lowest amount of infiltrated water relative to the amount of water desired to be infiltrated. The ratio between the roof area and the size of the infiltration area at this site, is 1.85 meaning that the roof is approximately twice as big as the available infiltration area. Although S10 has one of the lowest ratio between the roof area and the infiltration area, and thus better conditions for handling the amount of water to be infiltrated, it still has the lowest amount of infiltrated water. The reason for this is most probably found in the soil type at the site and its ability to infiltrate water. The soil at S10 was characterized as loam and has the lowest measured average K_{sat}-value of 2.46 cm/h. As discussed later, the soils saturated hydraulic conductivity has a great effect on the soils infiltration capacity, because this number describes the soil ability to move water through the soil layer. With a saturated hydraulic conductivity of 2.46 cm/h, the water will move slowly through the soil layer, which will create ponding on the top of the soil layer and resulting in generation of runoff.

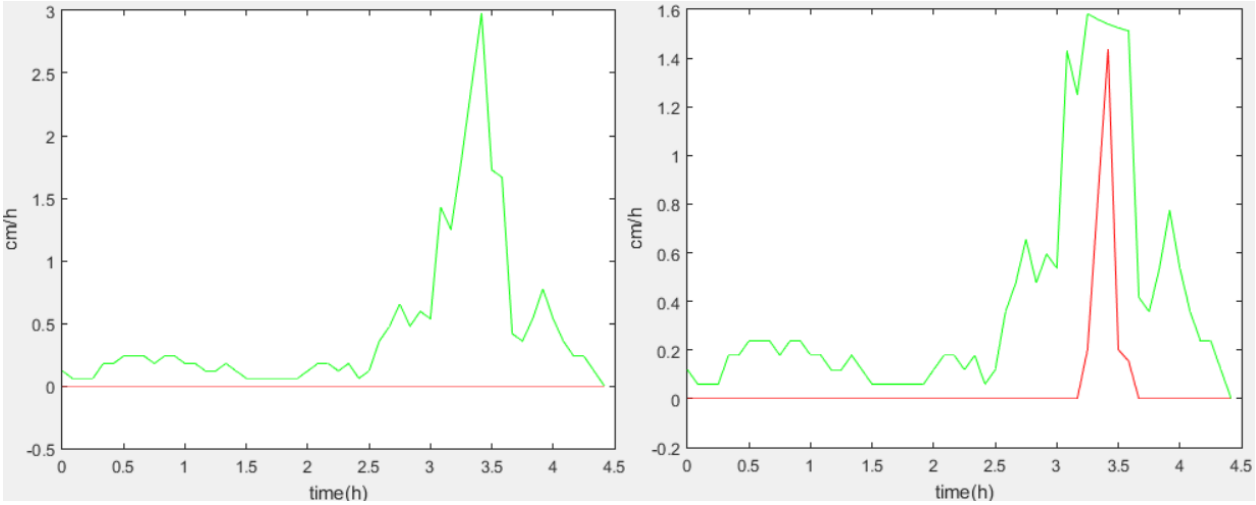

Figure 7.2 Shows the graph obtained for site R44. The red line represents the amount of generated runoff, while the green line represents the amount of infiltrated water. The graph to the left shows the result obtained by using the Green-Ampt model, while the graph to the right shows the result obtained by using the Philip model. The x-axis shows the duration of the rainfall and the y-axis shows the amount of water in cm/h.

On the contrary, there is site R44, which is the site with the highest amount of infiltration relative to the amount of generated water desired to be infiltrated at this site. This site has a rather high ratio between the size of the roof area and the size of the available infiltration area. The roof at this site is five times greater than the corresponding infiltration area, but the soil still manages to infiltrate 100 % using the Green-Ampt model and 88% using the Philip model, of the water generated from the roof. This is, again, most probably due to the soil type at the site, and its ability to infiltrate water. The soil at site R44 was characterized as sandy loam, and the average measured K_{sat}- value was computed to be 46 cm/h, which is the highest value used of all of the other sites.

Unlike in Oslo, where all of the roof areas was greater than the corresponding infiltration areas, the infiltration areas in Trondheim was bigger than the corresponding areas generating surface water. The soil at the different sites in Trondheim was either characterized as Loamy sand with a Ksat-value equal to 15.11 cm/h, or as sandy loam with a K_{sat}- value equal to 46.2 cm/h. Meaning that all of the sites investigated in Trondheim had good conditions for infiltration, which is also shown by the results from the calculations done. In the reference simulation all of the sites had an infiltration of 100% using both the Green-Ampt model and the Philip model. However, the established MATLAB- model does not say anything about how close it was before runoff would be generated,

but as sown later, there is no significant change in the amount of infiltration when changing the input parameters. This indicates that the capacity of the four sites in Trondheim has not been reached, and that these areas therefore probably will be able to withstand even larger areas generating surface water, than those used in these calculations.

Appendix 3 shows the generated graphs for all of the sites both in Oslo and Trondheim, for both Green-Ampt and Philip infiltration model. For the sites in Oslo it can be seen that the amount of generated runoff varies, but the generating of runoff occurs almost at the same time for all sites. The reason for this has most likely a connection to the shape of the hydrograph given in figure 6.7, and the change of infiltration capacity over time. The infiltration capacity decreases over time, and will reach a minimum constant value after some time, due to its dependence on the cumulative infiltration depth, F. At the beginning of the rainfall, the initial cumulative infiltration height is set to zero resulting in an infinity high infiltration capacity. During the rainfall, the cumulative infiltration depth increases due to the increased amount of infiltrated water. When studying equation 6.3, we see that with an increased cumulative infiltration depth the infiltration capacity decreases. As F increases, the term P/F approaches zero, because P is a constant, meaning that the infiltration capacity reaches a constant minimum value approximately equal to the saturated hydraulic conductivity. Figure 7.3 shows an example of the development of the infiltration capacity over time. The y-axis shows the infiltration capacity with the unit cm/h, while the x-axis shows the duration of the rainfall in hours. The rainfall event used for the calculations in Oslo has a duration of 4.5 h, and the heaviest part of the rainfall happens at the end of the event. The rain falling during the first two hours is infiltrated, but the rainfall from 2.5 to 4 hours generates runoff at most of the sites. At the beginning the infiltration capacity of the soil is at the highest, but as water continues to infiltrate and the soil gets more and more saturated, the infiltration capacity decreases. The soils infiltration capacity decreases rapidly the first time of the rainfall event, and as the graphs in appendix 3 and figure 7.3 shows, the infiltration capacity at 2.5 h has reached its constant value. Meaning that the heaviest part of the rainfall event occurs when the infiltration capacity has reached its constant minimum value.

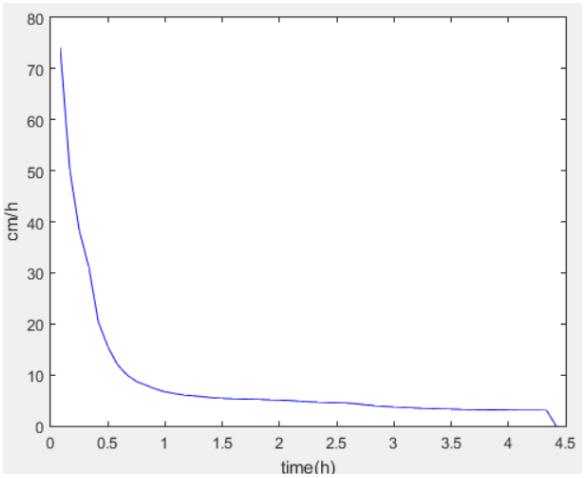

Figure 7.3 Shows an example of the development of the infiltration capacity over time. This graph is obtained for site S10 by using the Green-Ampt model.

7.2 Differences between Green-Ampt infiltration model and Philip infiltration model

Green-Ampt model and Philip model are two of the most popular infiltration models used for describing the process of infiltration, in hydrology. These two models are based on different assumptions for describing the change of infiltration capacity over time, but fundamentally there is no significant advantage to use one rather than the other one (Tarboton, 2003). However, when beginning working with this thesis, it was decided that the process of infiltration would be modeled by using both the Green-Ampt model and Philip model. This was done to investigate whether there would be significant differences in the results, depending on which infiltration model is chosen. Because of the lack of field data, the results cannot say something about how well the models correlate with the reality.

The amount of infiltrated water was calculated at each site by using both the Green-Ampt model and the Philip model, and the input parameters for each site was the same for both models. The calculated values are summarized in table 7.1, and in figure 7.1 and 7.2 show examples of the differences in results obtained by using the Green-Ampt model and Philip model can be seen. Table 7.1 shows that dependent on the site Green-Ampt infiltrates between approximately 6 % and 26 % more of the water than the Philip model with an average of approximately 14% more than the Philip model.

The calculations done in Trondheim shows no differences between the Green-Ampt model and the Philip-model. This is probably due to the fact that the infiltration rate at the sites are significantly smaller than the infiltration capacity at each time step. These values can therefore not be used to investigate the difference between the Green-Ampt model and the Philip model.

The reason behind the differences is most probably due to the different approximations done for describing the process of infiltration, resulting in that the models are based on different equations describing cumulative infiltration and thus the infiltration capacity (for formulas see section 5). In both models the infiltration capacity is calculated based on, among other, the measured saturated hydraulic conductivity. As will be seen in section 7.4, has the saturated hydraulic conductivity a great impact on the infiltration process. Therefore, could one important reason for the differences in results obtained from the two different models be the choice of K_p parameter in the Philip model. According to Rawls et al. (1992), the K_p parameter varies between $2/3K_{sat}$ and $1/3k_{sat}$. In this thesis the value $1/3K_{sat}$ was chosen for the K_p parameter, which gives a rather low value. It could be that another value for K_p would give a better correlation between the two different infiltration models.

The choice of which model to use is often dependent on personal preference and experience, and can be based on which one the different parameters can be obtained for, or which one gives the best fit to measured field data. In this thesis there cannot be drawn any conclusion whether one model correlates better with the reality or not, because of the lack of field data for verifying the MATLAB model. However, based on the results obtained in this thesis it appears that the Philip model calculates a lower amount of infiltrated water than the Green-Ampt model. For now, until the models have been verified, it may be safer to use the Philip model. This should though be further investigated as described in concluding remarks.

7.3 The impact of change in soil moisture content

The soil moisture content has a great impact on the infiltration capacity of the soil (Pitt et al., 2002). Table 6.7 shows that the measured initial soil moisture content varies from site to site, which is probably due to the different soil types. Clay, for example, has a greater ability to retain water than sand (Nyborg and Olsen, 2014). The soil samples taken in Oslo, was taken under a period with little precipitation. Both during the conduction of the infiltration test and the days before, the amount of precipitation was low. The maximum measured air temperature these days was in average 20°C, which may cause evaporation from the soil. These conditions indicate that the soil

was not saturated before starting the infiltration test, and thus the condition for infiltrating was good. In Trondheim the situation was slightly different. The soil samples taken in Trondheim was taken later that year, when the temperature was lower, resulting in a lower amount of evaporation. Additionally, it had rained all week before conducting the infiltration test. The small difference between the measured soil moisture content of the soil taken before and after the conduction of the infiltration test, indicates that the soil most probably already was quite saturated during the infiltration test. To be able to see how much the initial moisture content affects the results, it was decided to conduct simulations with saturated and unsaturated soil. In the calculations simulating an unsaturated soil, the field capacity, θ_{fc} was used as initial soil moisture content. θ_{fc} was chosen because it represents the amount of water in the soil that can be held against the force of gravity, and was calculated using equation 4.10. In the calculations simulating a saturated soil, the initial soil moisture content was set equal to the porosity, meaning that the pores are filled with water. Table 7.2 summarizes the different values used in the calculations.

The simulations and calculations of the amount of infiltration and runoff are quite time consuming, and the impact of change in initial soil moisture content has therefore only been computed for some of the sites. One site representing each soil type was picked randomly at each location. Table 7.2 shows the values used for the calculations done with the different initial soil moisture contents.

Site	θ_{fc}	θ_i	θ_i=n
Oslo			
B28AB	0.29	0.33	0.45
B65	0.20	0.31	0.40
L34	0.09	0.31	0.34
R44	0.08	0.30	0.32
S10	0.18	0.32	0.40
Trondheim			
Site 1	0.09	0.22	0.32
Site 3 SL	0.12	0.3	0.34

Table 7.2 The different values used for the calculations done with the different soil moisture contents, and the sites which the computations were conducted for.

To be able to compare the results obtained with the reference simulation, with the results obtained when changing the initial soil moisture content, all of the other input parameters were kept fixed, and only the initial soil moisture content was changed for each simulation. Table 7.3 summarizes

the computed amount of infiltration and generated runoff for all of the investigated sites, with both using Green-Ampt model and Philip model.

	Infiltration with $\theta_i=\theta_{fc}$		**Infiltration with $\theta_i=\theta_i$**		**Infiltration with θ_i=n**	
Site	**Infiltration [%]**	**Runoff [%]**	**Infiltration [%]**	**Runoff [%]**	**Infiltration [%]**	**Runoff [%]**
Green-Ampt infiltration model						
B28	99.74	0.26	98.59	1.41	92.05	7.95
B65	95.49	4.51	92.27	7.73	85.99	14.01
L34	100.00	0.00	100.00	0.00	100.00	0.00
R44	100.00	0.00	100.00	0.00	100.00	0.00
S10	69.13	30.87	61.31	38.69	52.97	47.03
Site 1	100.00	0.00	100.00	0.00	100.00	0.00
Site 3 SL	100.00	0.00	100.00	0.00	100.00	0.00
Philip infiltration model						
B28	95.69	4.31	92.41	7.59	63.28	36.72
B65	85.41	14.59	75.86	24.14	57.95	42.05
L34	95.84	4.16	83.79	16.21	76.92	23.08
R44	98.14	1.86	88.31	11.69	83.56	16.44
S10	62.30	37.70	50.31	49.69	30.66	69.34
Site 1	100.00	0.00	100.00	0.00	99.12	0.88
Site 3 SL	100.00	0.00	100.00	0.00	100.00	0.00

Table 7.3 The results obtained for the investigated sites for all of the different values of initial soil moisture content used in the simulations. The table is showing the results by using both the Green-Ampt model and the Philip model.

The results show that the amount of infiltrated water decreases with increasing soil moisture content. For example, the amount of infiltrated water decreases, calculated with the Green-Ampt model, at site S10 with 16.2 %, when the soil moisture content increases from 0.18 to 0.4 (from unsaturated soil to saturated soil). The results, computed for Oslo, also show that the values obtained when using the measured initial moisture content are closer to the results obtained when using an initial soil moisture content equal to the field capacity, then compared with the results obtained when using an initial moisture content equal to the porosity. This supports the theory that the soil was quite unsaturated, most of the places, when conducting the measurements of the saturated hydraulic conductivity.

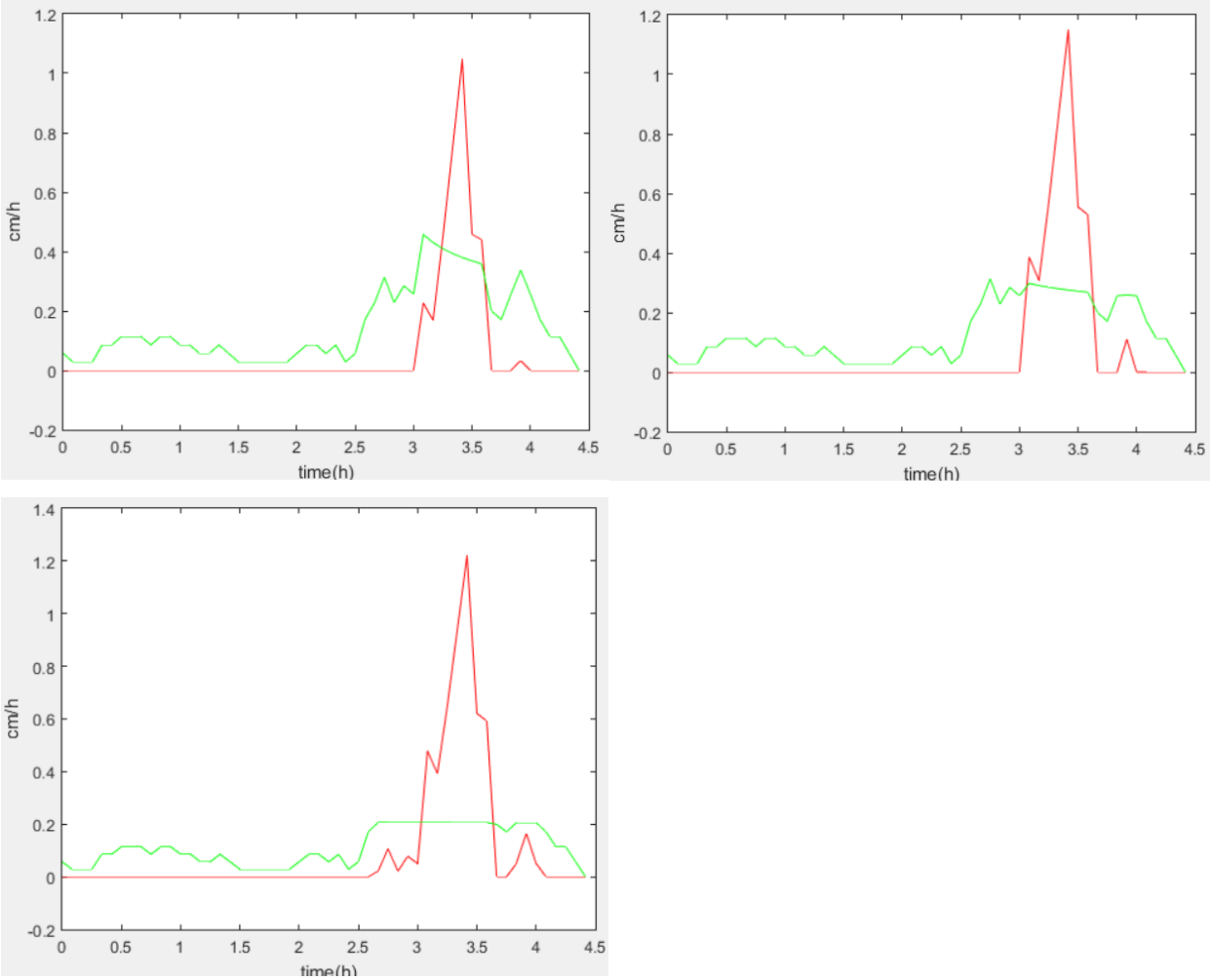

Figure 7.4 Shows the differences in result when using different initial soil moisture content. The graph to the upper left shows the result when the initial soil moisture content is equal to the field capacity. The graph to the upper right shows the result for the reference simulation (with the measured initial soil moisture content), and the last graph shows the result with an initial soil moisture content equal to the porosity. All of the three situations are calculated for site S10 by using the Green-Amp model. The red line represents the amount of generated runoff, while the green line represents the amount of infiltrated water.

When looking at the calculated percent-values obtained by using the Green-Ampt model, it seems that there is no change in the amount of infiltrated water at site L34 and R44 in Oslo, and site 1 and 3 in Trondheim, when changing the initial soil moisture content. Due to the high K_{sat}-value at site L34 and R44, and due to the big infiltration area at site 1 and 3, it seems that the soil still is capable to infiltrate the water even if it is nearly saturated. On the contrary, when studying the obtained

graphs showing the infiltration capacity, the effect of changing the initial soil moisture content can be seen.

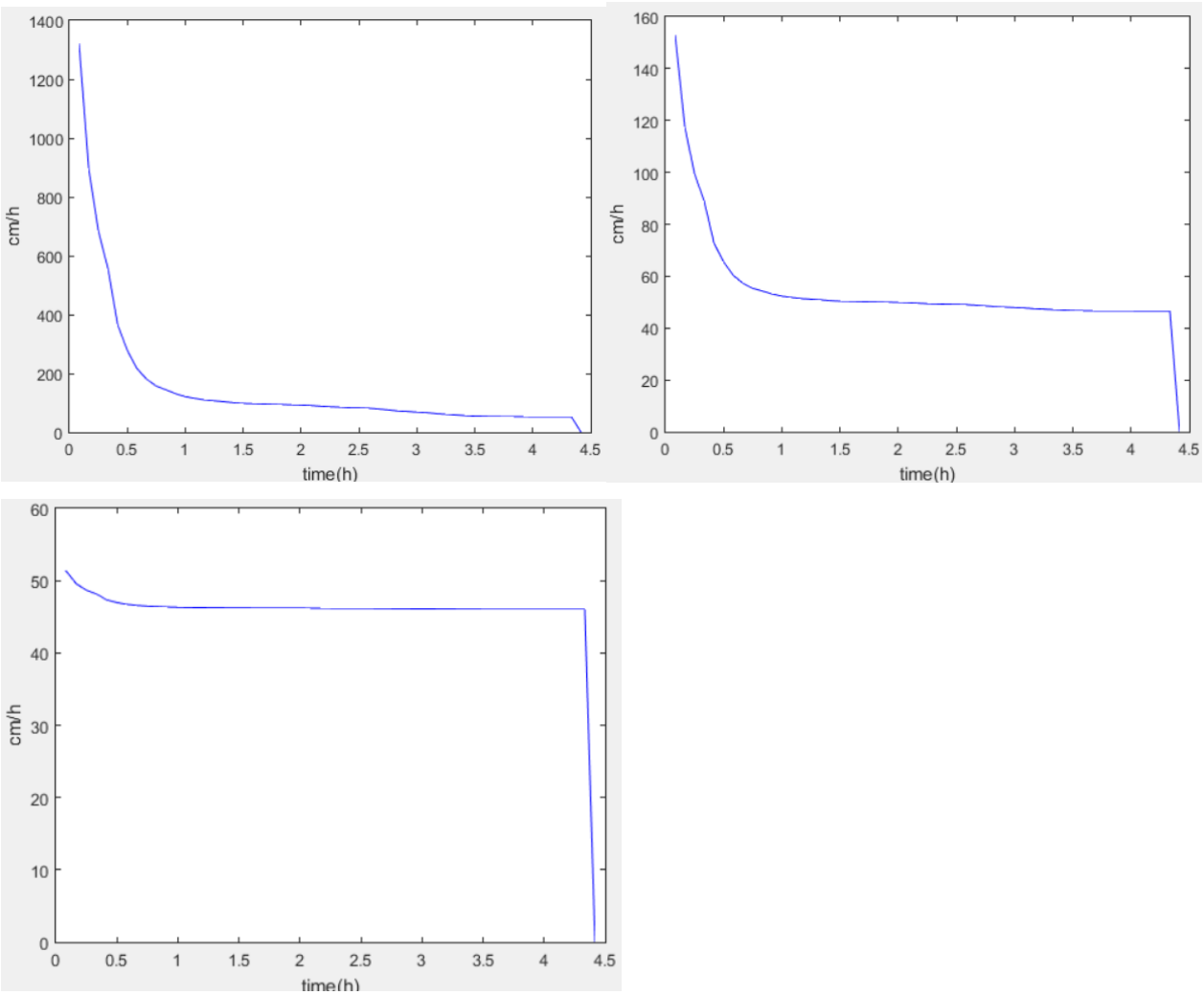

Figure 7.5 Shows the differences in initial infiltration capacity when using different initial soil moisture content. The graph to the upper left shows the result when the initial soil moisture content is equal to the field capacity. The graph to the upper right shows the result for the reference simulation (with the measured initial soil moisture content), and the last graph shows the development of the infiltration capacity with an initial soil moisture content equal to the porosity. All of the three situations are calculated for site R44 by using the Green-Amp model.

Figure 7.5 shows the calculated infiltration capacity graphs obtained for site R44 by using the Green-Ampt model. The y-axis represents the infiltration capacity with the unit cm/h, and the x-axis represents the time duration of the rainfall event. The graph to the left shows the development of the infiltration capacity over time for the unsaturated soil, and the graph to the right shows the

development of the infiltration capacity over time for the saturated soil. The graph in the middle shows the development of the infiltration capacity over time for the calculation done with the initial soil moisture content equal to the value measured in the field. When studying the graphs in figure 7.5, it is seen that the development of the infiltration capacity curve and particularly the initial infiltration capacity is affected by the initial soil moisture content. As the soil approaches saturation, the P parameter decreases, meaning that the term P/F approaches zero and the initial infiltration capacity is approximately equal to the soils saturated hydraulic conductivity. This is also seen in figure 7.5, with an increased soil moisture content, the initial infiltration capacity decreases, and for a saturated soil the initial infiltration capacity is almost equal to the constant minimum value. When the soil is unsaturated it has an initial infiltration capacity equal to 1322 cm/h, while decreasing as the initial soil moisture content is changed closer to a saturated soil. For the reference simulation, the initial infiltration capacity is equal to 153cm/h, while for the saturated soil the initial infiltration capacity has decreased to a value equal to 51 cm/h. In this specific case, the soil is still able to infiltrate all of the desired amount of water, using the Green-Ampt model, even if the soil is saturated. This is most probably due to the soil texture and the high K_{sat}- value measured at the site. In general, a reduction of infiltration capacity will increase the risk of ponding and result in more generated runoff.

According to the calculation where the initial soil moisture content was changed, it is suggested that the Philip model is more dependent on the initial soil moisture content than the Green-Ampt model. When comparing the results obtained when computing with an initial soil moisture content equal to the porosity, meaning that the soil is saturated, with the results obtained when computing with an initial soil moisture content equal to the moisture content measured in the field, it seems that the differences are grater for the Philip model than for the Green-Ampt model. This can easily be explained when looking at the equations used for calculating the infiltration capacity. In the Philip model, the initial soil moisture content is used to calculate the sorptivity of the soil. When setting θ_i equal to the porosity, n, the sorptivity gets approximately equal to zero (see equation 6.4.2). A sorptivity equal to zero will result in an infiltration capacity, fc, approximately equal to K_p (see equation 6.12), which in this thesis is set to $1/3K_{sat}$. The same is also happening for the Green-Ampt model. When setting θ_i equal to the porosity, the P parameter in equation 6.3 gets approximately equal to zero, resulting in an infiltration capacity equal to K_{sat}. Because K_p is equal to $1/3K_{sat}$, the Green-Ampt model is using a three times higher K_{sat} value than the Philip model,

resulting in a higher computed amount of infiltrated water compared to using the Green-Ampt model.

In the MATLAB- code for the established model in this thesis, there is added a function calculating an average soil moisture content based on the amount of rain days during the year. This function is only meant to be used if the soil moisture content was not measured in the field (see section 6.6.5). Based on the discussion above, it is suggested that if it is possible the initial soil moisture content should be measured in the field, and not be calculated with this function or be estimated in other ways. Because of its great impact on the computation of the amount of infiltrated water, the used value for the initial soil moisture content should be as close to the reality as possible in order to be able to get reliable results.

7.4 The impact of change in saturated hydraulic conductivity

The saturated hydraulic conductivity is a measure of the soils ability to lead the water through the soil layers, and depends on the soils permeability and the viscosity of the water. This parameter is therefore of great important when investigating the soils infiltration capacity. The measurements of K_{sat} for each site, done in Becker (2015), showed a great variation in measured K_{sat}- value form both site to site, but also from column to column at same site. In the reference simulation the average value computed for each site, was used in Oslo, and the computed median value for each site was used in Trondheim. Because of the great variation in measured K_{sat} value, some of the sites was simulated using different K_{sat}-values, to illustrate how K_{sat} affects the results. The sites chosen for this simulation are sites with great variation in measured K_{sat}-value, and the simulations were done by using the lowest measured value and the highest measured value at each site. The simulations were done using both the Green-Ampt model and the Philip model. Table 7.4 shows the sites chosen for this simulation and the different K_{sat}- values used in the calculations. R5 and R44 are sites in Oslo, while site 3 is in Trondheim.

Site	K_{sat} min	Average/median K_{sat}	K_{sat} max
R5	0.059	6.34	20.021
R44	12.939	46.00	88.82
Site 3 sandy loam	3.188	46.20	-
Site 3 loamy sand	3.188	15.11	-

Table 7.4 The different sites used in the simulation and the different K_{sat}-values used in the different calculations.

To be able to compare the results from the reference simulation, with the results obtained when changing the saturated hydraulic conductivity, all of the other input parameters were kept fixed, and only the K_{sat}-value was changed for each simulation. Table 7.5 summarizes the computed amount of infiltration and the amount of generated runoff, for all of the investigated sites, with both using Green-Ampt model and Philip model.

	K_{sat} min.		Average/median K_{sat}		K_{sat} max.	
Site	**Infiltration [%]**	**Runoff [%]**	**Infiltration [%]**	**Runoff [%]**	**Infiltration [%]**	**Runoff [%]**
Green-Ampt infiltration model						
R5	11.28	88.72	90.21	9.79	100.00	0.00
R44	77.30	22.70	100.00	0.00	100.00	0.00
Site 3 SL	98.28	1.72	100.00	0.00	-	-
Site 3 LS	100.00	0.00	100.00	0.00	-	-
Philip infiltration model						
R5	10.45	89.55	76.99	23.01	99.73	0.27
R44	54.92	45.08	88.31	11.69	99.85	0.15
Site 3 SL	95.20	4.80	100.00	0.00	-	-
Site 3 LS	99.74	0.26	100.00	0.00	-	-

Table 7.5 Results for the different sites obtained by changing the K_{sat}- value, for both Green-Amp model and Philip model.

The results show that the amount of infiltrated water decreases with decreasing K_{sat}- value, which is logical by the definition of saturated hydraulic conductivity. By decreasing the K_{sat}- value from 6.3 cm/h to 0.06 cm/h, and using the Green-Ampt model, the amount of infiltrated water decreased from 90% to 11% at site R5. On the other hand, when increasing the K_{sat}-value from 6.3 cm/h to 20.0 cm/h, the amount of infiltrated water at site R5 increases from 90% to 100%. Site 3 with sandy loam in Trondheim has a high capacity for infiltration, and the amount of infiltrated water was not

reduced when changing the initial soil moisture content, but as we can see does the change in K_{sat}-value change the result. By decreasing the K_{sat}- value to 3.188 cm/h the amount of infiltrated water at site 3 wit sandy loam decreases to 98% using the Green-Ampt model and to 95% using the Philip model. The change in the amount of infiltrated water is not large compared to the change in the K_{sat}- value, but is still shows the effect of change in K_{sat}-value. It is also suggested that the amount of infiltrated water is more dependent on the soils saturated hydraulic conductivity, than the soils initial moisture content.

When studying the equations used for computing the infiltration capacity, for both the Green-Ampt model and the Philip model, it can be seen that the infiltration capacity is highly dependent on the soils saturated hydraulic conductivity. A decrease in saturated hydraulic conductivity will result in a reduction of the infiltration capacity, see equation 6.3 and 6.12. This is also clearly shown when comparing the obtained fc-graphs for the different situations.

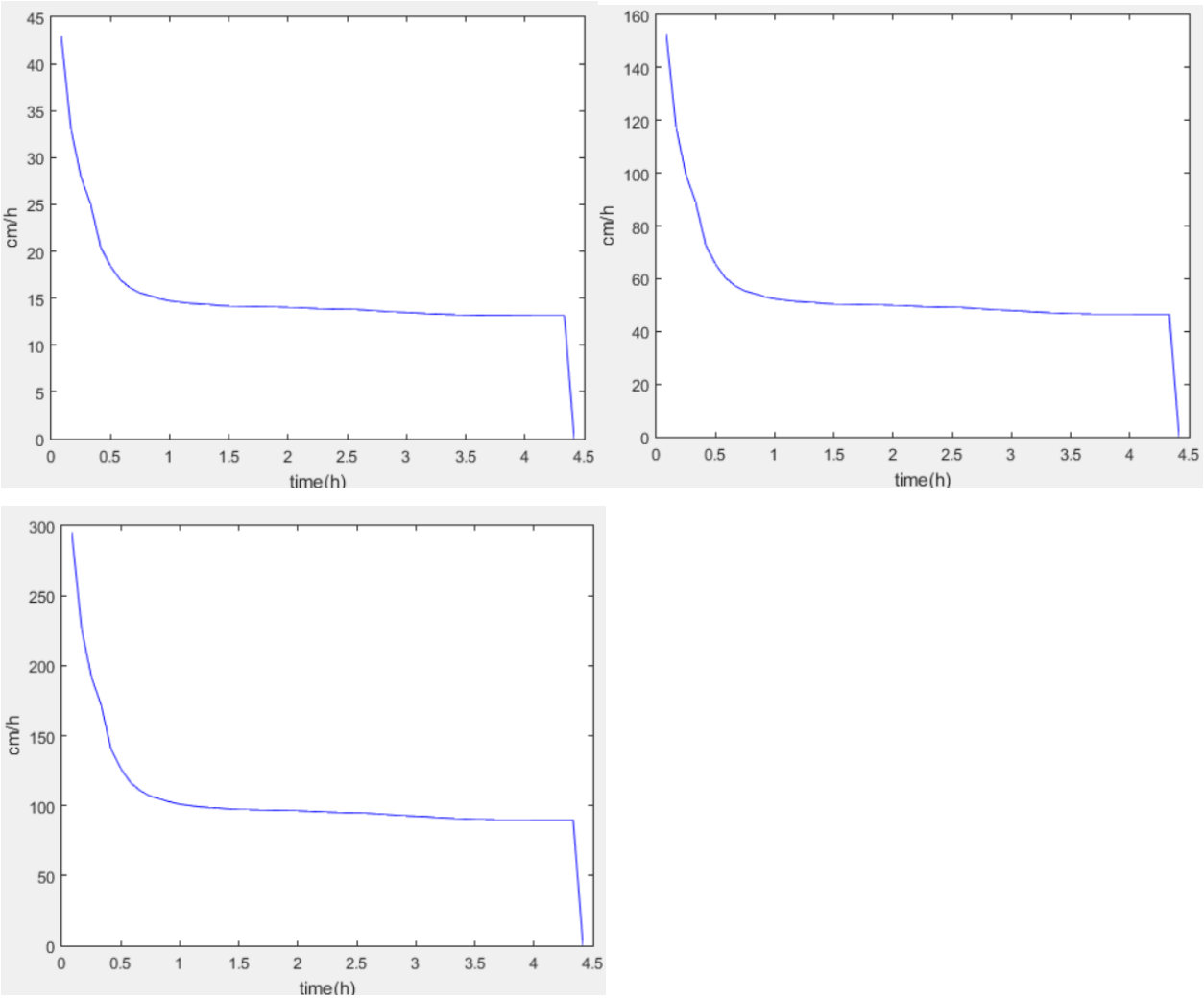

Figure 7.6 Differences in the infiltration capacity when changing the K_{sat}- values. The y-axis represents the infiltration capacity with the unit cm/h, and the x-axis represents the time duration of the rainfall event. The graph to the left shows the development of the infiltration capacity over time for K_{sat} equal to 12.94 cm/h, and the graph to the right shows the development of the infiltration capacity over time for K_{sat} equal to 88.82 cm/h. The graph in the middle shows the development of the infiltration capacity over time obtained with the reference simulation, meaning a K_{sat} equal to 46cm/h.

Figure 7.6 shows the calculated infiltration capacity graphs obtained for site R44 by using the Green-Ampt model. The y-axis represents the infiltration capacity with the unit cm/h, and the x-axis represents the time duration of the rainfall event. The graph to the left shows the development of the infiltration capacity over time for K_{sat} equal to 12.94 cm/h, and the graph to the right shows the development of the infiltration capacity over time for K_{sat} equal to 88.82 cm/h. The graph in the middle shows the development of the infiltration capacity over time obtained with the reference

simulation, meaning a K_{sat} equal to 46cm/h. When studying the results presented in table 7.5, there is no change in the amount of infiltrated water when changing the K_{sat}-value from 46cm/h to 88.82cm/h, when computing infiltration at site R44 using the Green-Ampt model. However, despite no change in the amount of infiltrated water, figure 7.6 shows that the infiltration capacity changes when changing the saturated hydraulic conductivity. Both figure 7.6 and equation 6.3 shows that the infiltration capacity is proportional with the K_{sat}-value. Meaning that when the K_{sat}-value is reduced by a half, the infiltration capacity is also equally reduced. This proportionality yields also for the Philip model.

These simulations show the importance of measuring the saturated hydraulic conductivity of the soil at multiple places at each site to ensure a representative K_{sat}- value for the calculations. Both the minimum K_{sat}- value and the maximum K_{sat}-value used in these calculations are actual values measured at a point at the site. The reason for the great variation in measured K_{sat}-value is most probably the effect of urbanization. Parts of the garden can be more compact due to former construction work, or the soil in some parts of the garden has been replaced. Roots, stones and insect activity in the soil can also lead to great local variations in saturated hydraulic conductivity. One measurement at one point is therefore not necessarily representative for the entire site.

7.5 The effect of soil suction on the amount of infiltration

As described in section 4.1, the wetting front capillary suction head is dependent on the soil moisture content and the pore size distribution, resulting in affecting the soils ability to infiltrate water. When the pores in the soil is only partly filled with water, the water is attached to the particle surface by surface-tension forces. These forces can be described by capillary forces and result in the water drawing closely up around the particle surfaces into the dry soil, leaving a center filled with air in between the particles. Due to the capillary force it is created menisci between the particle surfaces. As the curvature of this menisci decreases, the tension increases, meaning that the tension, also called the suction head, increases as water content decreases (Chow et al., 1988). The relationship between the matric potential, or suction head, and the volumetric water content are shown with soil moisture characteristic curves as described in section 4.1, and shown in figure 4.1. The soil moisture characteristic curve has to be developed for each soil type, because the differences related to the effect of differences in pore size distribution among soils (Miyazaki et al., 1993). By defining pressure as force over area, the reason why the tension head is higher in soil

with small pores than soil with larger pores can be explained. Since the ratio between the pores perimeter and cross section area is not proportional, will a smaller pore sustain a larger surface tension force around the pore perimeter relatively to its cross section, than larger pores can sustain.

Because of its dependent on soil moisture content and pore size distribution, the soil suction affects also the hydraulic conductivity of the soil. As the soil suction increases the moisture content is reduced which results in the number of pores occupied by water decreases. This will again result in fewer flow paths for the water to move in, reduced cross section and are more tortuous, leading to a reduction of the hydraulic conductivity. The relationship between soil suction and hydraulic conductivity can be seen in figure 4.1. According to Miyazaki et al. (1993), these curves are sensitive to the change in bulk density and disturbance of soil structures.

The relationship between the soils pore distribution and the tension head are seen when comparing the soil types and their corresponding wetting front capillary pressure head. According to the discussion above, should the soils with small pores have a higher suction head than soils with larger pores, which is confirmed when studying the computed values used for wetting front capillary pressure head at each site. As we can see are the values decreasing with increasing pore size distribution. Site B28 which is characterized with a silt clay loam soil has a ψ_f equal to 49 while site R44 which is characterized as a loamy sand soil has a ψ_f equal to 14. Two of the sites which are characterized as sandy loam has a smaller ψ_f than the site with loamy sand. This deviation is probably due to the fact that the wetting front capillary pressure head, bubbling pressure and the particle size distribution index was not measured in the field, but calculated using equation 6.22, 6.24, and 6.25. Some of the sites had either a too low clay content or a too high sand content, that was adjusted in order to be able to use equation 6.24 and 6.25 for calculating the bubbling pressure and the pore size distribution index. This could also be a reason for the deviation.

The wetting front capillary pressure head will also affect the infiltration capacity. This is clearly revealed when studying the equations used for calculating the infiltration capacity for both Green-Ampt model and Philip model. The infiltration capacity increases with increasing wetting front capillary suction head. Site B28 has the highest value for ψ_f resulting in the highest initial infiltration capacity of 1050 cm/h, while site S75sl, with the lowest value for ψ_f, has an initial infiltration capacity of 337cm/h. However, it does not mean that the site with the highest ψ_f has the highest initial infiltration capacity. The infiltration capacity is also dependent on other factors like

the saturated hydraulic conductivity of the soil, the cumulative infiltration height and the ratio of porosity and initial soil moisture content, which is seen by studying the results. To illustrate this, site S75sl has as mentioned the lowest value for ψ_f, but simultaneously a relatively high K_{sat}-value, resulting in an initial infiltration capacity of 337cm/h, which is not the lowest value. Site L34, on the other hand, has the second lowest value for ψ_f and a K_{sat}- value equal to 15 cm/h, resulting in an initial infiltration capacity of 156cm/h. Site S10 does also stand out. This site has an average value for ψ_f, but the lowest measured K_{sat}-value of 2.46 cm/h, resulting in the lowest initial infiltration capacity of 74cm/h.

7.6 Impact of the ratio between the roof area and the infiltration area

The amount of water to be infiltrated is dependent on the size of the roof and the size of the infiltration area, incremental rainfall and the duration of the time interval. The rainfall intensity, w, is computed for each time step, by dividing the incremental rainfall by the length of the time step. In the calculations done for considering whether there will occur ponding or not during the time step, the rainfall intensity is used. Resulting in, among other, the ratio between the infiltration capacity, fc, and the rainfall intensity determines the amount of infiltrated water and the amount of runoff generated. Since the model established in this thesis considers both the amount of water falling onto the roof and the amount of water falling directly onto the infiltration area, the rainfall intensity used in the calculations has to be adjusted. The adjusted rainfall intensity, w', includes both the rainfall intensity from the roof, w_{roof}, and the rainfall intensity from the infiltration area, $w_{infiltration\ area}$. $W_{infiltration\ area}$ is easily computed by dividing the incremental rainfall by the duration of the time step, while the rainfall intensity from the roof is computed by first multiplying the rainfall intensity falling onto the roof with the area of the roof to compute the water volume generated from the roof. This water volume is then divided by the size of the infiltration area to obtain the rainfall intensity from the roof charging the infiltration area. The adjusted rainfall intensity can thus be described by the equation

$$w' = w_{roof} + w_{infiltration\ area} = \left(\frac{V_{water\ volume\ roof}}{A_{infiltration\ area}}\right) + w_{infiltration\ area} \qquad (7.1)$$

Where the water volume generated from the roof is computed by

$$V_{water\ volume\ roof} = \left(\frac{A_{roof}}{numbers\ of\ downspouts}\right) * w \qquad (7.2)$$

As we can see w' is highly dependent on the ratio between the water volume generated from the roof, which in turn is dependent on the size of the roof area, and the size of the infiltration area. If the generated water volume from the roof is significantly greater than the size of the infiltration area, the adjusted rainfall intensity gets high and there is a greater risk of ponding to occur. On the contrary, when the water volume generated from the roof is small, and the size of infiltration area is big, the adjusted rainfall intensity gets low and the risk of ponding decreases.

In the literature it is recommended that the infiltration area should be 1-2 times bigger than the roof area. Whether the water volume generated from the roof is infiltrated or not depends also on other factors like the soils saturated hydraulic conductivity and the degree of saturation, but the results show that the ratio between the area of the roof and the infiltration area affects the amount of infiltrated water and the amount of generated runoff. In Trondheim the size of the infiltration areas computed, are much greater than the corresponding roof area, and all of the water is infiltrated even when the K_{sat-} value was lowered to 3.188 cm/h.

To illustrate the effect of the ratio between the size of the roof area and the size of the infiltration area, the amount of infiltration was calculated at site R5 using different sizes of the infiltration area. The two last columns to the right, in table 7.6, are showing the percentage change in size of the infiltration area and percentage change in amount of infiltrated water compared to the reference simulation.

Size of the roof (m^2)	**Size of the infiltration area (m^2)**	**Infiltration %**	**Runoff %**	**%-change in size of infiltration area**	**%-change in amount of infiltrated water**
		Green-Ampt			
16	10	90.21	9.79	Reference simulation	
16	16	96.70	3.30	60%	6.49%
16	24	99.29	0.71	140%	9.08%
16	32	100.00	0.00	220%	9.79%
		Philip			
16	10	76.99	23.01	Reference simulation	
16	16	86.64	13.36	60%	9.65%

16	24	93.67	6.33	140%	16.68%
16	32	96.34	3.66	220%	19.35%

Table 7.6 The percentage change in size of the infiltration area and percentage change in amount of infiltrated water compared to the reference simulation. Both for Green-Ampt model and Philip model.

To be able to compere the different results, all of the other input parameters where kept fixed, and only the size of the infiltration area was changed. The simulation was done for three different sizes of the infiltration area; equal to the roof area, 1.5 times the roof area, and twice the size of the roof area, and was computed with both using the Green-Ampt model and the Philip model.

The results show that by increasing the infiltration area with 60% the amount of infiltrated water increases with 6.5 % using the Green-Ampt model and with 9.7% using the Philip model. The amount of infiltrated water continues to increase when increasing the infiltration area with 140% and 220%. By increasing the infiltration area to twice the size of the roof area, corresponding to an increase of 220%, the amount of infiltrated water increases with 9.8% using the Green-Ampt model and with 19.4% using the Philip model. These specific percentage changes in the amount of infiltrated water are only representative for site R5, but an increase in of the size of the infiltration area will result in an increase in the amount of infiltrated water also for the other sites. The percentage increase of infiltrated water will however be dependent on the soil type and the soils infiltration properties. When considering a site with a very sandy soil, it could be enough to have an infiltration area as big as the roof area. While when considering a site with a very high clay content, the infiltration area might be more than three times as large as the roof area in order to be able to infiltrate the entire amount of generated runoff.

7.7 Comparison of places with the same soil type

When comparing the sites characterized with the same soil type, it is seen that there are great variations in the amount of infiltrated water. One of the reasons for the great variations are probably the fact that the ratio between the size of the roof and the size of the infiltration area is not equal at each site, but the most decisive reason is most probably the differences in the values used for the different input parameters. Both the values describing the saturated hydraulic conductivity, initial soil moisture and wetting front capillary suction head has great variations in places with the same soil type. The amount of infiltrated water varies from 61% to 90% at the sites characterized as loamy soil, while the amount of infiltrated water varies from 70% to 100% at the sites characterized as sandy loam soil. By definition, the sandy loam should infiltrate more than the loam, which it to

some extent also does, but there is no clear distinction between the amount of infiltration into the two different soil types. This is most probably due to urbanization, and the effect of compaction of the soil. The consequence of urbanization and compaction can clearly be seen when studying the K_{sat}- values for each site characterized with the same soil type. Table 6.2 shows that, in Oslo, the K_{sat}-values measured in soil characterized as silt clay loam varies from 10.35cm/h to 19.10cm/h, for the soils with loamy soil K_{sat} varies from 0cm/h to 42.5cm/h, the K_{sat} values measured in sandy loam varies from 0.55cm/h to 46.04cm/h, and the K_{sat}- value measured in soil characterized as loamy sand varies from 12.94 cm/h to 88.82 cm/h. This shows that there is no clear distinction between the measured K_{sat}- values for the different soil types. Based on the soil properties the saturated hydraulic conductivity should increase with increasing coarseness, meaning that the K_{sat}-value should increase from silt clay loam, to loam, to sandy loam and to loamy sand with the coarsest texture. This is not the case with the measurements taken in Oslo. Some of the K_{sat} values measured at sites with loam and sandy loam are lower than the smallest K_{sat}-value measured at sites with silt clay loam, and the range of the measured values for loam and sandy loam are almost identical. The situation in Trondheim is not much different. The soil was characterized as sandy loam, with a K_{sat}- value varying from 3.188cm/h- 145cm/h, and as loamy sand with a K_{sat}- value varying from 8.59cm/h to 68,83 cm/h. Again, sandy loam should have a lower K_{sat}- value than loamy sand, but there is no clear distinction in saturated hydraulic conductivity between the two different soil types.

At site S75 in Oslo and site 2 and 3 in Trondheim, one of the five soil samples taken at each site was characterized as another soil texture than the other four samples. For these sites, the amount of infiltrated water was therefore computed by using both of the two different soil types found at the site, in order to investigate the differences. The results obtained for the sites in Trondheim showed no differences using the two different soil types because of the high capacity for infiltration, and can therefore not be used for compering. For site S75, however, there was obtained differences in the result when changing the soil type of the site. The ratio between the size of the roof area and the size of the infiltration area is the same for each of the two calculations, but because of the change of soil type the input parameter values are different for the two calculations. The two different soil types found at the site was sandy loam (SL) and Loam (L). By changing the soil type from loam to sandy loam, the amount of infiltrated water increased from 83.5% to 93.5% by using the Green-Ampt model and from 67.6% to 72.6% by using the Philip model. Figure 7.7 shows the

different amount of infiltration obtained by using the Green-Ampt model. The diagram to the left shows the development of the amount of infiltration and the amount of generated runoff over time for the loamy soil, while the diagram to the right shows the development of the amount of infiltration and the amount of generated runoff over time for the sandy loamy soil. The red line in these two diagrams, represents the amount of runoff, while the green line represents the amount of infiltration. The majority of the soil samples were characterized as Loam, so the calculation done by using the input parameter values for Loamy soil, is most probably more representative for this site. However, this calculation was done to show how a different soil type would affect the amount of infiltration at a site.

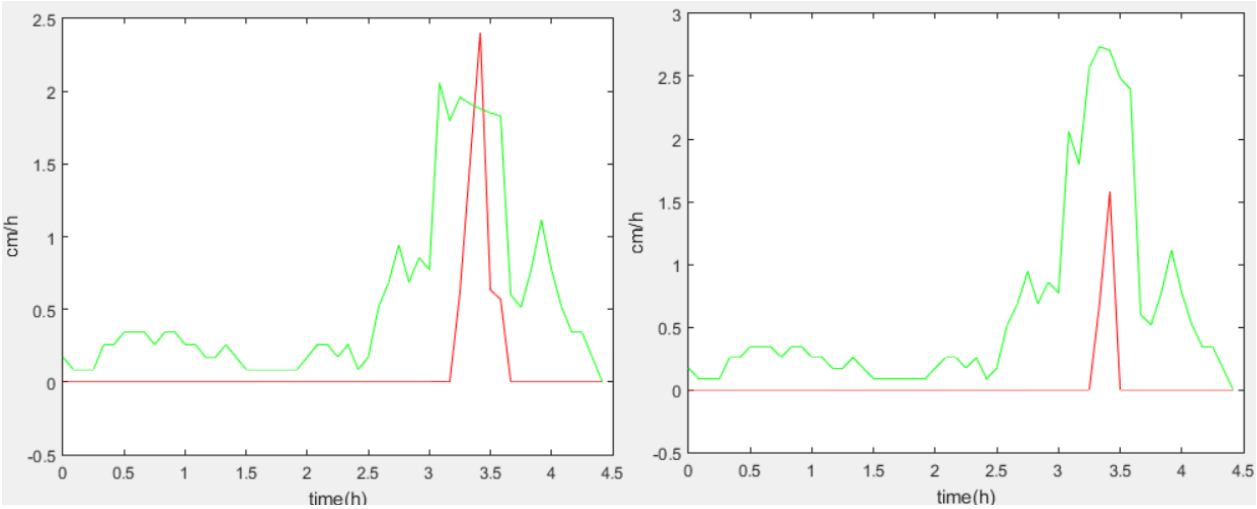

Figure 7.7 The results obtained with the different soil types found at site S75. The graph to the left shows the results for the loamy soil, and the graph to the right shows the result for the Sandy loam soil. Both graphs are calculated by using the Green- Ampt model. The red line represents the amount of generated runoff, while the green line represents the amount of infiltrated water.

This comparison of sites with the same soil type shows that there can be great variations in the amount of infiltrated water most probably due to urbanization and the effect of compaction of the soil. The results show that information obtained from soil maps is not necessarily sufficient to be able to find the infiltration capacity of the area. Even though several sites are characterized with the same soil type, the effect of urbanization and soil compaction can lead to a great variation in saturated hydraulic conductivity at each site. Resulting in one site may be able to infiltrate more water than another despite the same soil type. Therefore, there is suggested that when investigating the condition for downspout disconnection it is important to measure the saturated hydraulic

conductivity at each site, and preferably at multiple point at each site, to be able to find a representative K_{sat}-value used for the whole site. It also shows that when investigating the possibility for downspout disconnection, and thus the possibility for infiltration into urban soil, it should be expected that there may be different types of soil at the same site, which will affect the infiltration capacity for the site.

7.8 Downspout disconnection as a measure for stormwater managing

Infiltration of water into the soil is a complex process with many different factors affecting the soils ability to transport the water through the soil layers. Therefore, is it also many factors to take into account when considering downspout disconnection, especially in an urban area. As discussed in the previously sections, the amount of infiltrated water is dependent on the soils saturated hydraulic conductivity, the initial soil moisture content, the wetting front capillary suction head, the rainfall intensity and the ratio between the size of the roof area generating surface runoff and the size of the available infiltration area. The infiltration process is also affected by other factors, like the amount of organic matter and the degree of swelling, but their impact on infiltration were not considered in this thesis.

In connection with the discussion of this thesis, it was shown that there was great variation in the measured K_{sat}- values both between the different sites, but also between the five points measured at each site. The measurements showed that when investigating infiltration into urban soil it has to be expected that there are great local variations in the soils saturated hydraulic conductivity, most probably because of the compaction of soil due to urbanization. Because of this great variation in saturated hydraulic conductivity, and because of its major influence on the amount of infiltrated water, it is important that the soils K_{sat}- value is measured in the field, and preferably at multiple points at the site, to ensure a representable value. The soils initial moisture content is another factor affecting the amount of infiltrated water. The amount of infiltrated water decreases as the initial soil moisture content increase, and should also be measured in the field at each site. The initial soil moisture content is not constant, due to its dependence on the soil properties and the amount and duration of the rainfalls. When dimensioning for downspout disconnection, the infiltration capacity of a saturated soil should therefore also be considered, and the infiltration area should be designed to be able to handle most of the water even when the soil is saturated in order to ensure a safe stormwater management. This is particularly important in areas like Trondheim where it in periods

of the year can be long rainfall events where the soil does not have time to drain completely before the next rainfall. The wetting front capillary pressure head affects the amount of infiltrated water because of its dependent of soil moisture content and the pore size distribution. Because of this dependence, the wetting front capillary pressure head is affecting the soils saturated hydraulic conductivity. The higher ψ_f, the lower is the soils saturated hydraulic conductivity, and the value of ψ_f should therefore be evaluated when considering downspout disconnection. This may even be more important when considering infiltration into urban soil, because the relationship between ψ_f and K_{sat} is sensitive to bulk density and disturbance of the soil structure.

Based on the discussion in this thesis and the evaluation of the different K_{sat}- values at each site, done in Becker (2015), it seems that when considering infiltration into urban soil, it has to be taken into account that the soil not always behave as expected. Therefore, when considering downspout disconnection in urban areas it is not enough to use soil maps in order to find representative input parameter for the calculations of the site's infiltration capacity. In order to be able to obtain a good evaluation of the site, thorough field investigations should be conducted to find representative values for the different input parameters.

The rainfall intensity and the ratio between the size of the roof area and the size of the available infiltration area, is also important to take into account when considering downspout disconnection. The rainfall events used in this thesis, both in Oslo and Trondheim, are rather heavy rainfalls, and are not characterized as every day rainfalls. However, these rainfall events were still used in the calculations since it due to climate change is expected that such rainfall events like these will appear more often in the future. But since the rainfall intensity and the size of the roof area, among other, determines how large the corresponding infiltration area needs to be, it is important that the roof area is measured and that it is decided which rainfall intensity it should be dimensioned for, when considering downspout disconnection. Another factor affecting the size of the infiltration area is the soils saturated hydraulic conductivity. According to Paus et al. (2015), the saturated hydraulic conductivity should be greater than 10 cm/h in order to obtain good infiltration capacity. Almost all, except for two, of the K_{sat}- values used in the calculations for Oslo are greater than 10cm/h, and in Trondheim all of the used values are greater. This combined with the high values for the amount of infiltrated water, suggests that some of the sites, investigated in this thesis, are suitable for downspouts disconnection. In Trondheim, all of the sites showed great ability for infiltrating water

according to the calculations conducted in this thesis. However, because of the size of the available infiltration area and the location of the site, it is suggested that site 3 and 4 has the best conditions for infiltrating water in Trondheim. In Oslo, the variation in the amount of infiltrated water is bigger. Site B28, L34 and R44 has approximately 100% infiltration when using the Green- Ampt model, and it is therefore suggested that these sites are capable to handle most of the rainfall without implementing further measures. The sites R5 and S75 has a lower infiltration capacity than the previously mentioned sites, but because of the large size of the gardens at these sites, it is suggested that these sites are also capable to handle most of the rainfall without implementing further measures. The remaining sites has a lower infiltration capacity, and to be sure that the stormwater is managed safe, it is recommended that other measures are considered in addition. Because the infiltration area cannot handle the amount of stormwater, it should be considered whether the infiltration area could be made larger or not, or combining downspout disconnection with other measures like an infiltration trench or a rain garden.

As a general rule when considering downspout disconnection, the following is suggested. If the soil at the site is sandy and the infiltration area is one to twice as big as the roof area, it can be assumed that the infiltration capacity is good enough to infiltrate the amount of generated stormwater. Silty soil covers however a rather large range of K_{sat}- values depending on the percentage of silt in the soil, and the K_{sat}- value of the site should therefore be measured. Dependent on the soils ability to infiltrate water, it may be enough that the infiltration area is one to twice as big as the roof area, but this should be considered especially if the soils saturated hydraulic conductivity is of the lower value. The same yield also for a soil with a very high clay content. Whether this soil has a large enough infiltration capacity or not is dependent on the percentage of silt and sand fraction in the soil. The calculations done in this thesis also shows that for a site with a very high clay content, and thus a low K_{sat}- value, it is recommended to use an infiltration area three times or more, as big as the size of the roof area. Finally, when considering downspout disconnection, the rainfall intensity, the ratio between the size of the roof area and the size of the infiltration area, and the degree of urbanization of the soil should always be considered.

8. Concluding Remarks

In this thesis a MATLAB- model was established, based on field investigations, for modeling the effect of downspout disconnection by computing the amount of infiltrated water and the amount of runoff. Based on the rainfall intensity, the ratio between the roof area and the infiltration area, and some soil properties, the MATLAB-model is capable, to some degree, to reflect the infiltration process which happens in the soil. The model can thus calculate the amount of infiltrated water and the amount of generated runoff during a specific rainfall event, by using both the Green-Ampt model and the Philip model. A significantly amount of infiltration is observed, resulting in the suggestion that downspout disconnection can reduce the amount of stormwater considerably, if most of the water is infiltrated. The model is however based on some assumptions and there has been made some simplifications that should be looked into in further works. The model takes not overland flow into consideration, meaning that the model is disregarding that rainwater which is falling onto the ground forms a thin sheet flow on the surface due to gravitational forces. The model does not include water flowing into the infiltration area and some water flowing out, but assumes that the rainwater is falling onto the ground and infiltrates and has no horizontal movement. Which leads to the next simplification that should be looked into in further works. Rainwater infiltrating into the ground infiltrates both vertically and horizontally, but this model is only considering the vertical movement of the wetting front. Therefore, the model is also not considering that as the flow out from the downspout reaches the infiltration area, the soil closest to the downspout is getting saturated first and that the wetting front is moving both vertically and horizontally into the rest of the soil. this should be considered in future work. Another thing that should be corrected in further work, is that the model requires a constant rainfall event. Since it during a rainfall event can be minutes without rain fall, the rainfall event had to be divided into time intervals of 5 minutes each, and summing up the precipitation falling during this 5 minutes in order to avoid this problem. In order to be able to model as close to the reality as possible, this problem should be corrected, and the model should be able to calculate the infiltration during a rainfall event where some of the time steps has no precipitation. In further work it should also be conducted more field work in order to be able to verify the model, and to see which of the infiltration models used in this thesis are closest to the reality.

In connection with the assessment of further development of the established MATLAB- model in this thesis, the purpose of the model should be taken into consideration. The model, as it is

presented in this thesis, can be used when evaluating whether a site is suitable for downspout disconnection or not. The current model can also show if a site is able to infiltrate all of the generated stormwater, or whether downspout disconnection should be combined with other measures in order to obtain a safe stormwater management. However, if the purpose of the model is to be used for dimensioning, the current model should first be developed according to the discussion presented above.

Regardless whether the model is used for evaluation of the site, or if it is developed to be able to be used in dimensioning, the establishing of this model is a step in the right direction in relation to use downspout disconnection as a measure for managing stormwater. As downspout disconnection becomes a more frequently used measure, the need to understand its influence on the urban hydrology is increasing. There will thus be an increased need to promote close cooperation between hydrology and hydraulics in order to develop downspout disconnection as a measure for stormwater managing.

9. References

AHMED, F., GULLIVER, J. & NIEBER, J. A new technique to measure infiltration rate for assessing infiltration of BMPs. 12th International Conference on Urban Drainage, 2011.

ATTAWAY, S. 2011. *Matlab : A Practical Introduction to Programming and Problem Solving,* Burlington, Elsevier Science.

BECKER, M. A. 2015. *Beregning av mettet hydraulisk konduktivitet ved bruk av MPD- infiltrometer, for vurdering av frakopling av taknedløp.* NTNU.

BOCKHEIM, J. 1974. Nature and properties of highly disturbed urban soils. Philadelphia, Pennsylvania. *Div. S-5, Soil Science Society of America, Chicago, Illinois*.

BRAKENSIEK, D. L. 1977. Estimating the effective capillary pressure in the Green and Ampt Infiltration Equation. *Water Resources Research,* 13**,** 680-682.

BRASKERUD, B., PAUS, K. & EKLE, A. 2013. Anlegging av regnbed. En billedkavakade over 4 anlagte regnbed. NVE rapport 3/2013. Oslo, Norge.

BRATTLI, B. 2009. *Fysisk og kjemisk hydrogeologi,* Trondheim, Norges teknisk-naturvitenskapelige universitet, Institutt for geologi og bergteknikk.

BROOKS, R. H. & COREY, A. T. 1964. Hydraulic properties of porous media. *colorado State Univ. Hydrology Papers*.

BRUTSAERT, W. 1976. The concise formulation of diffusive sorption of water in a dry soil. *Water Resources Research,* 12**,** 1118-1124.

BUTLER, D. & DAVIES, J. 2010. Urban Drainage, Third Edition. 3 ed.: Taylor and Francis.

CHOW, V. T., MAIDMENT, D. R. & MAYS, L. W. 1988. *Applied hydrology,* New York, McGraw-Hill.

COUNTY, P. G. S. 1999a. Low-impact development design strategies: an integrated design approach. *Department of Environmental Resources, Programs and Planning Division, Prince George's County, Maryland*.

COUNTY, P. G. S. 1999b. Low-Impact Development Hydraulic Analysis. *Department of Environmental Resources, Programs and Planning Division, Prince George's County, Maryland*.

DINGMAN, S. L. 2008. *Physical hydrology,* Long Grove, Ill, Waveland Press.

EAGLESON, P. S. 1970. *Dynamic hydrology,* New York, McGraw-Hill.

GHORBANI DASHTAKI, S., HOMAEE, M., MAHDIAN, M. & KOUCHAKZADEH, M. 2009. Site-Dependence Performance of Infiltration Models. *An International Journal - Published for the European Water Resources Association (EWRA),* 23**,** 2777-2790.

GREEN, W. H. & AMPT, G. 1911. Studies on Soil Phyics. *The Journal of Agricultural Science,* 4**,** 1-24.

GREGORY, J. H., DUKES, M. D., JONES, P. H. & MILLER, G. L. 2006. Effect of urban soil compaction on infiltration rate. *Journal of Soil and Water Conservation,* 61**,** 117-124.

HORN, R., DOMŻŻAŁ, H., SŁOWIŃSKA-JURKIEWICZ, A. & VAN OUWERKERK, C. 1995. Soil compaction processes and their effects on the structure of arable soils and the environment. *Soil and Tillage Research,* 35**,** 23-36.

HORTON, R. E. 1941. An approach toward a physical interpretation of infiltration-capacity. *Soil science society of America journal,* 5**,** 399-417.

LINDHOLM, O., ENDRESEN, S., THOROLFSSON, S., SÆGROV, S., JAKOBSEN, G. & AABY, L. 2008. Veiledning i klimatilpasset overvannshåndtering Norsk Vann Rapport 162, Hamar.

MIYAZAKI, T., HASEGAWA, S. & KASUBUCHI, T. 1993. *Water flow in soils,* New York, Marcel Dekker.

NAWAZ, M., BOURRIE, G. & TROLARD, F. 2013. Soil compaction impact and modelling. A review. *Agron. Sustain. Dev.*

NYBORG, Å. & OLSEN, H. 2014. *Tekstur i plogsjkt* [Online]. Available: http://www.skogoglandskap.no/filearchive/fakta_15-2014_tekstur_i_plogsjikt.pdf [Accessed 21.12.15.

PAUS, K. H., MUTHANNA, T. M. & BRASKERUD, B. C. 2015. The hydrological performance of bioretention cells in regions with cold climates: seasonal variation and implications for design. In press. IWA Publishing

PAZWASH, H. 2011. *Urban storm water management,* Boca Raton, Fla, CRC Press.

PHILIP, J. 1957. The theory of infiltration: 1. The infiltration equation and its solution. *Soil science,* 83**,** 345-358.

PHILIP, J. R. 1993. Approximate Analysis of falling- head lined Borehole Permeameter. *Resources Research 29(11): 3763-3768*.

PHILLIP, J. C. 2016. *Urban Soils* [Online]. Available: https://www.ces.ncsu.edu/fletcher/programs/nursery/.../m57.pdf [Accessed 25.05.2016.

PITT, R., CHEN, S.-E., CLARK, S., STRECKER, E. W. & HUBER, W. C. 2002. Compacted urban soils effects on infiltration and bioretention stormwater control designs.

RAWLS, W. J., AHUJA, L. R., BRAKENSIEK, D. L., SHIRMOHAMMADI, A. & MAIDMENT, D. 1992. *Infiltration and soil water movement*, McGraw-Hill Inc.

RAWLS, W. J. & BRAKENSIEK, D. Prediction of soil water properties for hydrologic modeling. Watershed Management in the Eighties, 1985. ASCE, 293-299.

REGCLIM. 2005. *Norges klima om 100 år.Usikkerhet og risiko* [Online]. Available: http://regclim.met.no/presse/download/regclim_brosjyre2005.pdf [Accessed 18.11.15.

RICHARDS, L. A. 1931. Capillary conduction of liquids through porous mediums. *Journal of Applied Physics,* 1**,** 318-333.

SHARMA, M., GANDER, G. & HUNT, C. 1980. Spatial variability of infiltration in a watershed. *Journal of Hydrology,* 45**,** 101-122.

SOANE, B. D., BLACKWELL, P. S., DICKSON, J. W. & PAINTER, D. J. 1980. Compaction by agricultural vehicles: A review I. Soil and wheel characteristics. *Soil and Tillage Research,* 1**,** 207-237.

TARBOTON, D. G. 2003. Rainfall-runoff processes. *Utah State University*.

TARBUCK, E. J., LUTGENS, F. K. & TASA, D. 2011. *Earth : an introduction to physical geology,* Boston, Prentice Hall/Pearson.

ØDEGAARD, H., NORHEIM, B. & NORSK VANN, B. A. 2014. *Vann- og avløpsteknikk,* Hamar, Norsk Vann.

10. Appendix

Appendix 1: MATLAB-Code

MATLAB-code for the Green- Ampt infiltration model

```
data= xlsread('inputsheet .xlsx','GreenAmpt');
n=size(data); % imports the input parameters from the excel-sheet
    n=n(1);
    t=data(1:n-1,10);% stores the values as variables
    I=data(1:n-1,11);
    w=data(1:n-1,12);
    deltat=data(1:n-1,13);
    arealtak= data(1,14);
    antalllop=data(1,15);
    Lengde=data(1,16);
    Bredde=data(1,17);
    Volumtak=data(1,18);
    nyw=data(1:n-1,19);

    jordtype=1;
    ksat=data(1:jordtype,1);
    por=data(1:jordtype,2);

    yf=data(1:jordtype,3);
    ya=data(1:jordtype,4);
    b=data(1:jordtype,5);
    ofc=data(1:jordtype,6);
    P=data(1:jordtype,7);
l=[ ksat por yf ya b ofc P];

tables = {};
infiltrations = zeros(size(l,1),1);
runoffs = zeros(size(l,1),1);
rains = zeros(size(l,1),1);
for j=1:size(l,1)

    ksat(j)= l(j,1);

    por(j)=l(j,2);
    yf(j)=l(j,3);
    ya(j)=l(j,4);
    b(j)=l(j,5);
    ofc(j)=l(j,6);
    P(j)=l(j,7);

m=[t I nyw deltat];% establishing table m

    for i=5:15
    m(:,i)=zeros;
    end
```

```
for i=1:size(m,1)% follows the corresponding flowsheet
    m(1,5)=0;
    m(1,6)=Inf;
    m(1,1)=0;

    if i>1
        m(i,5)=m(i-1,12);
    end
   if i>1
       m(i,6)=ksat(j)*(1+P(j)/m(i,5));
   end

    if m(i,6)< m(i,3)
        m(i,9)=m(i,5);
        m(i,10)=0;
        m(i,11)=m(i,1);
        m(i,13)=0;

        syms f(x)
        ln=@log;
        m(i,13)=0;
        f(x)=m(i,13)==((m(i,1)+m(i,4))-m(i,11))-((x-m(i,9))/ksat(j))-
(P(j)/ksat(j))*ln((m(i,9)+P(j))/(x+P(j)));
        sol=vpasolve(f,x,[0 inf]);
        m(i,12)=sol;

    else
            m(i,7)=m(i,5)+ (m(i,4)*m(i,3));

           m(i,8)=ksat(j)*(1+(P(j)/m(i,7)));


        if m(i,8)> m(i,3)
            m(i,12)=m(i,7);

        else

            m(i,9)=(ksat(j)*P(j))/(m(i,3)-ksat(j));
            m(i,10)=(m(i,9)-m(i,5))/m(i,3);
            m(i,11)=m(i,1)+m(i,10);

            syms f(x)
            ln=@log;
            m(i,13)=0;
            f(x)=m(i,13)==((m(i,1)+m(i,4))-m(i,11))-((x-m(i,9))/ksat(j))-
(P(j)/ksat(j))*ln((m(i,9)+P(j))/(x+P(j)));
            sol=vpasolve(f,x,[0 inf]);
            m(i,12)=sol;


        end
    end
    m(i,14)=m(i,12)-m(i,5);
```

```
    m(i,15)=(m(i,4)*m(i,3))-m(i,14);
    m(i+1,1)=m(i,1)+m(i,4);

end

figure

infcap=m(:,6);
infiltration=m(:,14);
runoff=m(:,15);
rain=m(:,2);
time=m(:,1);
plot(time,infcap,'color','b')
xlabel ('time(h)')
ylabel ('cm/h')

figure
plot(time,runoff,'color','r')
hold on;
plot(time,infiltration,'color','g')
xlabel('time(h)')
ylabel('cm/h')

tables{j} = m;
infiltrations(j) = sum(infiltration);
runoffs(j) = sum(runoff);
rains(j) = sum(rain);
end

A=[rains infiltrations runoffs];
disp(A)

disp(m)
```

MATLAB- code for the Philip infiltration model

```
data= xlsread('inputsheet .xlsx','Philip');
n=size(data); % imports the inputparameters from the excel-sheet
n=n(1);
t=data(1:n-1,11);% stores the values as variables
I=data(1:n-1,12);
w=data(1:n-1,13);
deltat=data(1:n-1,14);
arealtak=data(1,15);
antalllop=data(1,16);
Lengde=data(1,17);
Bredde=data(1,18);
Volumtak=data(1,19);
nyw=data(1:n-1,20);
jordtype=1;
ksat=data(1:jordtype,1);
por=data(1:jordtype,2);
yf=data(1:jordtype,3);
ya=data(1:jordtype,4);
b=data(1:jordtype,5);
```

```
o0=data(1:jordtype,6);
Sp=data(1:jordtype,7);
Kp=data(1:jordtype,8);

for o0=data(1:jordtype,6)
    if isnan(o0)
        o0=0.7*por;% has to be calculated
    end
end

l=[ksat por yf o0 Sp Kp];
tables={};
infiltrations=zeros(size(l,1),1);
runoffs=zeros(size(l,1),1);
rains=zeros(size(l,1),1);


for j=1:size(l,1)
    ksat(j)=l(j,1);
    por(j)= l(j,2);
    yf(j)=l(j,3);
    o0(j)=l(j,4);

    Sp(j)=l(j,5);
    Kp(j)=l(j,6);

m=[t I nyw deltat];%establishing table m
for i=5:14
    m(:,i)=zeros;
end

for i=1:size(m,1)%follows the corresponding flowsheet
    m(1,5)=0;
    m(1,6)=Inf;
    m(1,1)=0;

    if i>1
        m(i,5)=m(i-1,13);
    end

   if i>1
    m(i,6)=Kp(j)+((Kp(j)*Sp(j))/(sqrt(Sp(j)^2+4*Kp(j)*m(i,5))-Sp(j)));
   end

    if m(i,6)>m(i,3)
        m(i,7)=m(i,5)+(m(i,3)*m(i,4));
        m(i,8)=Kp(j)+(Kp(j)*Sp(j))/(sqrt(Sp(j)^2+4*Kp(j)*m(i,7))-Sp(j));

        if m(i,8)>m(i,3)
            m(i,13)=m(i,7);
        else
            m(i,9)=(Sp(j)^2*(m(i,3)-Kp(j)/2))/(2*(m(i,3)-Kp(j))^2);
            m(i,10)=(m(i,9)-m(i,5))/m(i,3);
            m(i,11)=m(i,1)+m(i,10);
```

```
            m(i,12)=m(i,11)-(1/(4*Kp(j)^2))*(sqrt(Sp(j)^2+4*Kp(j)*m(i,9))-
Sp(j))^2;
            m(i,13)=(Sp(j)*((m(i,1)+m(i,4))-
m(i,12))^0.5)+(Kp(j)*((m(i,1)+m(i,4))-m(i,12)));

        end
    else
        m(i,9)=m(i,5);
        m(i,10)=0;
        m(i,11)=m(i,1);
        m(i,12)=m(i,11)-(1/(4*Kp(j)^2))*(sqrt(Sp(j)^2+4*Kp(j)*m(i,9))-
Sp(j))^2;
        m(i,13)=(Sp(j)*(((m(i,1)+m(i,4))-
m(i,12))^0.5))+(Kp(j)*((m(i,1)+m(i,4))-m(i,12)));
    end
    m(i,14)=m(i,13)-m(i,5);
    m(i,15)=(m(i,3)*m(i,4))-m(i,14);
    m(i+1,1)=m(i,1)+m(i,4);
end
figure
infcap=m(:,6);
infiltration=m(:,14);
runoff=m(:,15);
rain=m(:,2);
time=m(:,1);
plot(time,infcap,'color','b')
xlabel ('time(h)')
ylabel ('cm/h')

figure
plot(time,runoff,'color','r')
hold on;
plot (time, infiltration,'color','g')
xlabel('time(h)')
ylabel('cm/h')
tables{j}=m;
infiltrations(j)=sum(infiltration);
runoffs(j)=sum(runoff);
rains(j)=sum(rain);
end
A=[rains infiltrations runoffs];
disp(A)

disp(m)
```

Appendix 2: Input parameters used for the reference simulation

Sample	**Soil texture**	**Ksat**	**porosity**	**ψf**	**ψa**	**λ**	**Initial moisture content**	**Roof area**	**# downspouts**	**Area of infiltration**
Oslo										
B20A	Loam	12.10	0.4	27.81	36.29	0.29	0.33	152	6	5
B28AB	Silt clay loam	15.30	0.45	49.38	63.18	0.26	0.33	142	6	7
B30	Sandy loam	10.46	0.34	17.68	24.39	0.41	0.26	85	3	5
B65	Loam	15.15	0.4	30.57	40.20	0.32	0.31	179	6	7
E14	Loam	15.23	0.4	39.20	51.82	0.32	0.33	251	4	7
L34	Sandy loam	35.00	0.34	12.76	17.79	0.43	0.31	127	4	7
R5	Loam	6.34	0.4	23.55	30.93	0.30	0.31	64	4	10
R29	Sandy loam	18.42	0.34	18.06	24.90	0.41	0.28	129	4	4
R44	Loamy sand	46.00	0.32	13.85	19.69	0.48	0.30	104	3	7
S10	Loam	2.46	0.4	20.74	27.43	0.32	0.32	74	4	10
S75(bcde)	Loam	18.77	0.4	38.73	51.11	0.31	0.30	227	3	10
S75(a)	Sandy loam	29.96	0.34	11.71	16.42	0.45	0.19	227	3	10

Trondheim										
Site 1	Loamy sand	15.11	0.32	17.67	25.28	0.5	0.22	17	1	51
Site 2	Sandy loam	46.2	0.34	24.78	34.99	0.47	0.3	64	1	80
Site 2	Loamy sand	15.11	0.32	17.67	25.28	0.5	0.22	64	1	80
Site 3	Sandy loam	46.2	0.34	24.78	34.99	0.47	0.3	63	1	94
Site 3	Loamy sand	15.11	0.32	17.67	25.28	0.5	0.22	63	1	94
Site 4	Loamy sand	15.11	0.32	17.67	25.28	0.5	0.22	47.5	1	123

Appendix 3: Obtained graphs form the calculations

The graph to the left shows the amount of infiltrated water (green line) and the amount of generated runoff (red line). The graph to the right shows the development of the infiltration capacity over time.

Results: Reference simulation

Calculations done by using Green Ampt infiltration model.

The different sites in Oslo:

B20

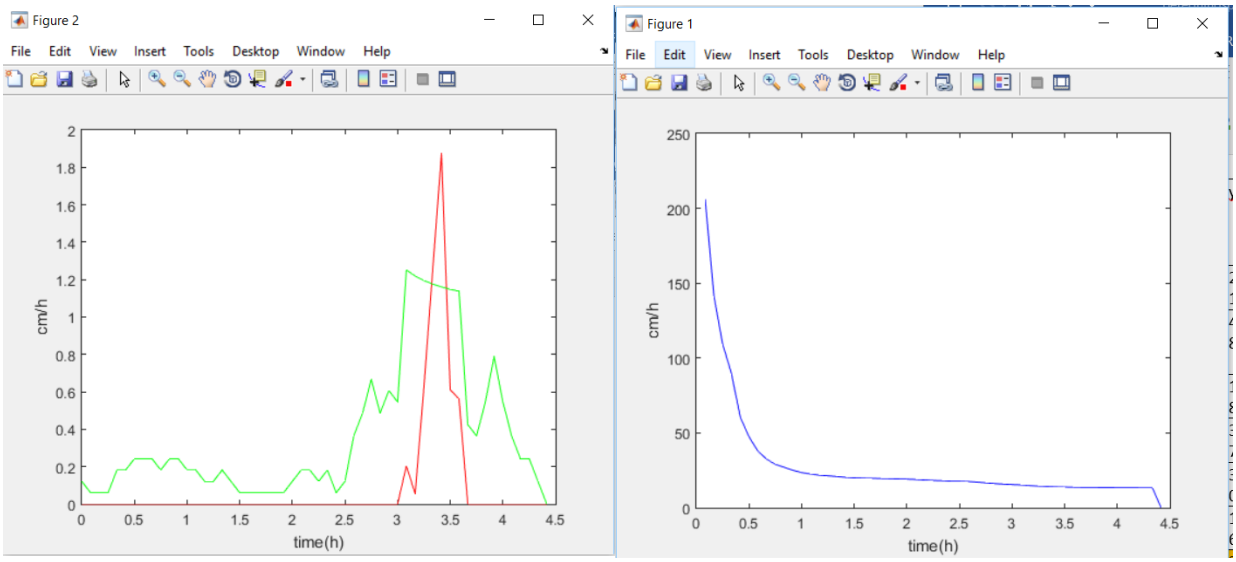

B28

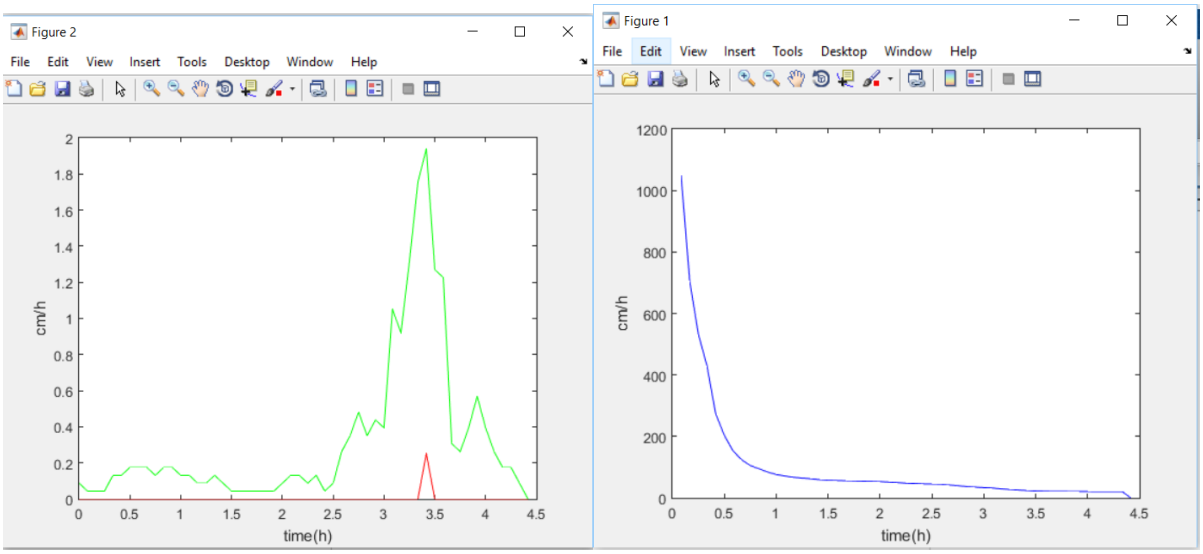

B30

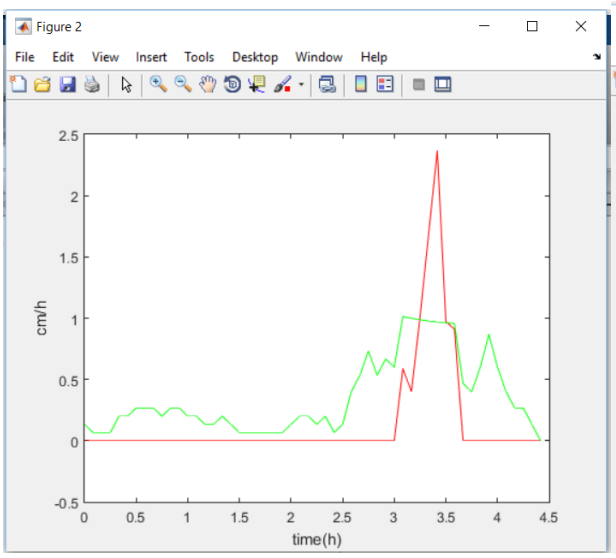
Figure 2
File Edit View Insert Tools Desktop Window Help
cm/h
time(h)

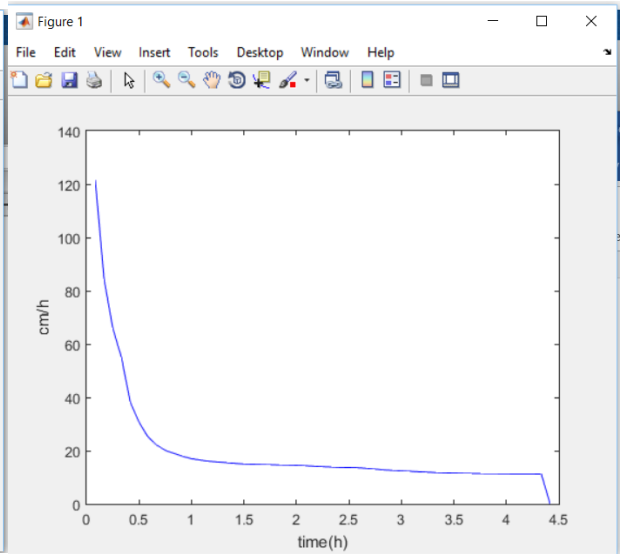
Figure 1
File Edit View Insert Tools Desktop Window Help
cm/h
time(h)

B65

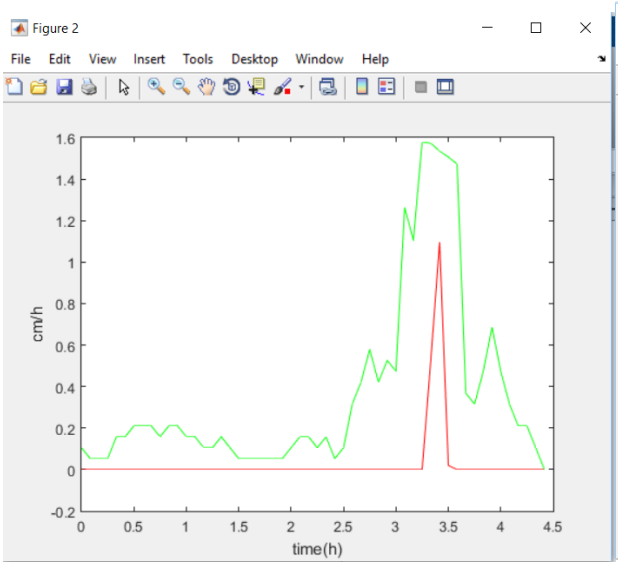
Figure 2
File Edit View Insert Tools Desktop Window Help
cm/h
time(h)

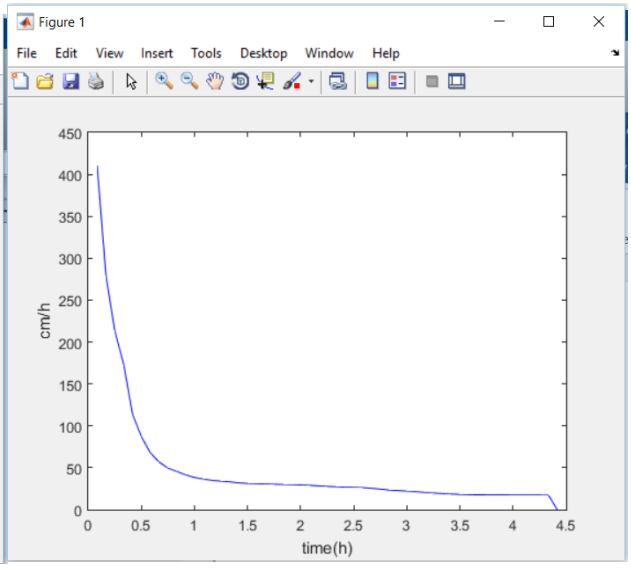
Figure 1
File Edit View Insert Tools Desktop Window Help
cm/h
time(h)

E14

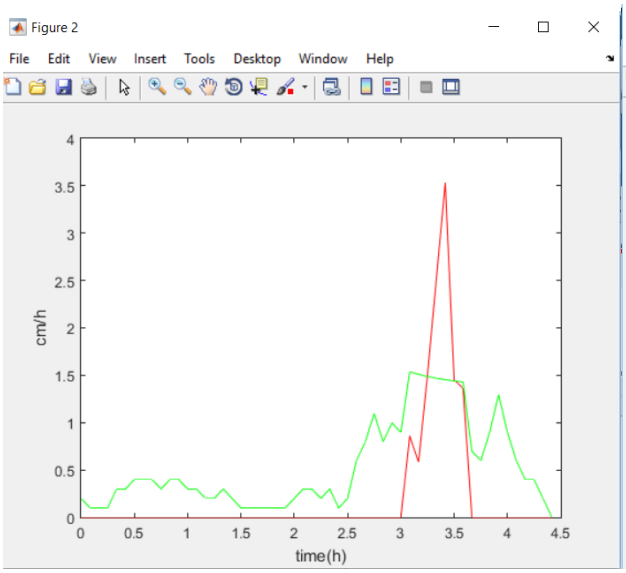
Figure 2
File Edit View Insert Tools Desktop Window Help
cm/h
time(h)

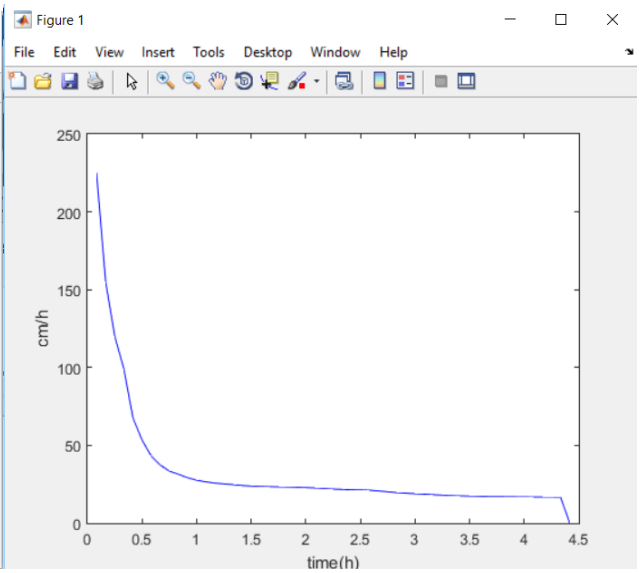
Figure 1
File Edit View Insert Tools Desktop Window Help
cm/h
time(h)

L34

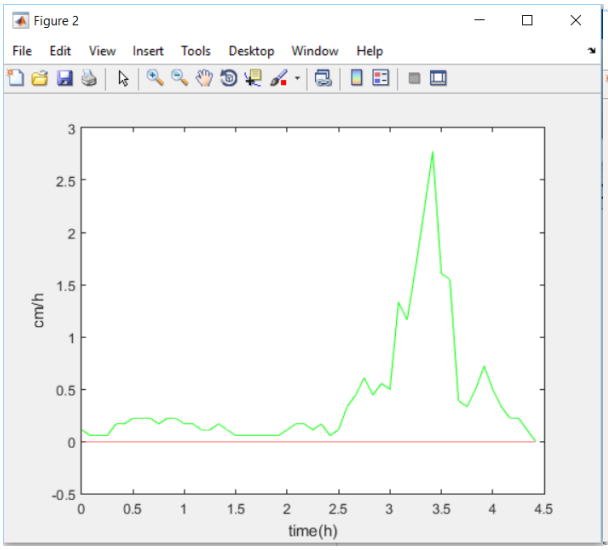
Figure 2
File Edit View Insert Tools Desktop Window Help
cm/h
time(h)

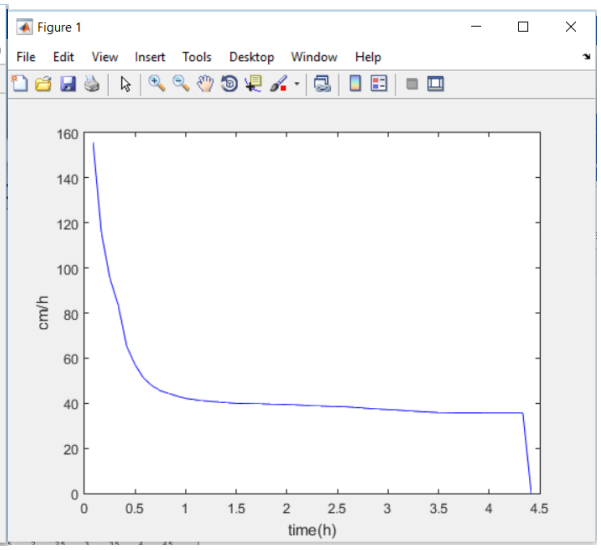
Figure 1
File Edit View Insert Tools Desktop Window Help
cm/h
time(h)

R5

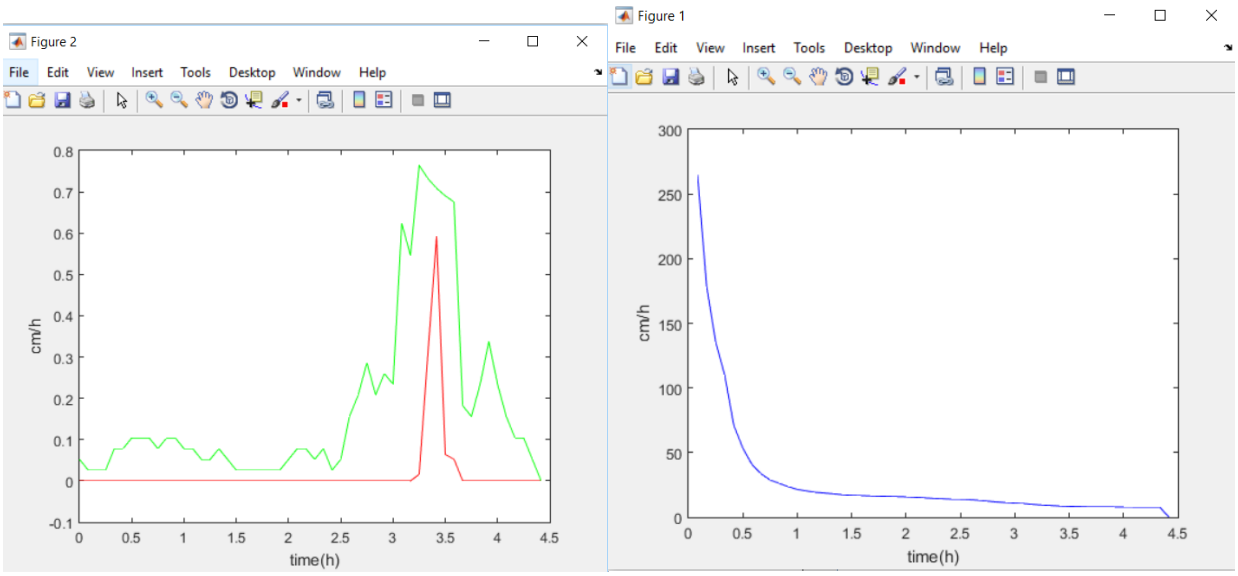
Figure 2
File Edit View Insert Tools Desktop Window Help
cm/h
time(h)
Figure 1
File Edit View Insert Tools Desktop Window Help
cm/h
time(h)

R29

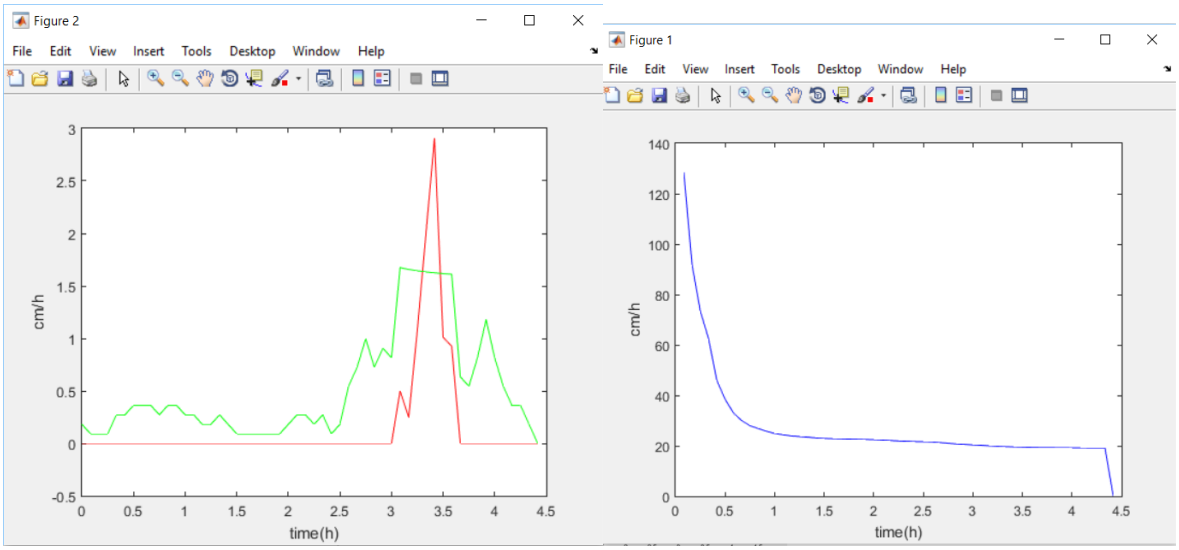
Figure 2
File Edit View Insert Tools Desktop Window Help
cm/h
time(h)
Figure 1
File Edit View Insert Tools Desktop Window Help
cm/h
time(h)

R44

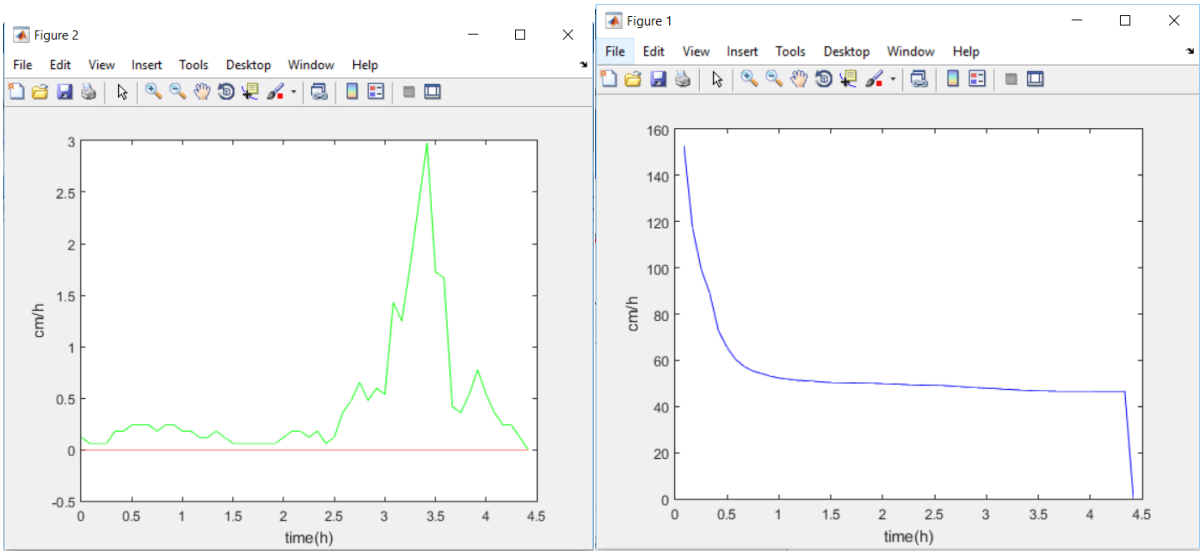
Figure 2
File Edit View Insert Tools Desktop Window Help
cm/h
time(h)
Figure 1
File Edit View Insert Tools Desktop Window Help
cm/h
time(h)

S10

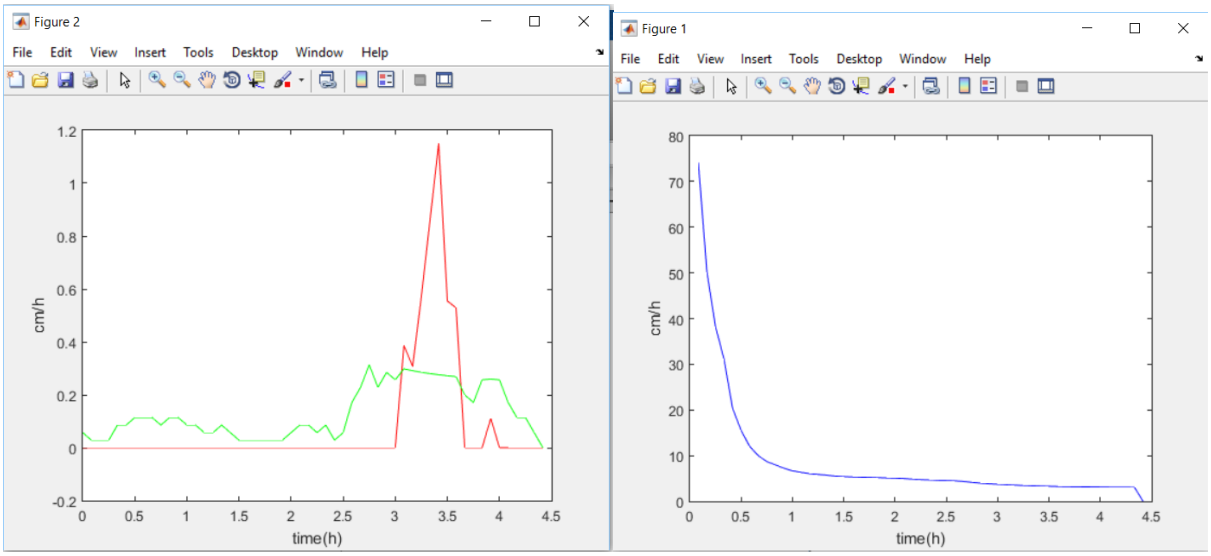
Figure 2
File Edit View Insert Tools Desktop Window Help
cm/h
time(h)
Figure 1
File Edit View Insert Tools Desktop Window Help
cm/h
time(h)

S75 (with Loamy soil)

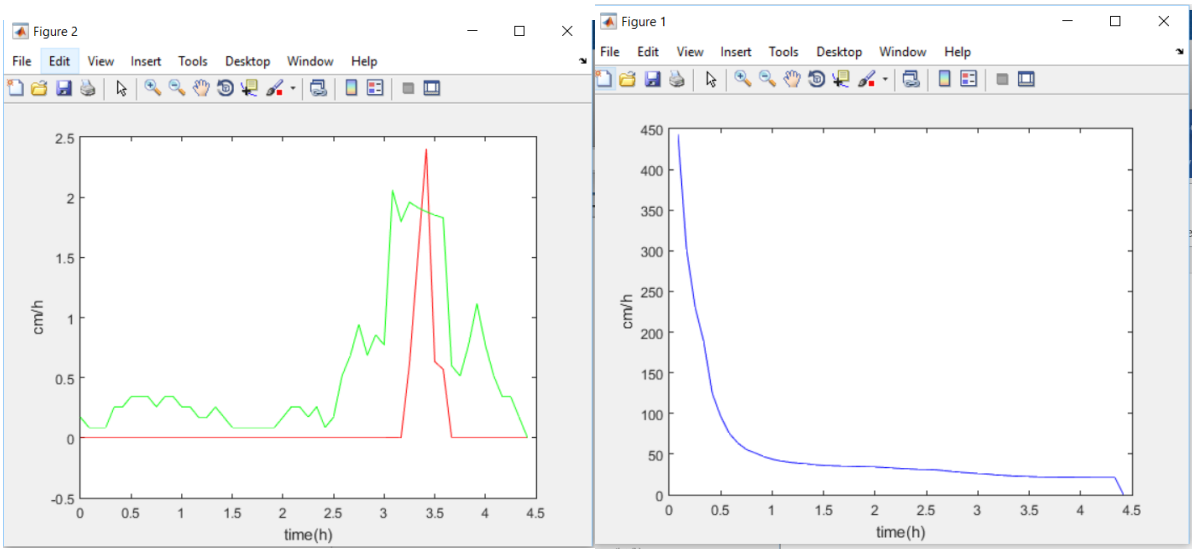

S75 (with sandy loam)

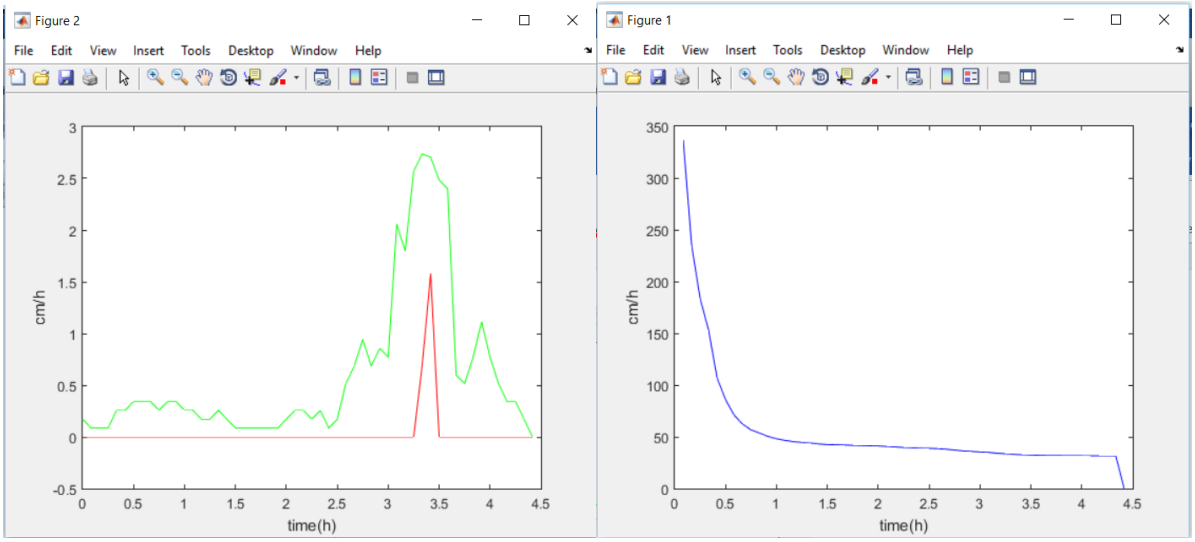

The different sites in Trondheim:

Site 1

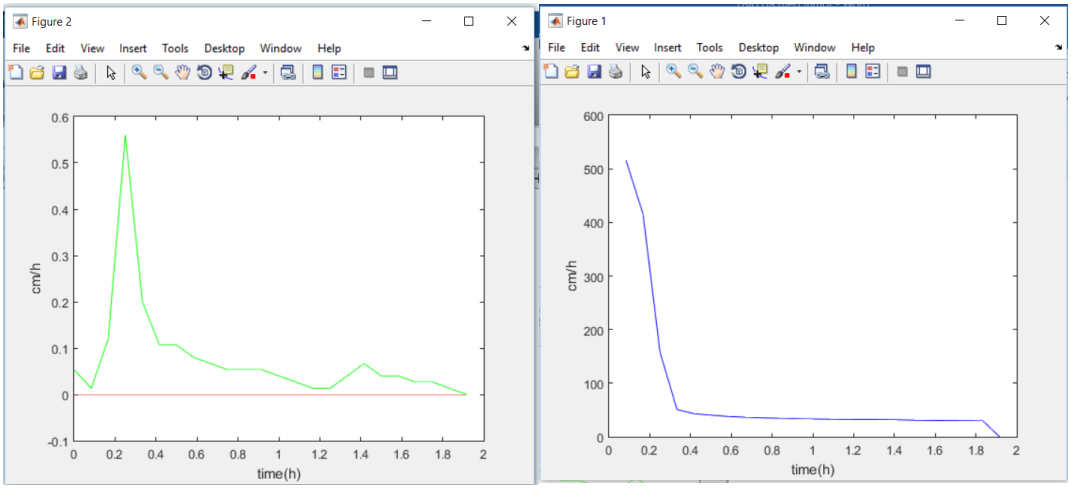

Site 3 with sandy loam

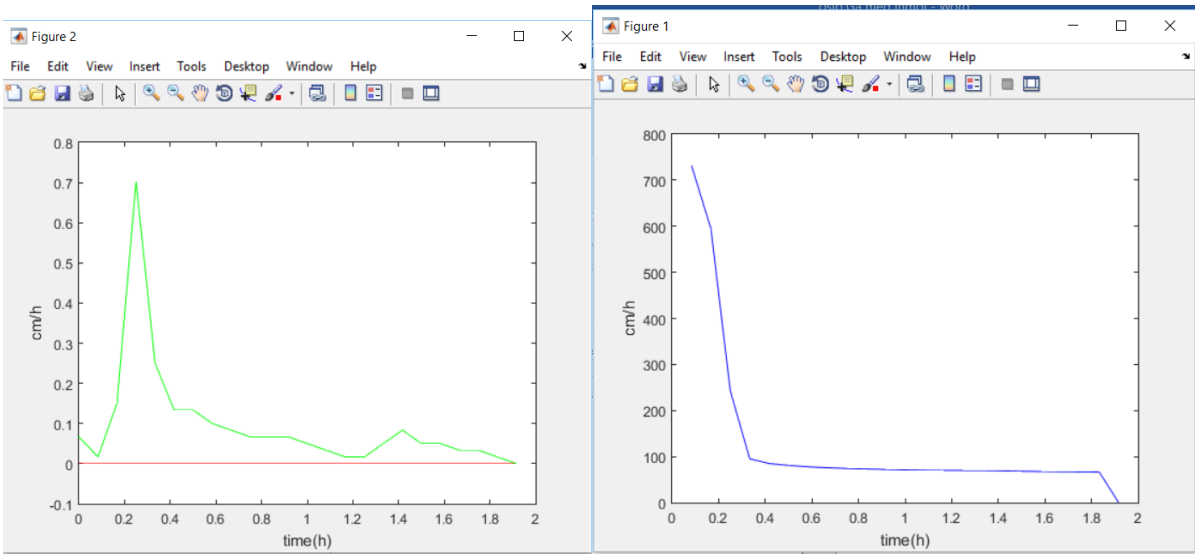

Calculations done by using Philip infiltration model

The different sites in Oslo

B20ab

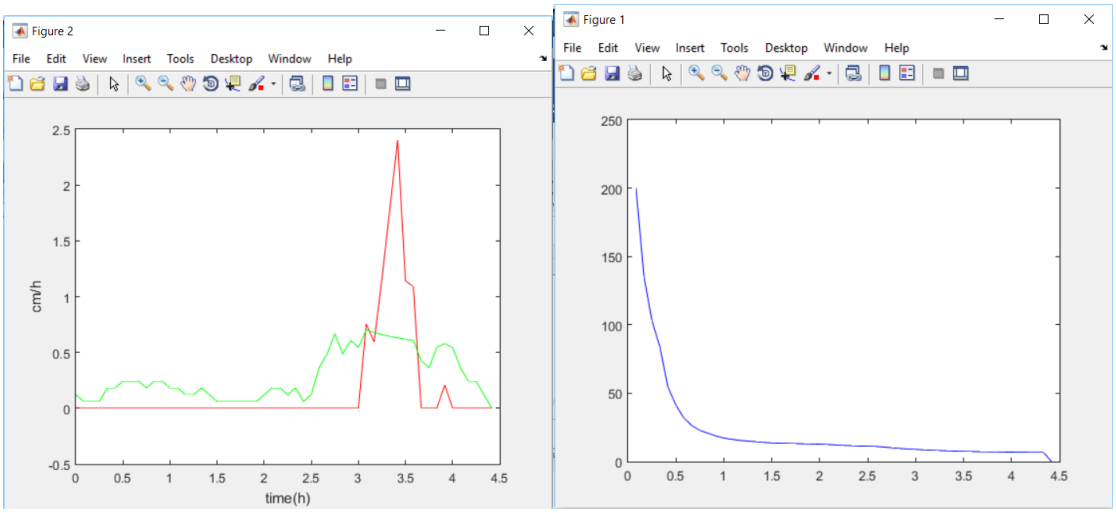

B28 ab

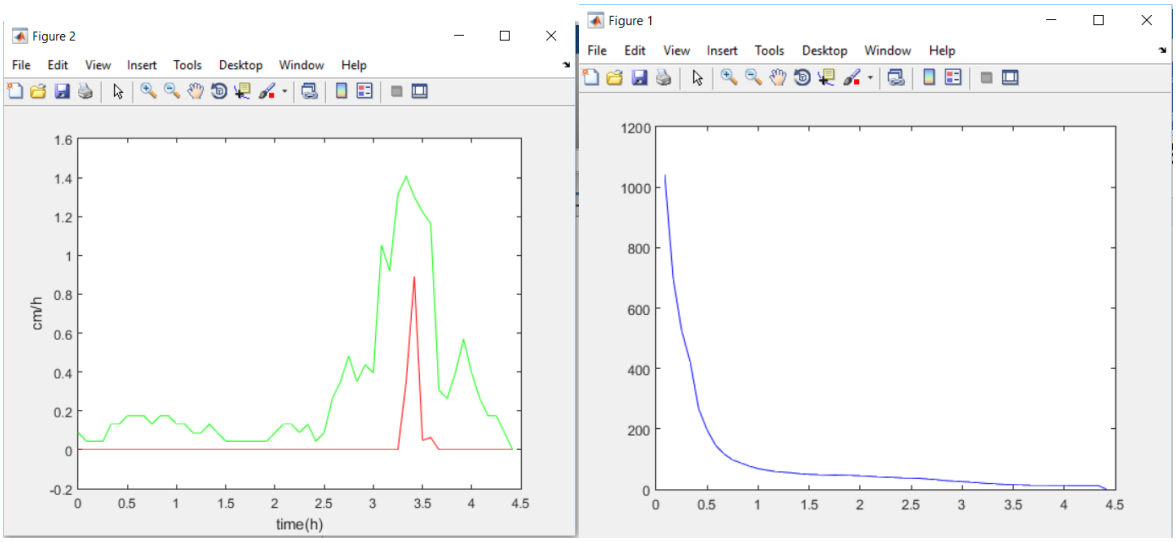

B30

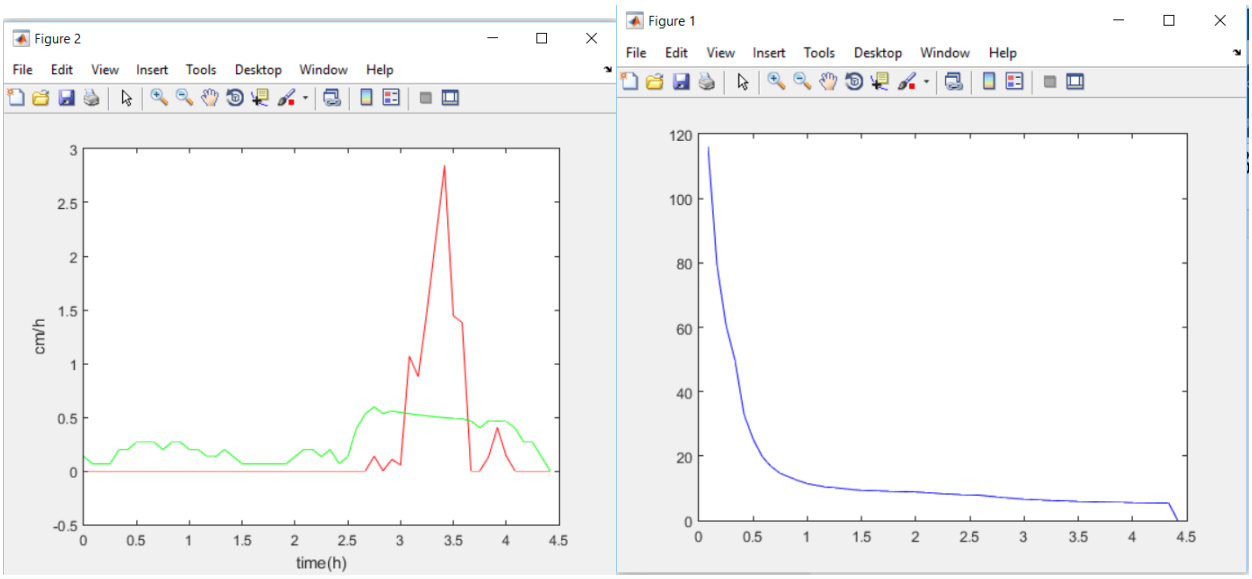
Figure 2
File Edit View Insert Tools Desktop Window Help
cm/h
time(h)
Figure 1
File Edit View Insert Tools Desktop Window Help

B65

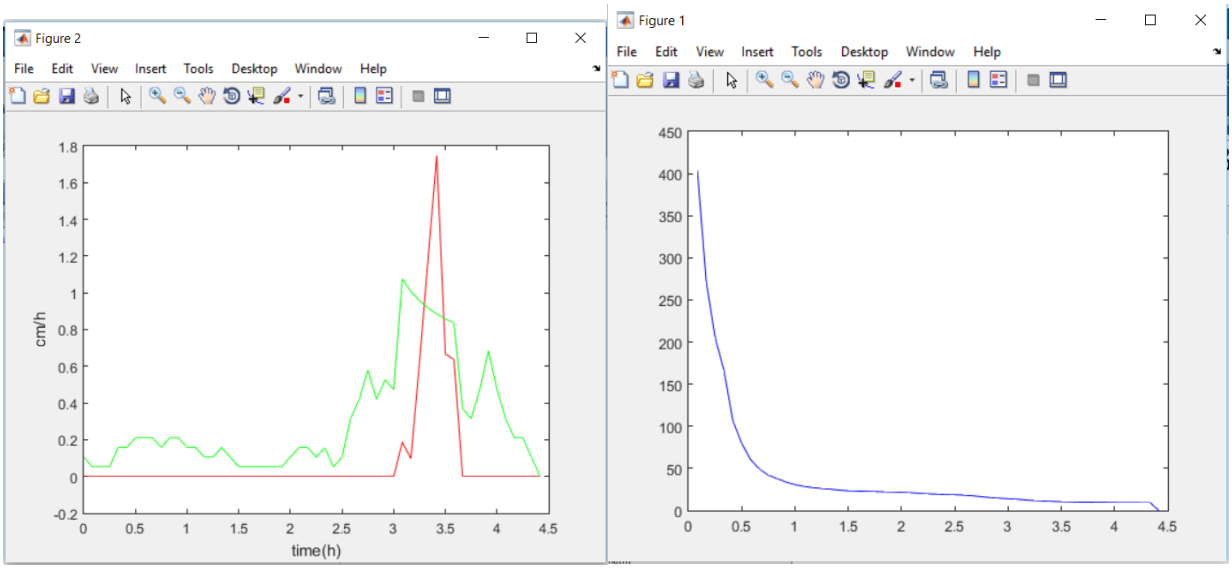
Figure 2
File Edit View Insert Tools Desktop Window Help
cm/h
time(h)
Figure 1
File Edit View Insert Tools Desktop Window Help

E14

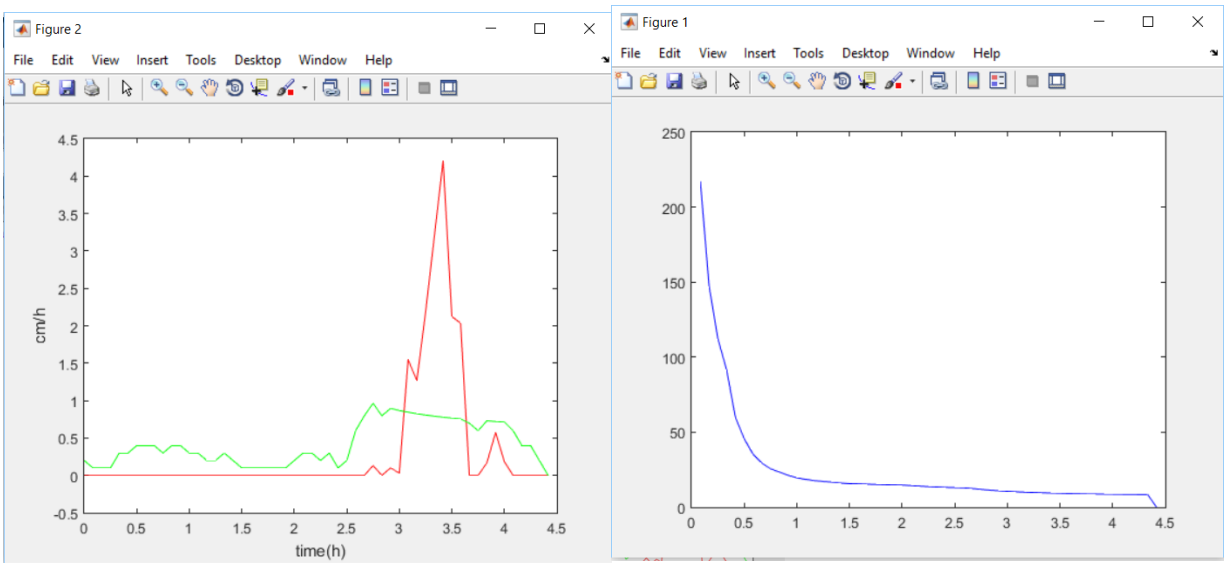
Figure 2
File Edit View Insert Tools Desktop Window Help
cm/h
time(h)
Figure 1
File Edit View Insert Tools Desktop Window Help

L34

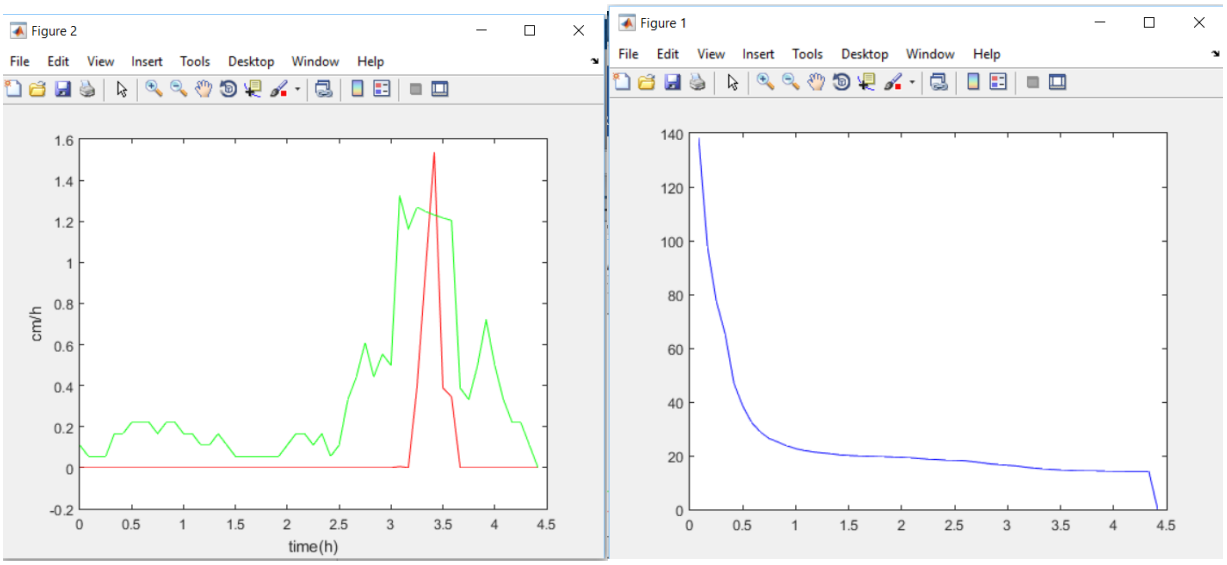
Figure 2
File Edit View Insert Tools Desktop Window Help
cm/h
time(h)
Figure 1
File Edit View Insert Tools Desktop Window Help

R5

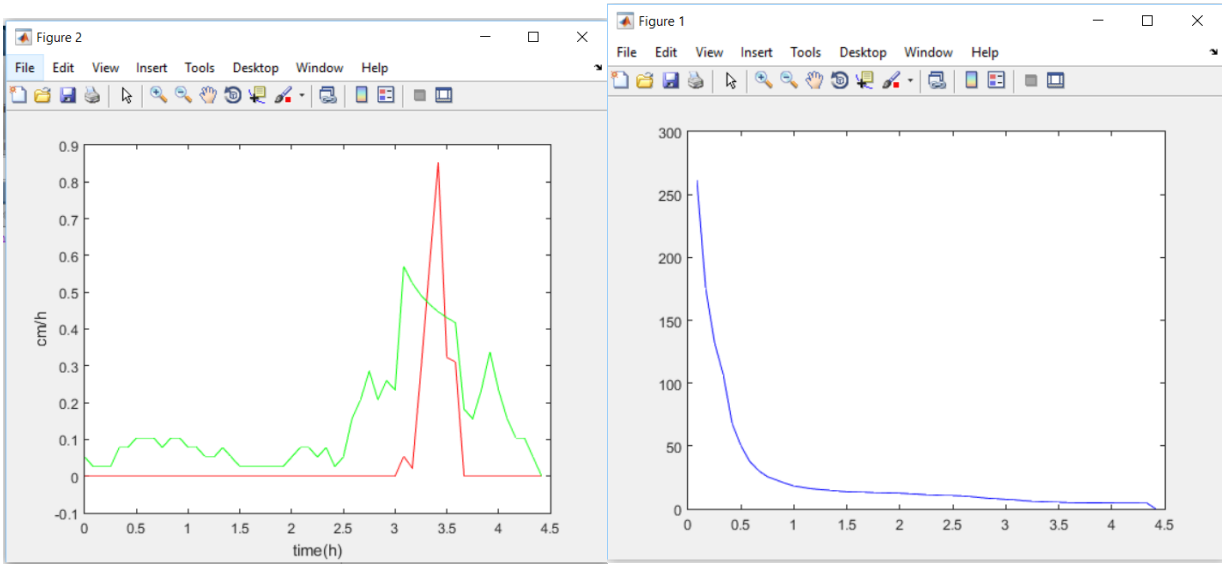
Figure 2
File Edit View Insert Tools Desktop Window Help
cm/h
time(h)
Figure 1
File Edit View Insert Tools Desktop Window Help

R29

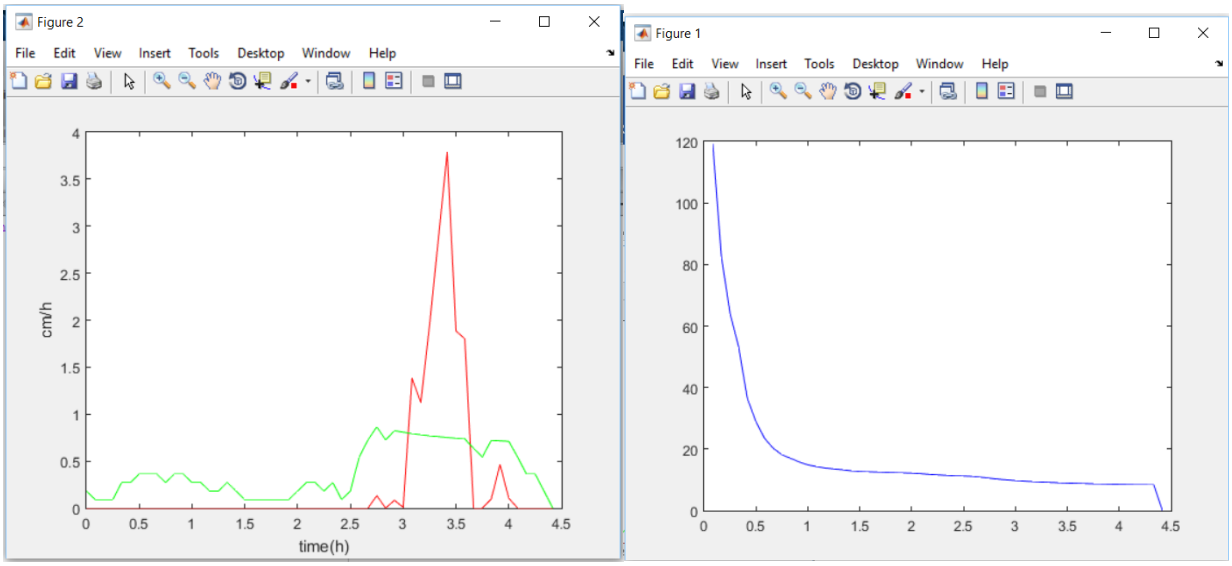
Figure 2
File Edit View Insert Tools Desktop Window Help
cm/h
time(h)
Figure 1
File Edit View Insert Tools Desktop Window Help

R44

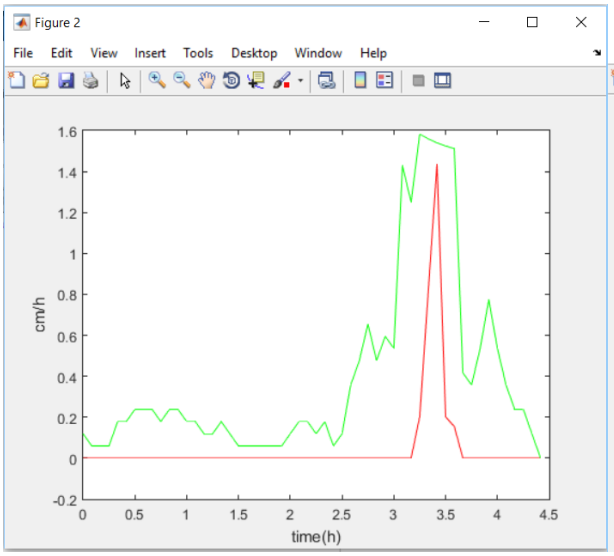
Figure 2
File Edit View Insert Tools Desktop Window Help
cm/h
time(h)

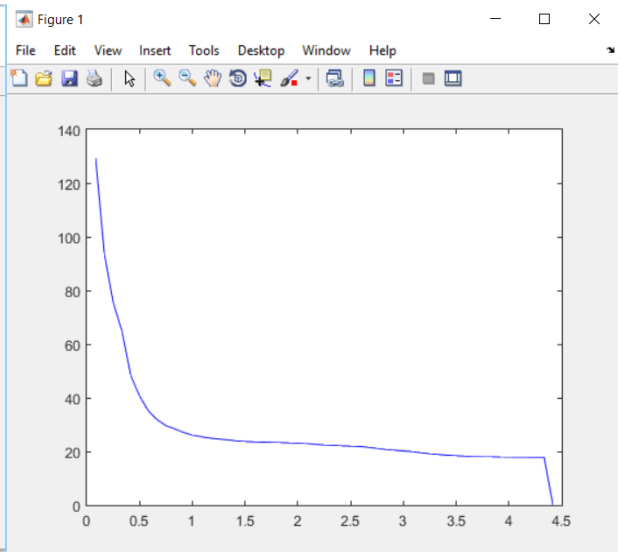
Figure 1
File Edit View Insert Tools Desktop Window Help

S10

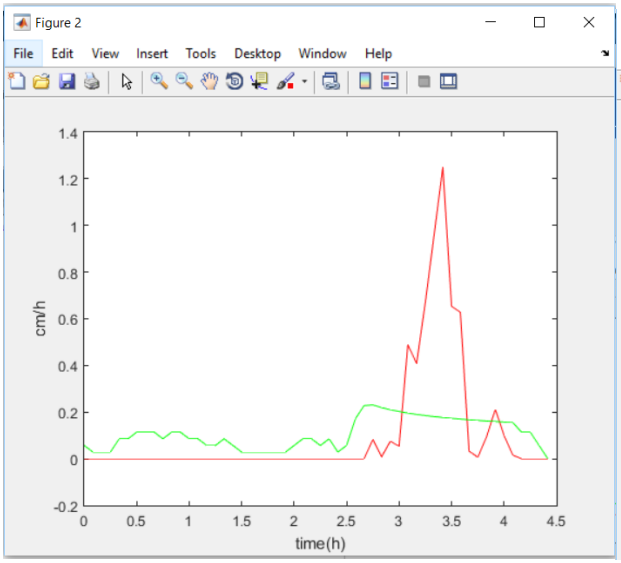
Figure 2
File Edit View Insert Tools Desktop Window Help
cm/h
time(h)

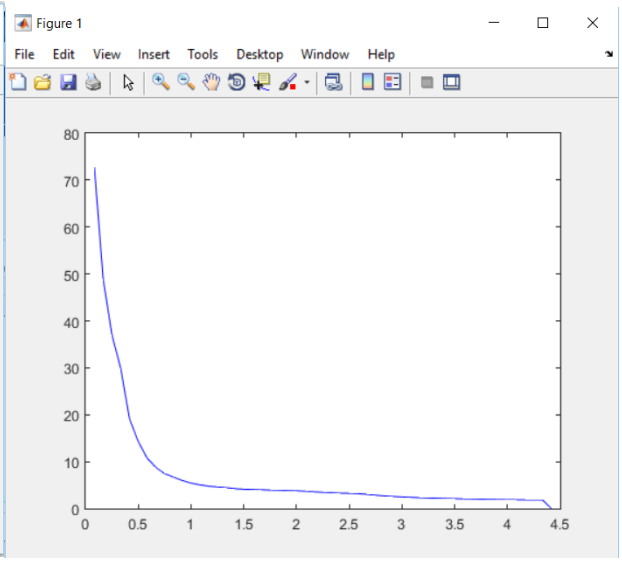
Figure 1
File Edit View Insert Tools Desktop Window Help

S75 (with loamy soil)

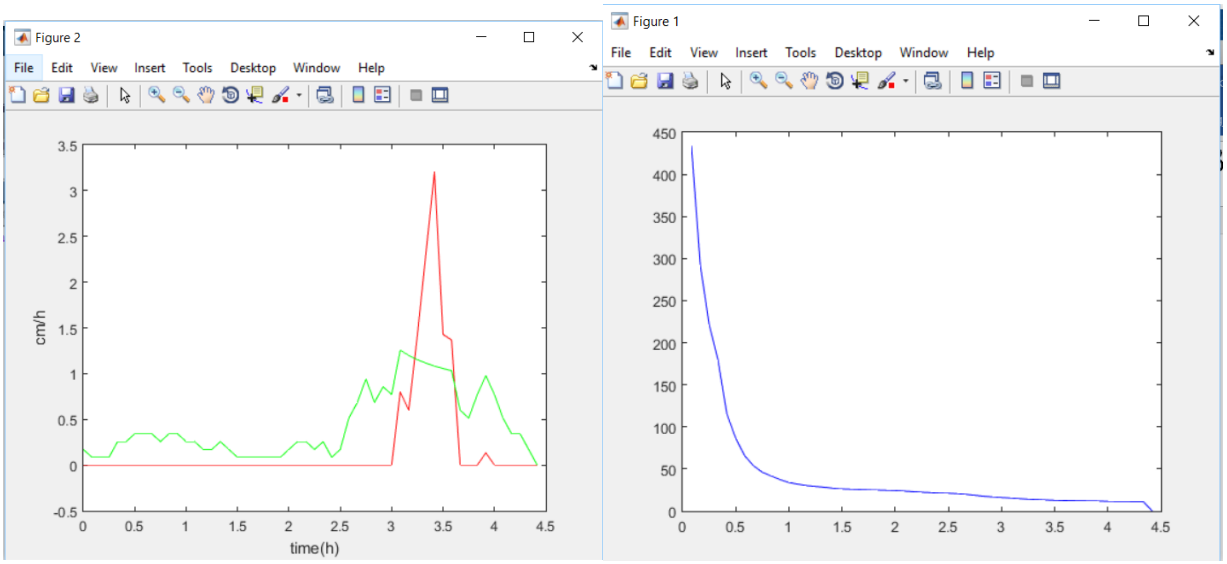

S75 (with sandy loam)

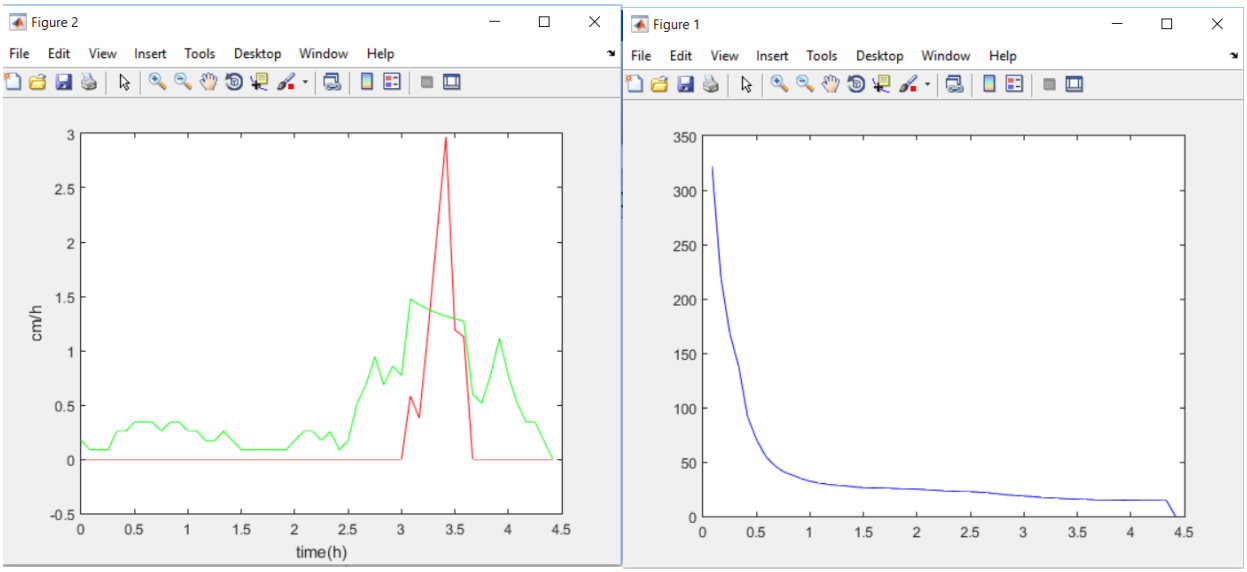

The different sites in Trondheim

Site 1: loamy sand

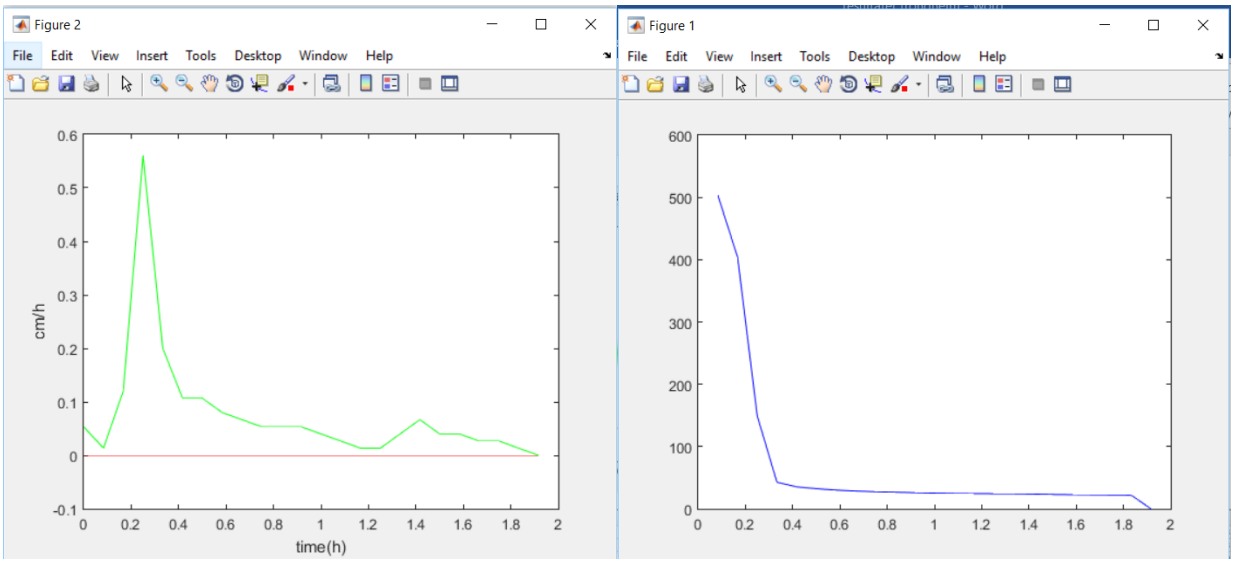

Site 2: loamy sand

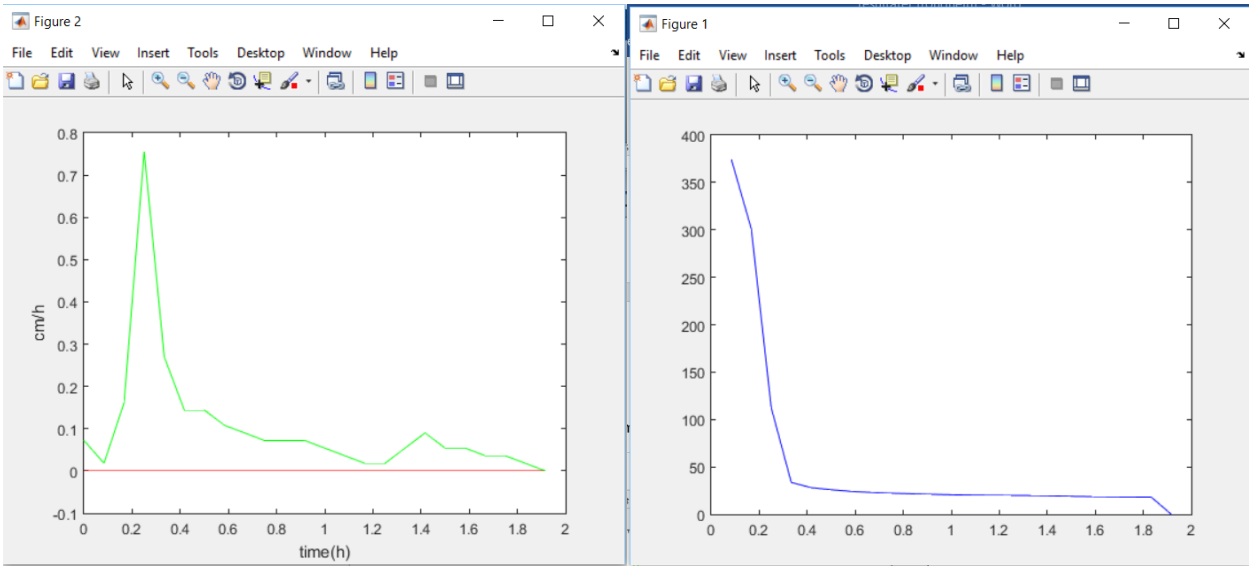

Site 2: sandy loam

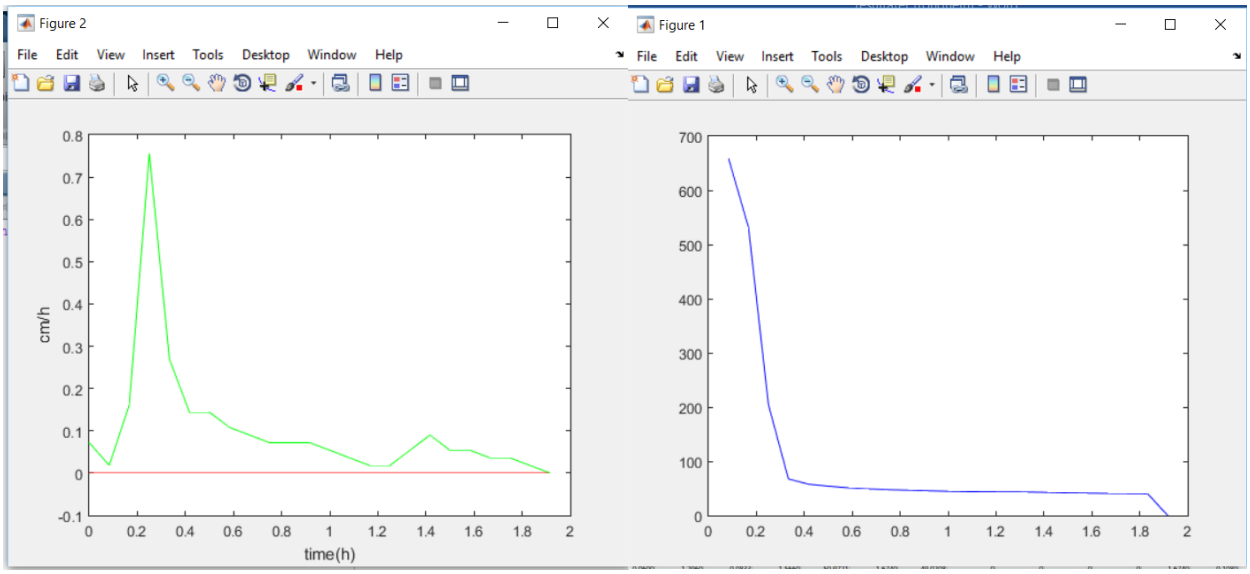

Site 3: sandy loam

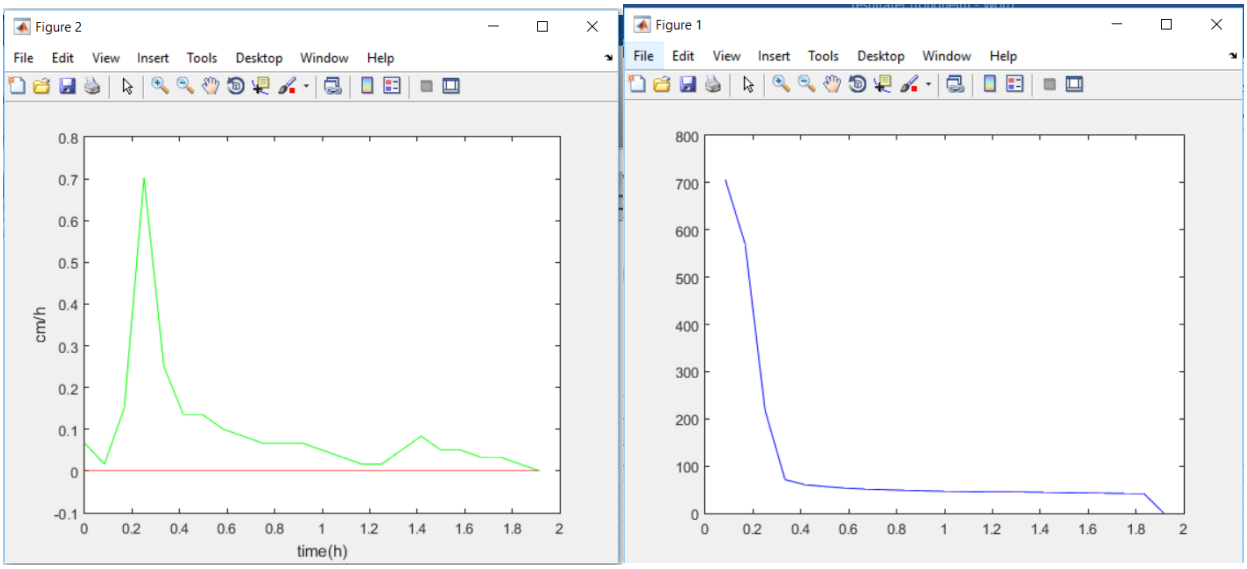

Site 3: loamy sand

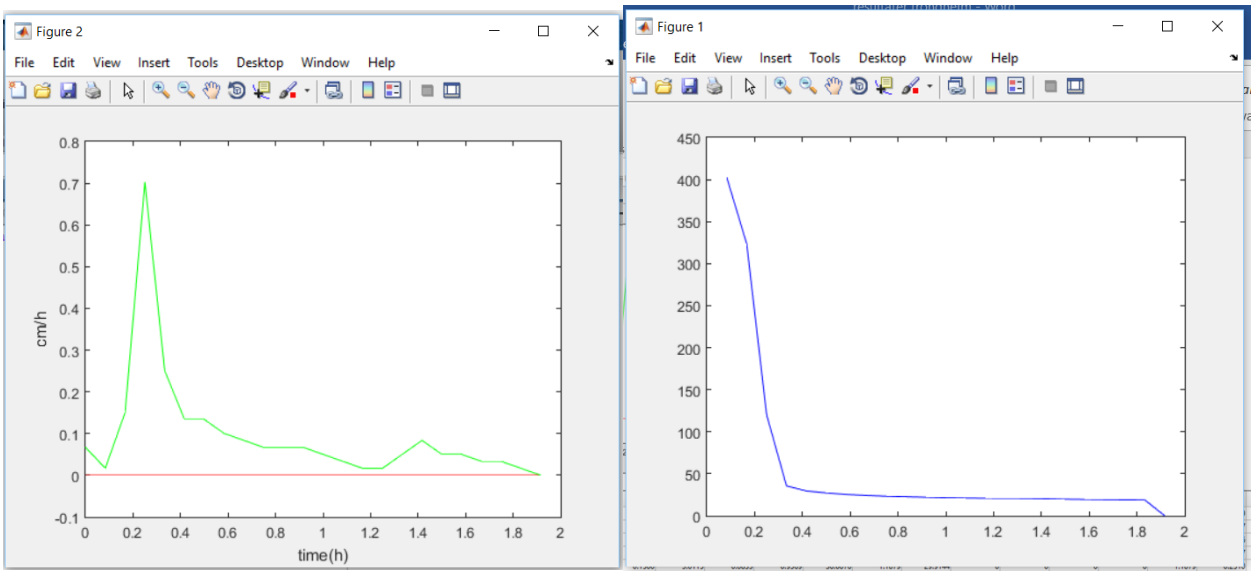

Site 4: loamy sand

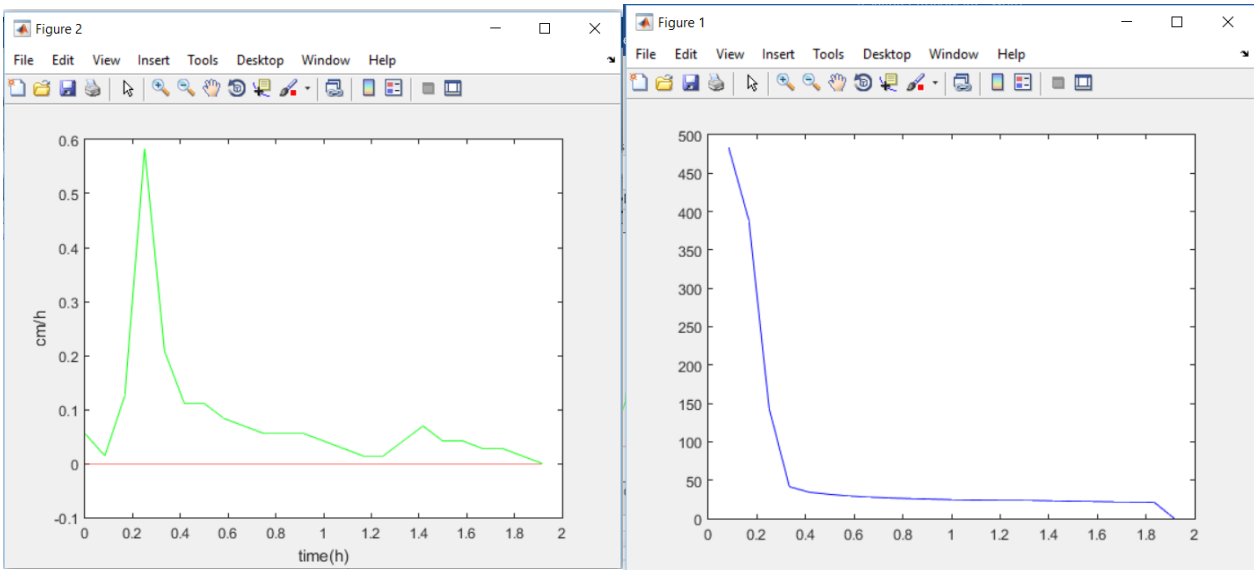

Results: Initial soil moisture content equal to the field capacity

Calculations done by using Green- Ampt infiltration model

The different sites in Oslo

S10

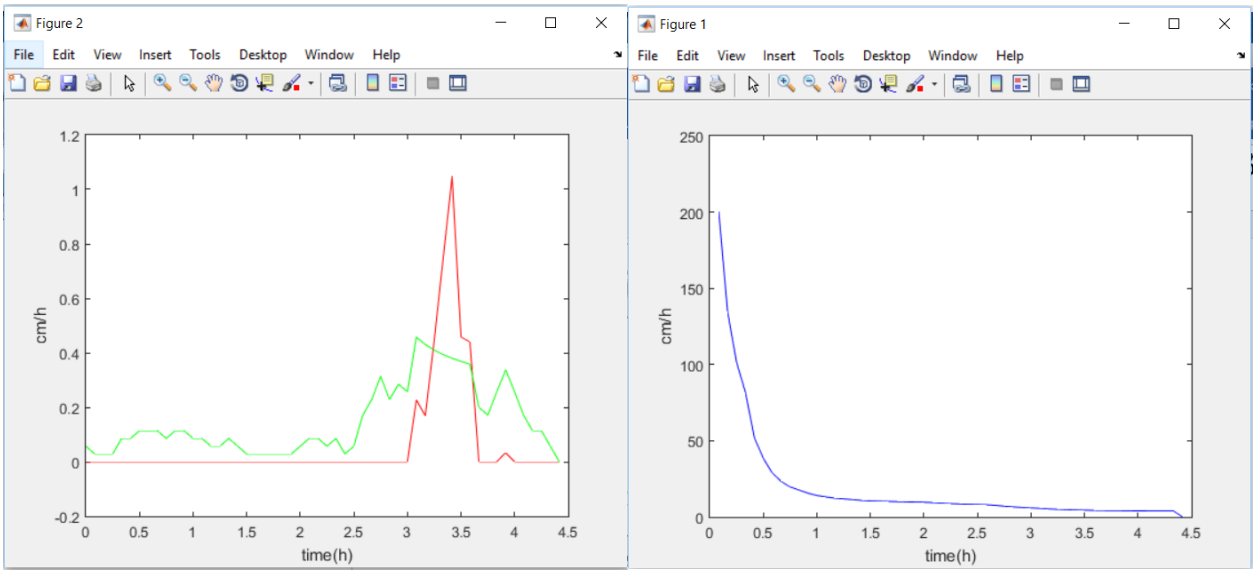

L34

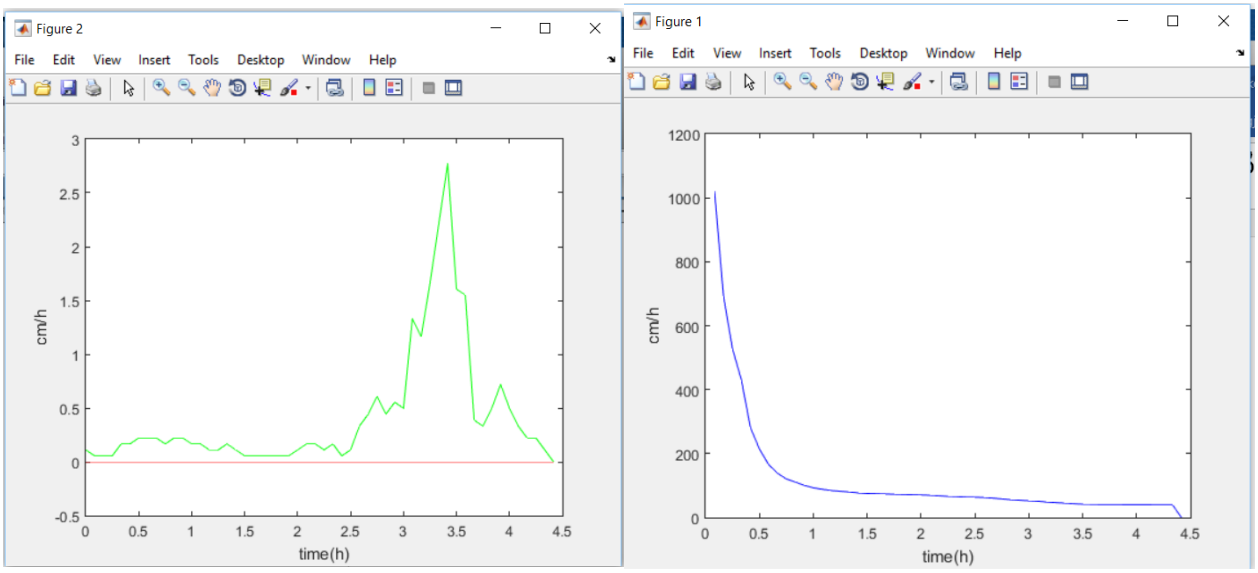

B28ab

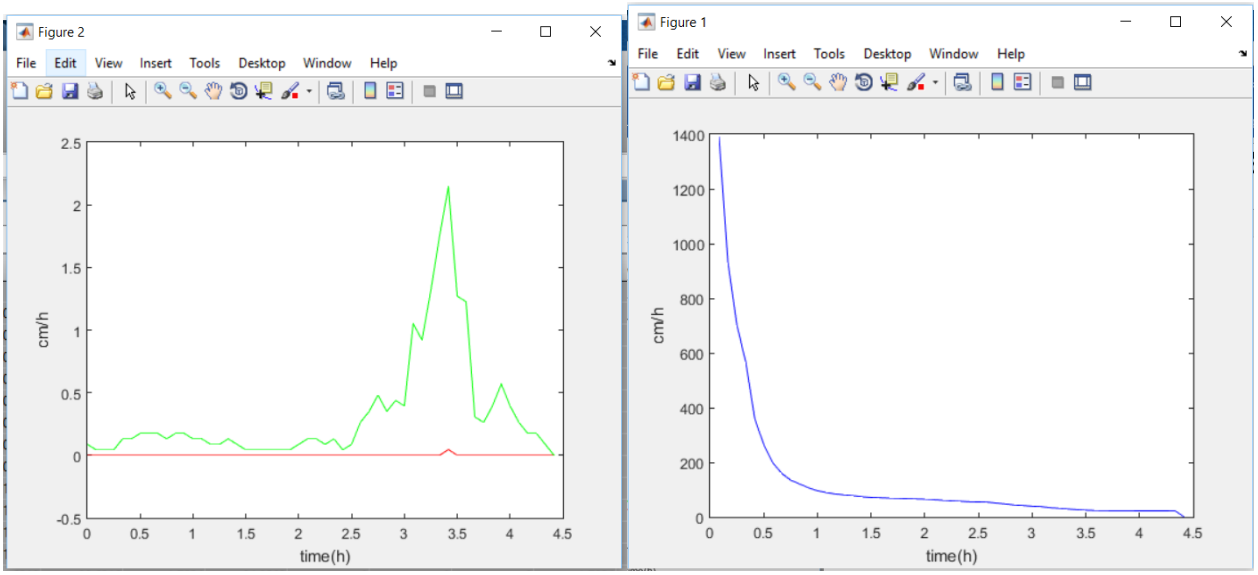
Figure 2
File Edit View Insert Tools Desktop Window Help
cm/h
time(h)
Figure 1
File Edit View Insert Tools Desktop Window Help
cm/h
time(h)

B65

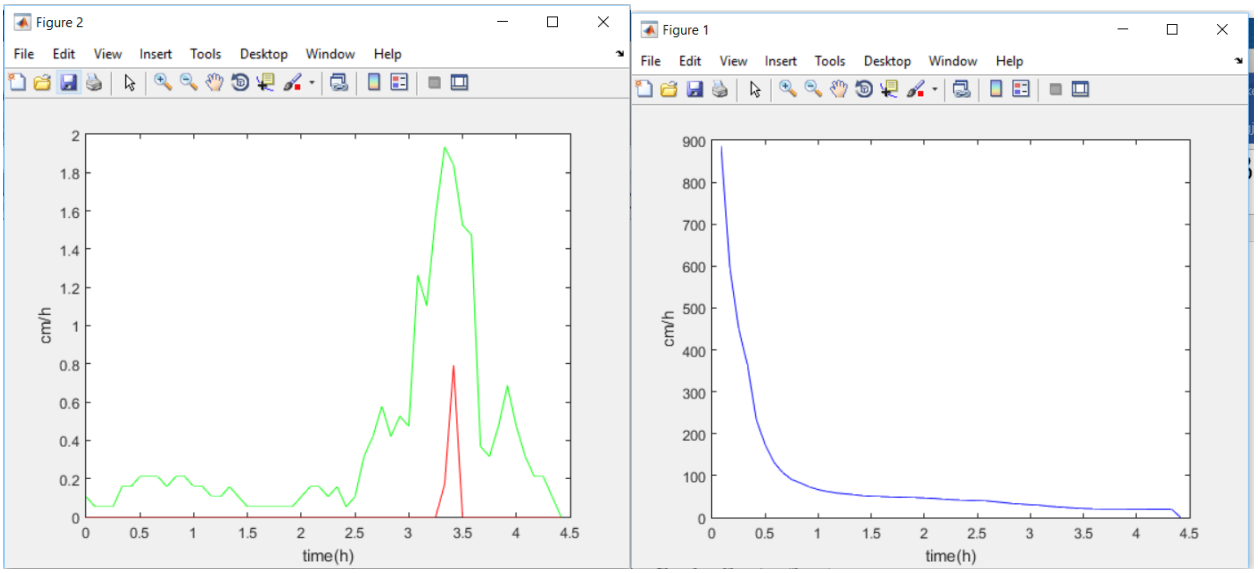
Figure 2
File Edit View Insert Tools Desktop Window Help
cm/h
time(h)
Figure 1
File Edit View Insert Tools Desktop Window Help
cm/h
time(h)

R44

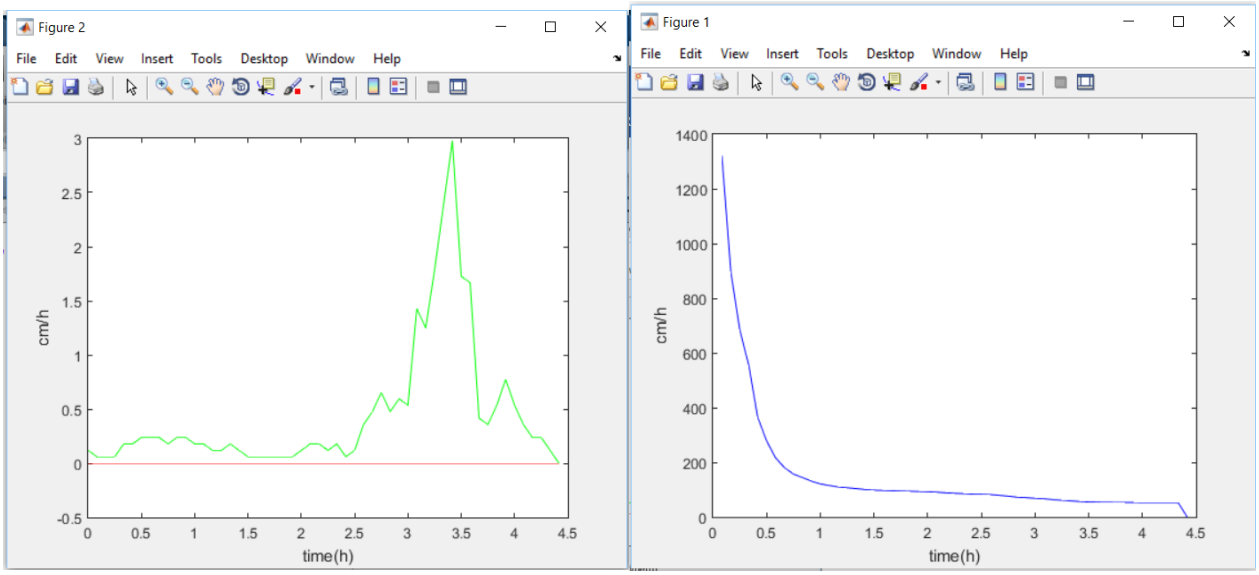

The different sites in Trondheim

Site 1: loamy sand

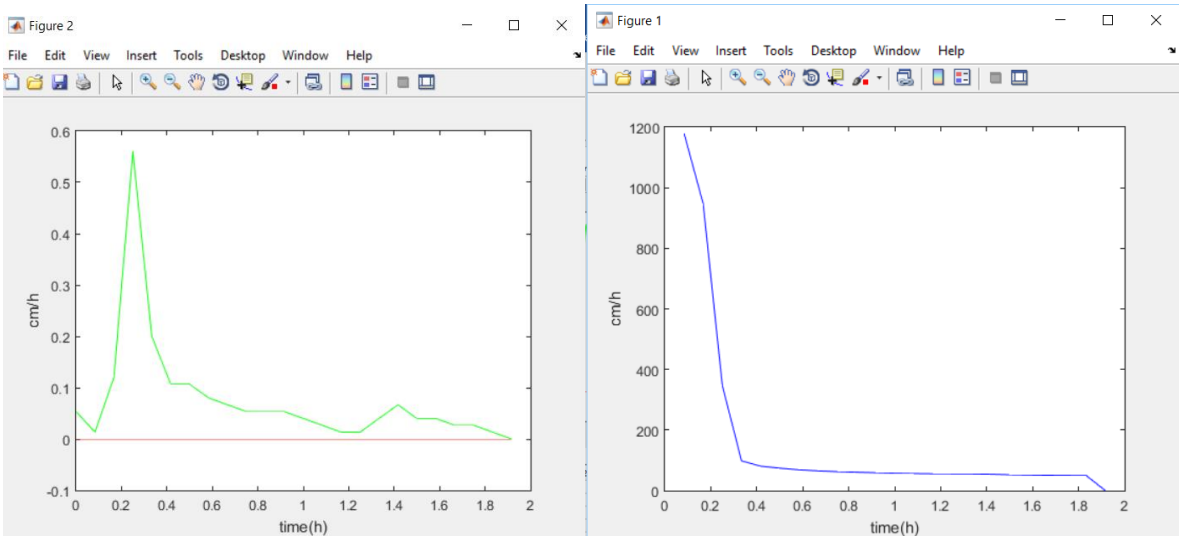

Site 3: sandy loam

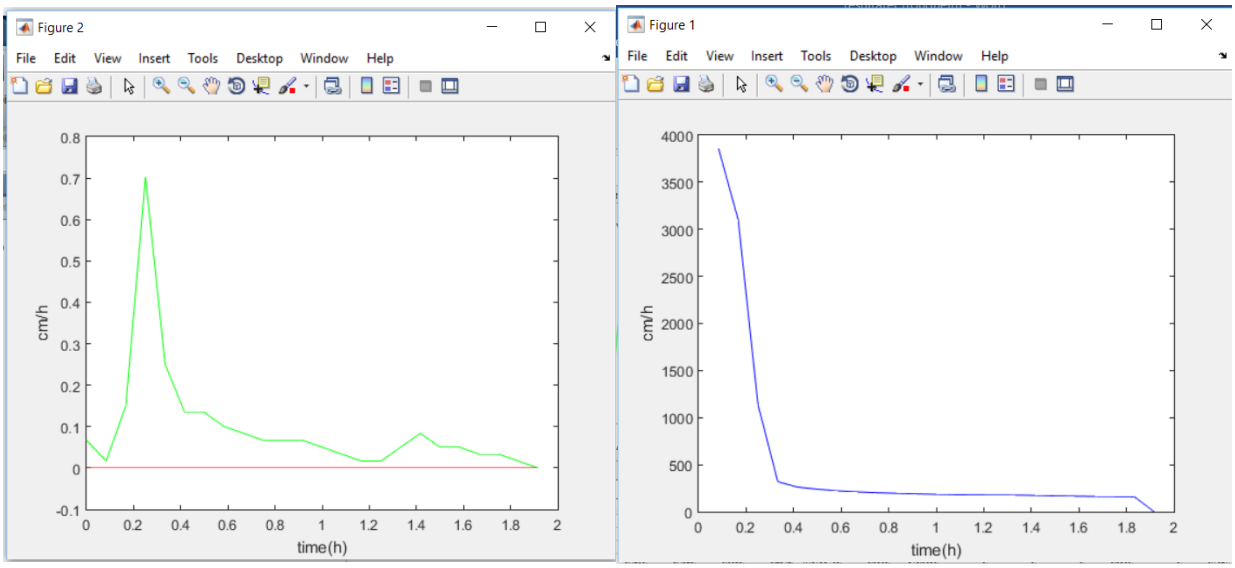

Computation done with Philip infiltration model

The different sites in Oslo

S10

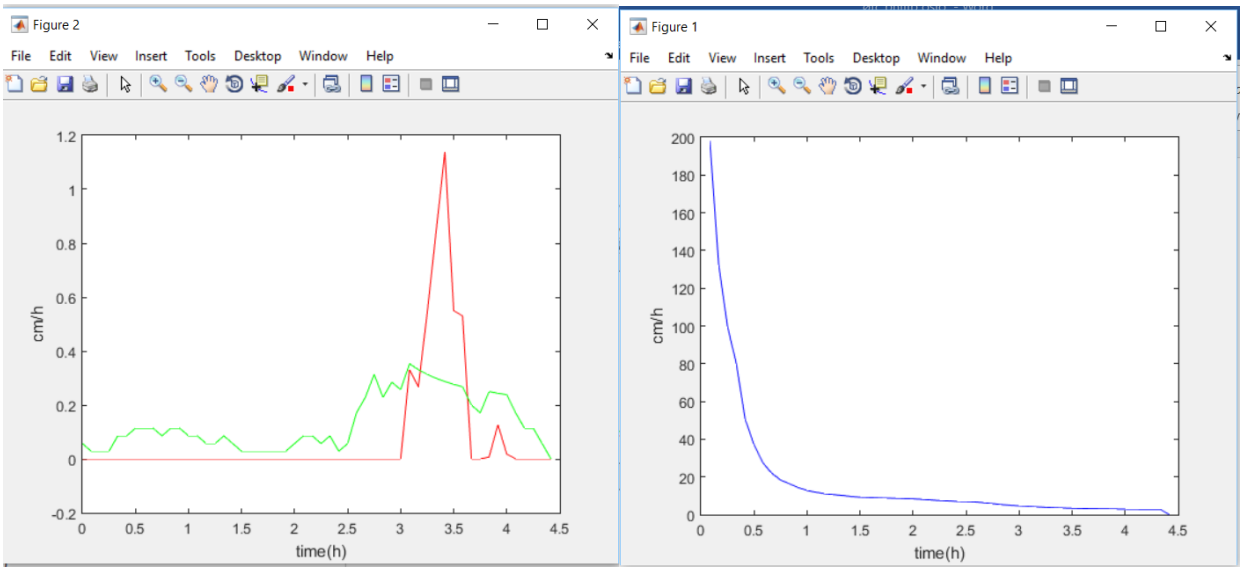

L34

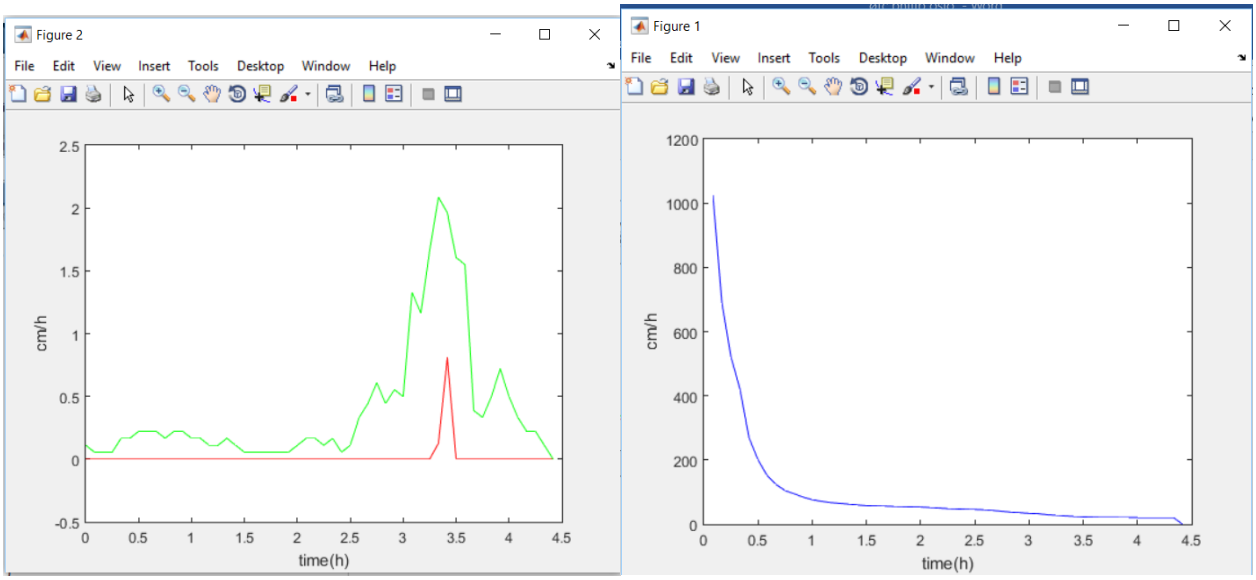
Figure 2
File Edit View Insert Tools Desktop Window Help
cm/h
time(h)
Figure 1
File Edit View Insert Tools Desktop Window Help
cm/h
time(h)

B28

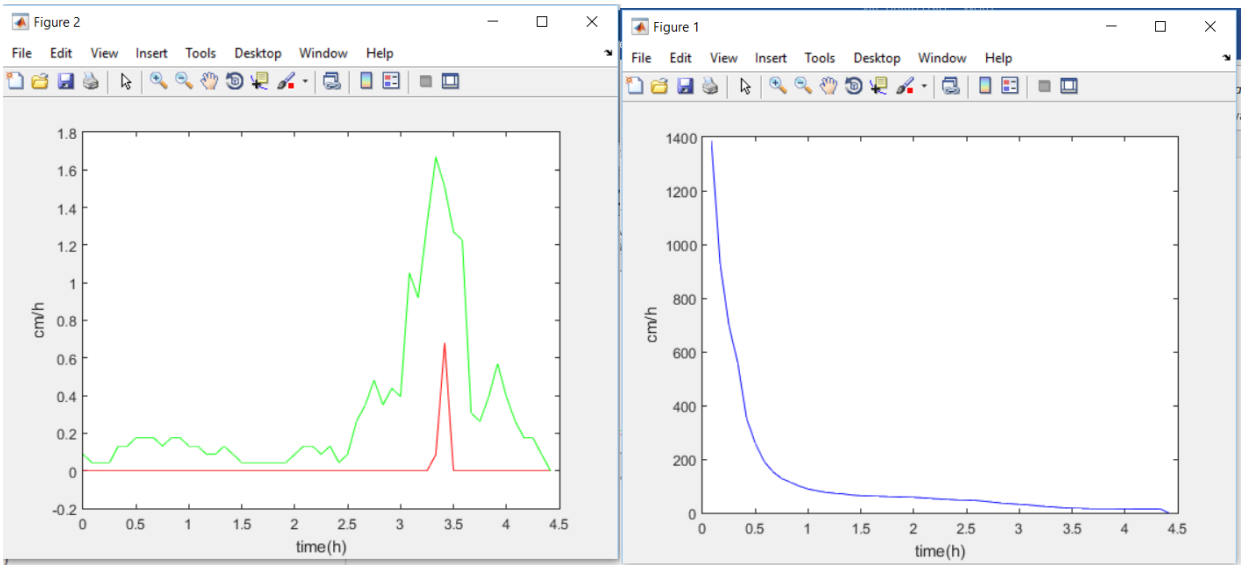
Figure 2
File Edit View Insert Tools Desktop Window Help
cm/h
time(h)
Figure 1
File Edit View Insert Tools Desktop Window Help
cm/h
time(h)

B65

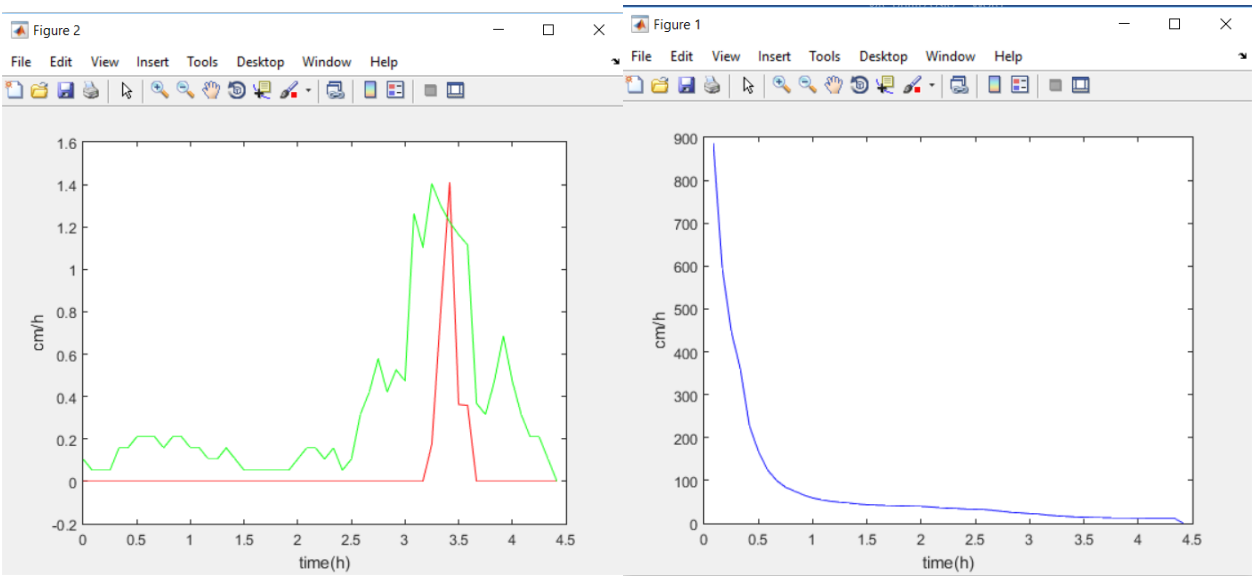
Figure 2
File Edit View Insert Tools Desktop Window Help
cm/h
time(h)
Figure 1
File Edit View Insert Tools Desktop Window Help
cm/h
time(h)

R44

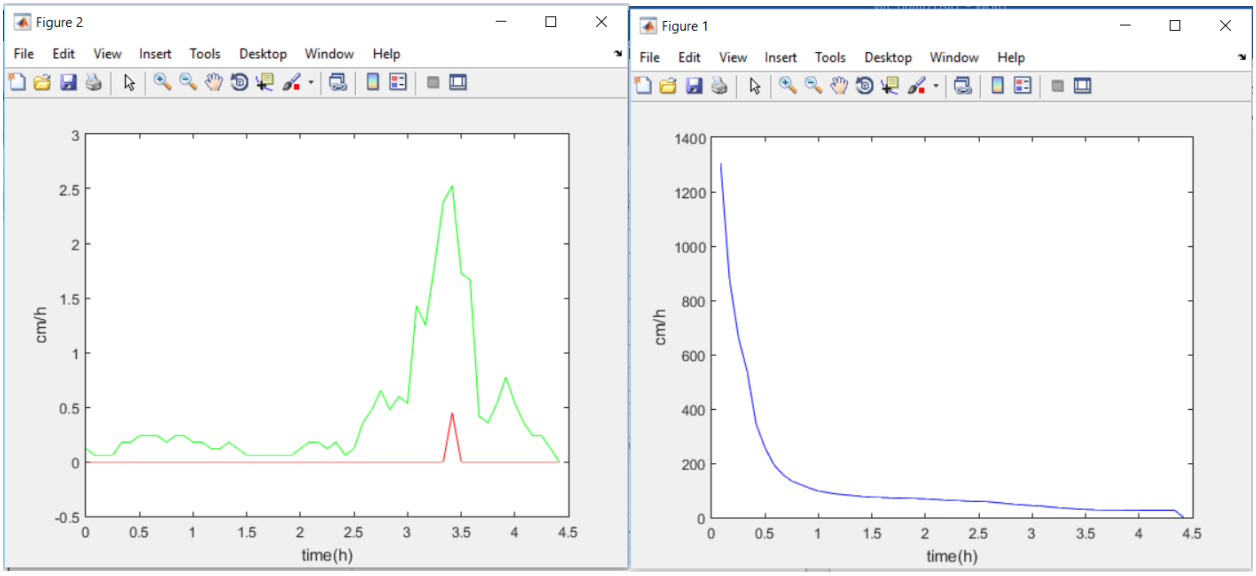
Figure 2
File Edit View Insert Tools Desktop Window Help
cm/h
time(h)
Figure 1
File Edit View Insert Tools Desktop Window Help
cm/h
time(h)

The different sites in Trondheim:

Site 1

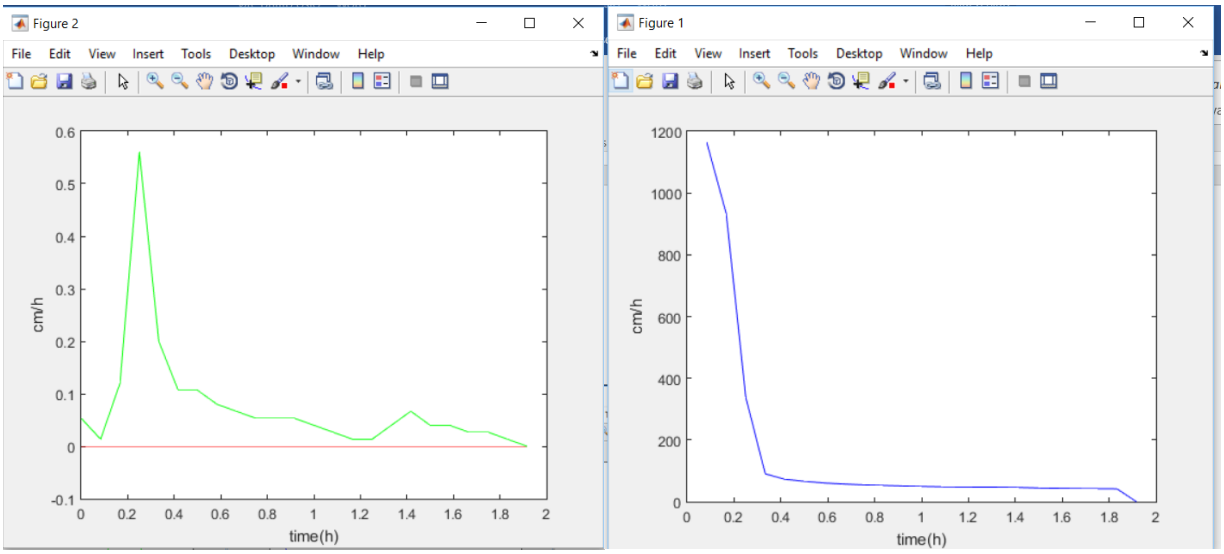

Site 3 sandy loam

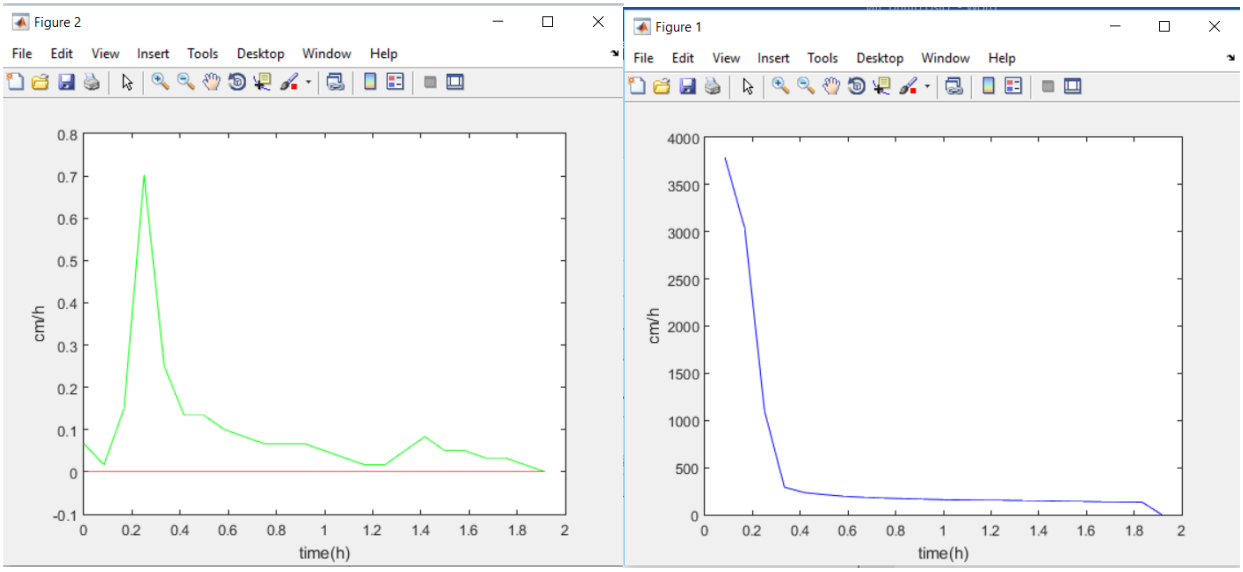

Results: Initial soil moisture content equal to the porosity

Computed by using Green-Ampt infiltration model

The different sites in Oslo

S10

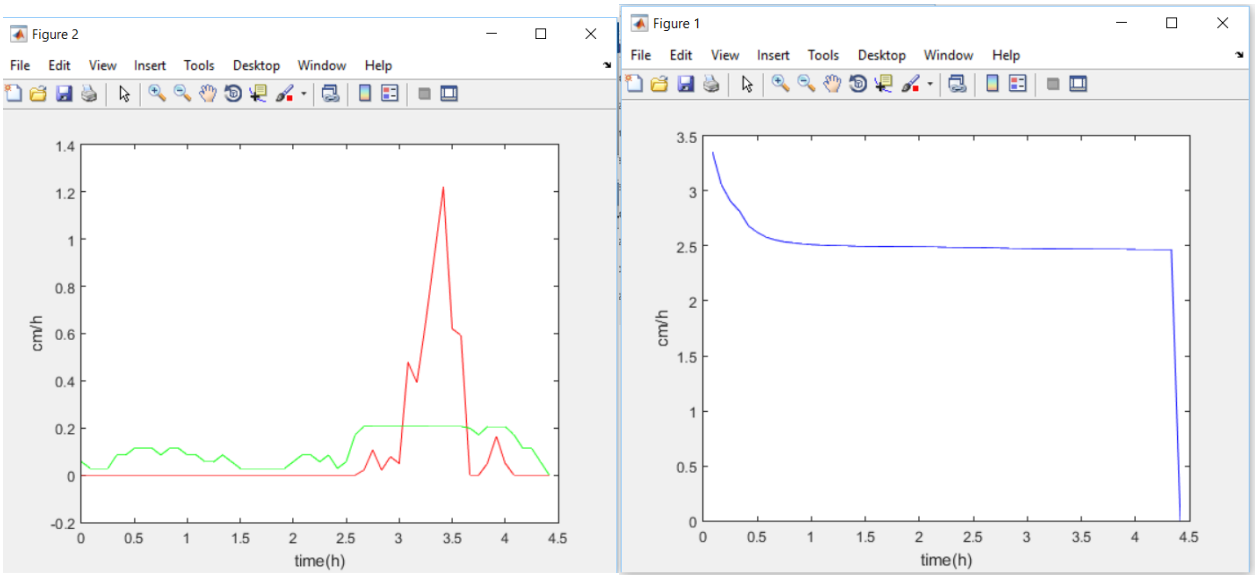

L34

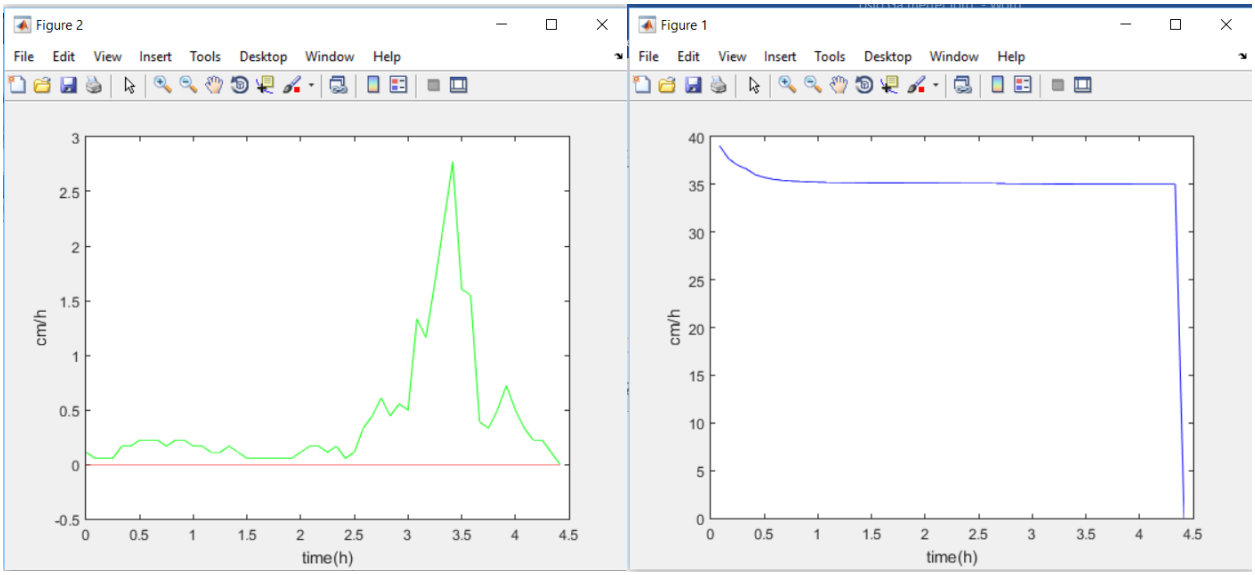

B28

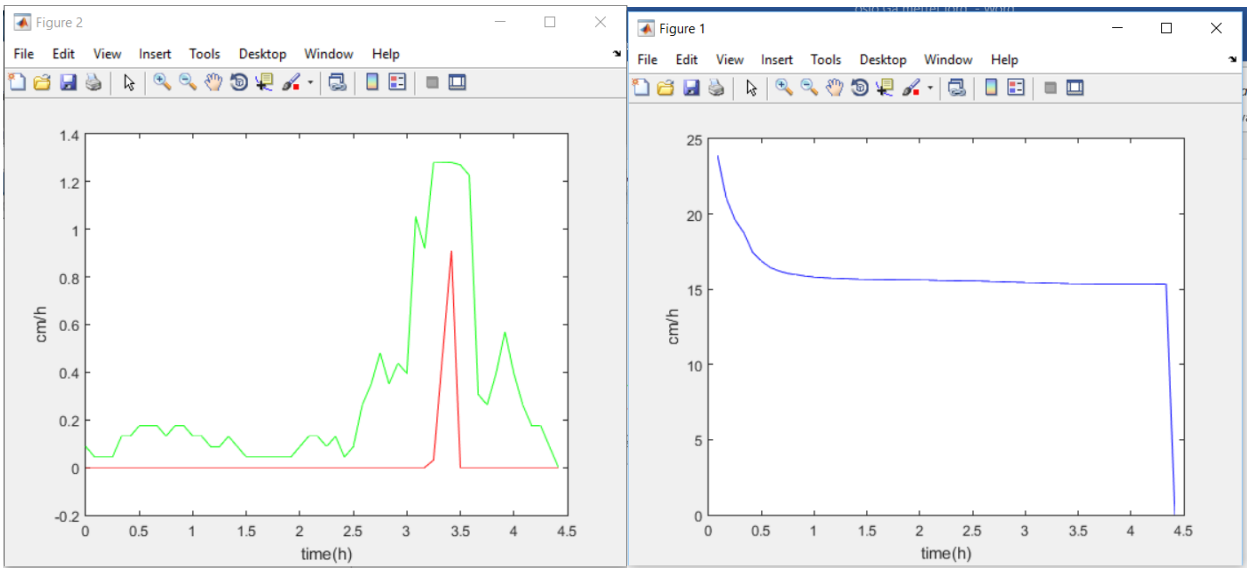
Figure 2
File Edit View Insert Tools Desktop Window Help
cm/h
time(h)
Figure 1
File Edit View Insert Tools Desktop Window Help
cm/h
time(h)

B65

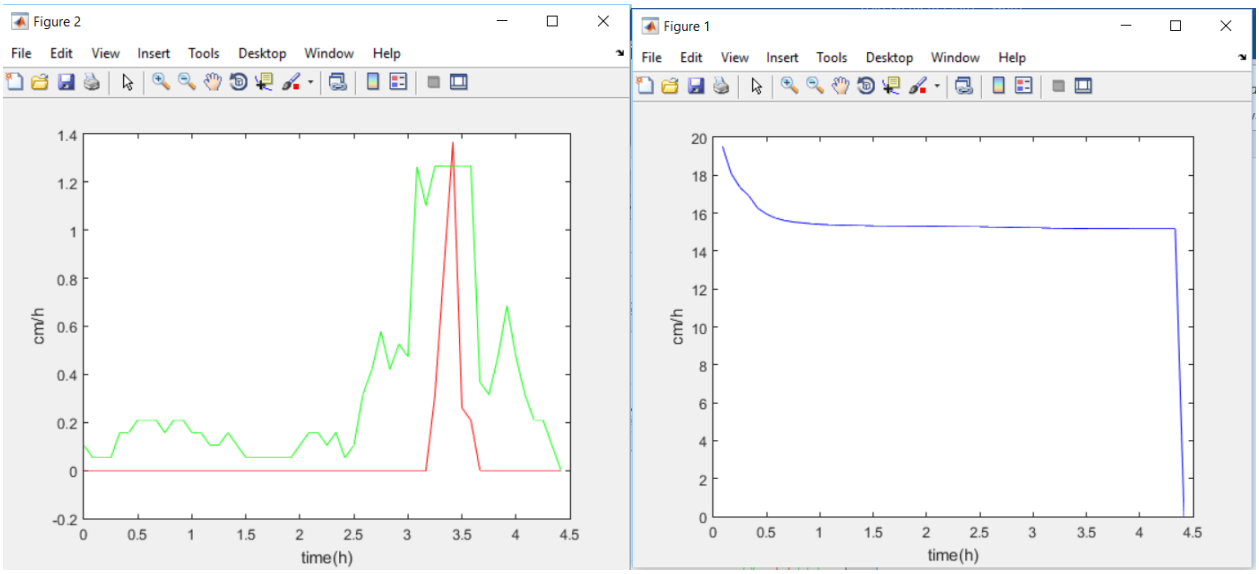
Figure 2
File Edit View Insert Tools Desktop Window Help
cm/h
time(h)
Figure 1
File Edit View Insert Tools Desktop Window Help
cm/h
time(h)

R44

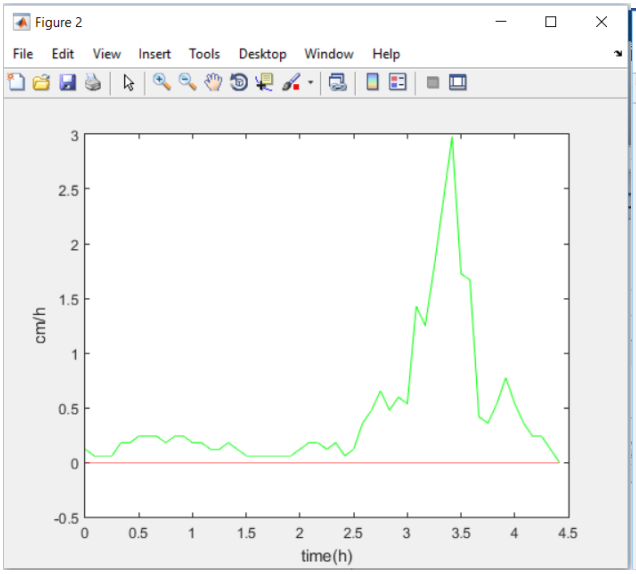

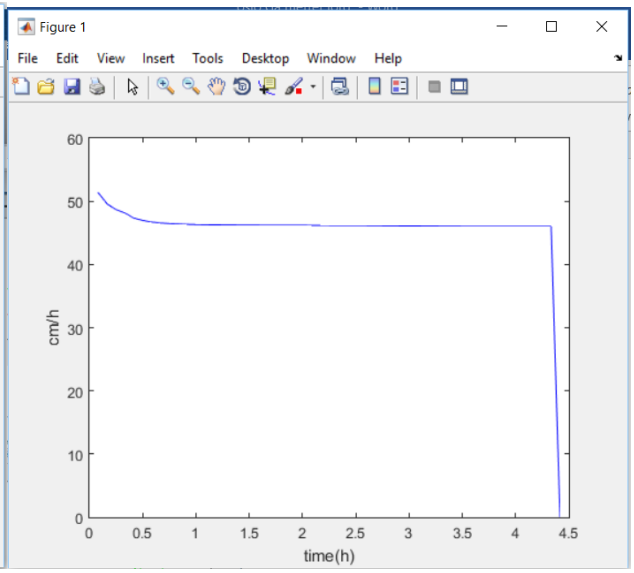

The different sites in Trondheim:

Site 1

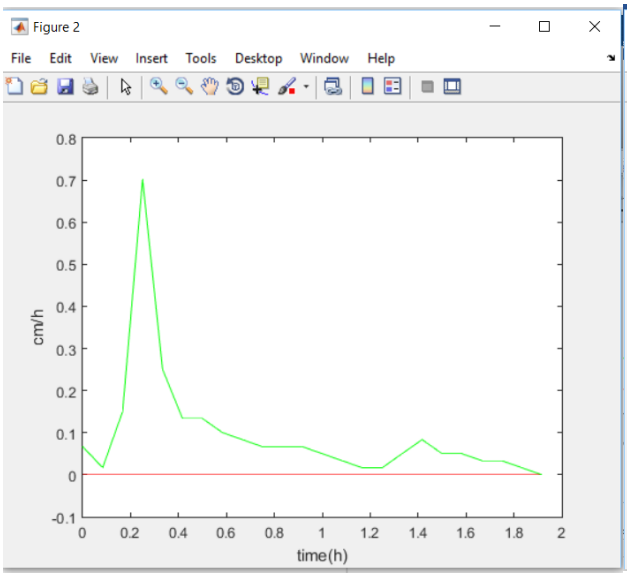

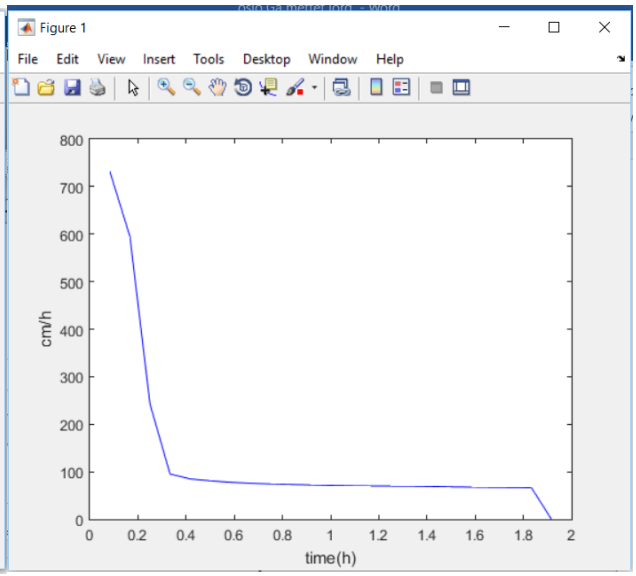

Site 3 with sandy loam

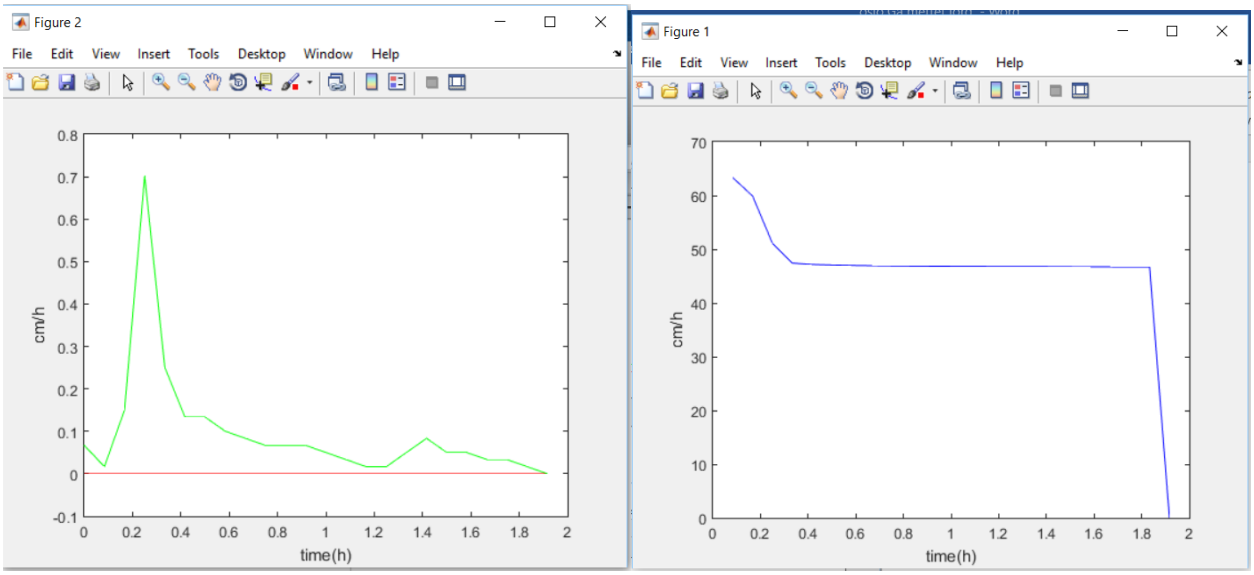

Calculated by using Philip infiltration model

The different sites in Oslo

S10

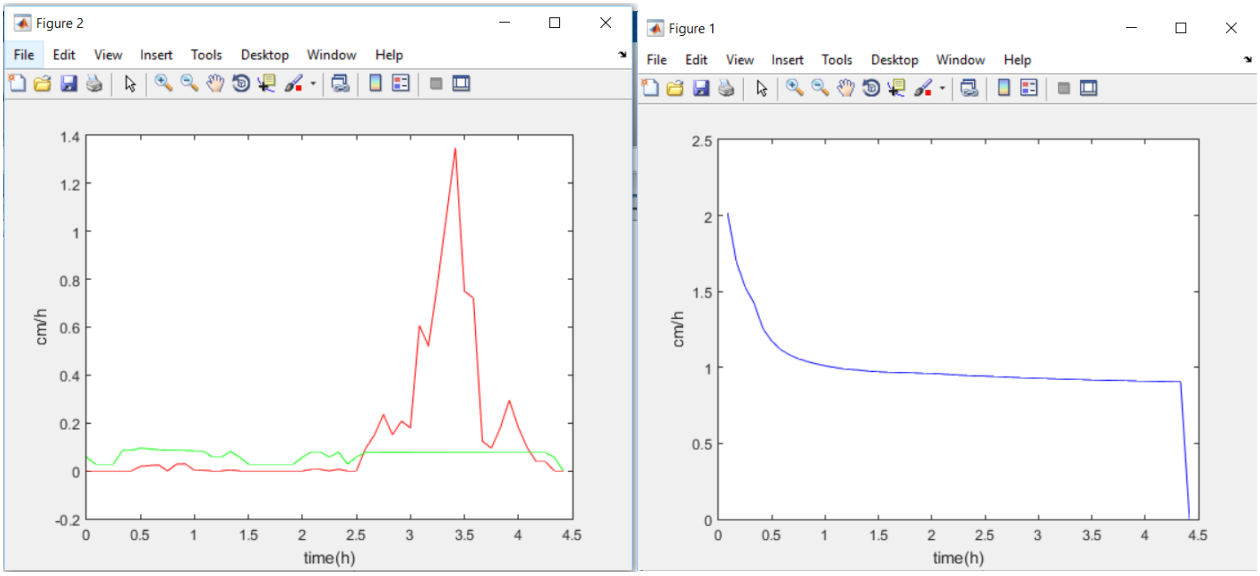

L34

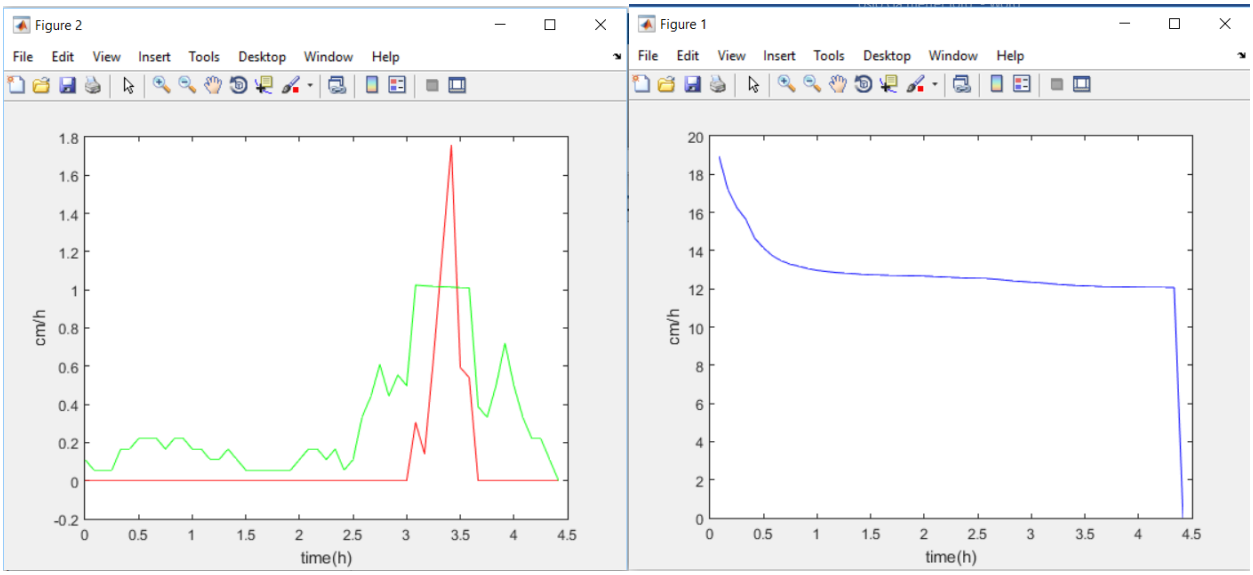
Figure 2
File Edit View Insert Tools Desktop Window Help
cm/h
time(h)
Figure 1
File Edit View Insert Tools Desktop Window Help
cm/h
time(h)

B28

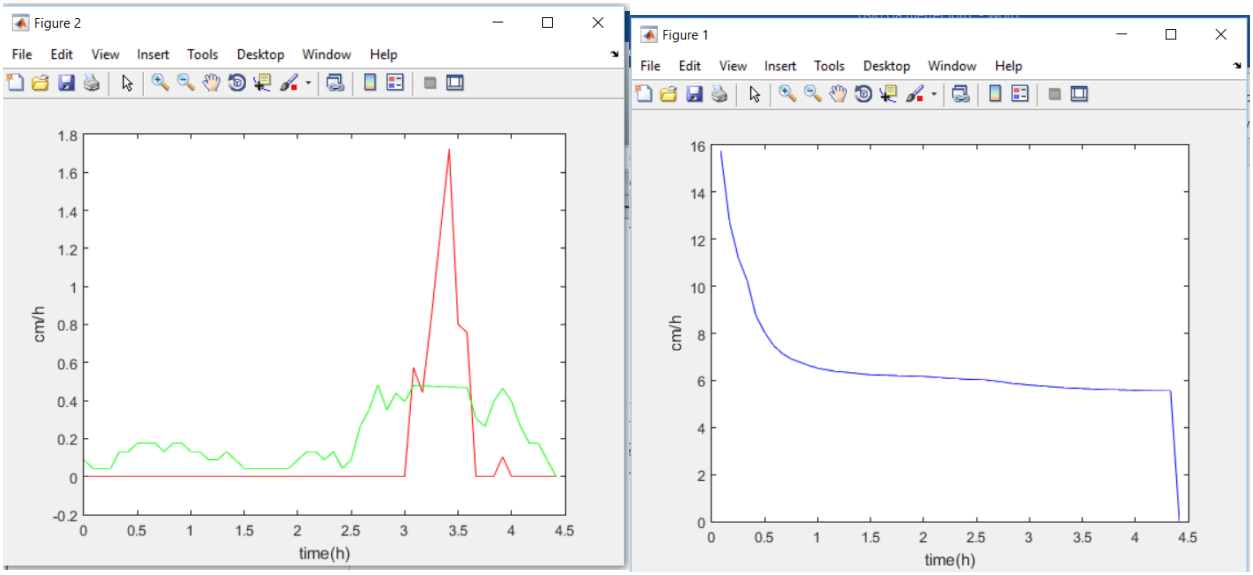
Figure 2
File Edit View Insert Tools Desktop Window Help
cm/h
time(h)
Figure 1
File Edit View Insert Tools Desktop Window Help
cm/h
time(h)

B65

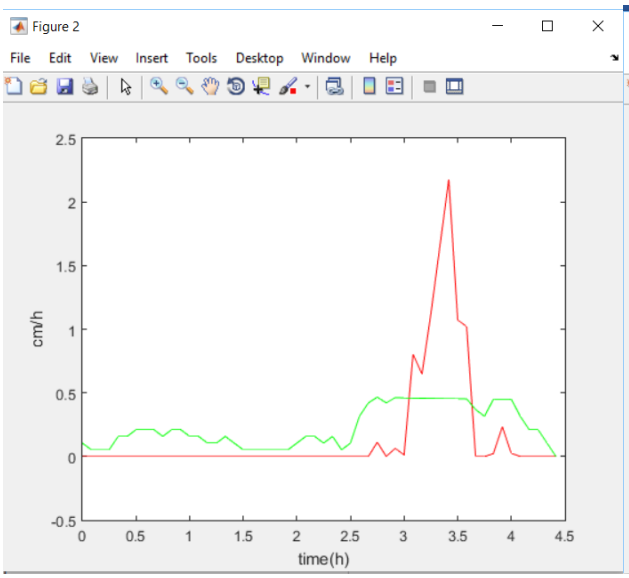
Figure 2
File Edit View Insert Tools Desktop Window Help
cm/h
time(h)

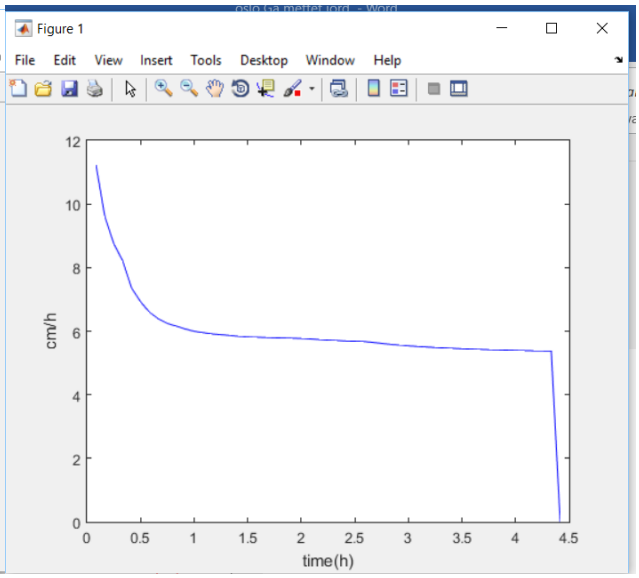
Figure 1
File Edit View Insert Tools Desktop Window Help
cm/h
time(h)

R44

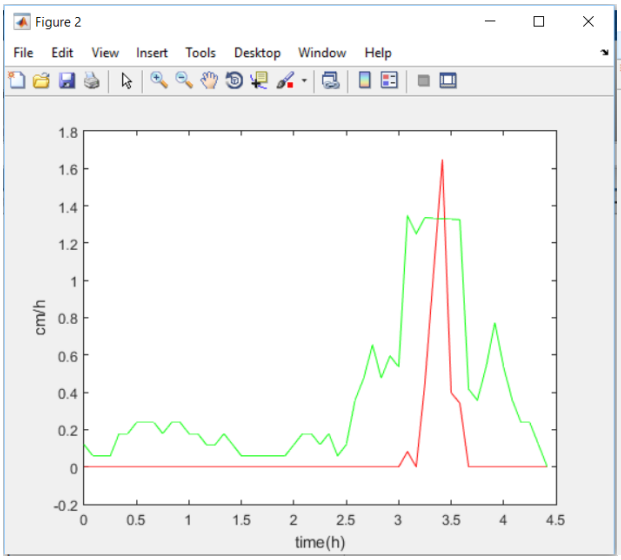
Figure 2
File Edit View Insert Tools Desktop Window Help
cm/h
time(h)

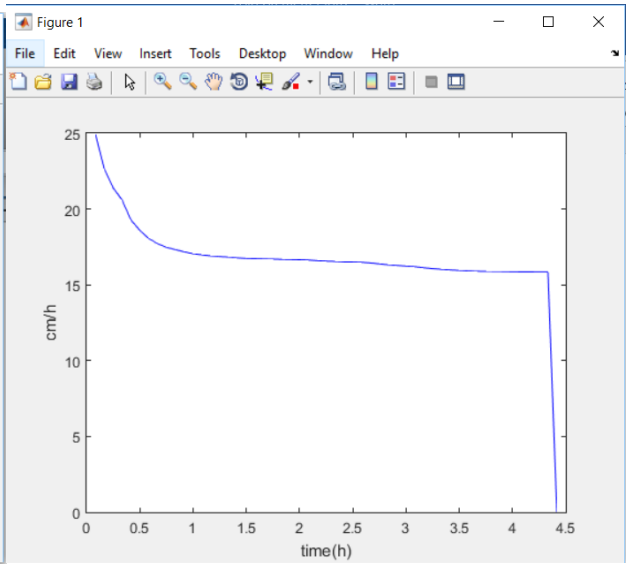
Figure 1
File Edit View Insert Tools Desktop Window Help
cm/h
time(h)

The different sites in Trondheim

Site 1

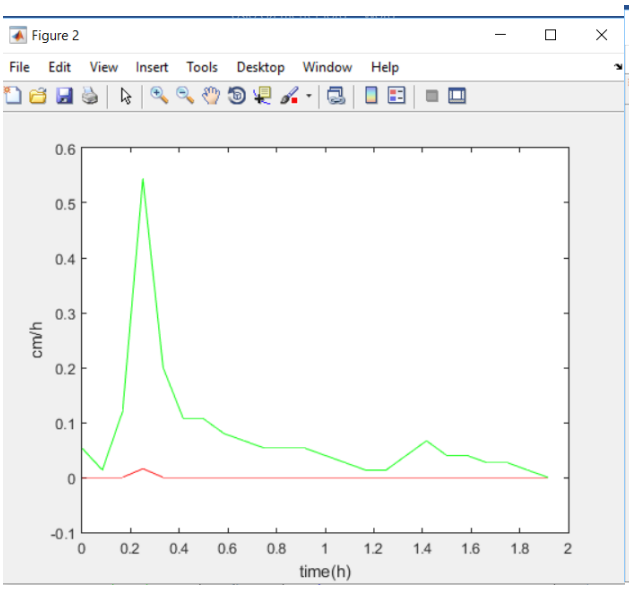

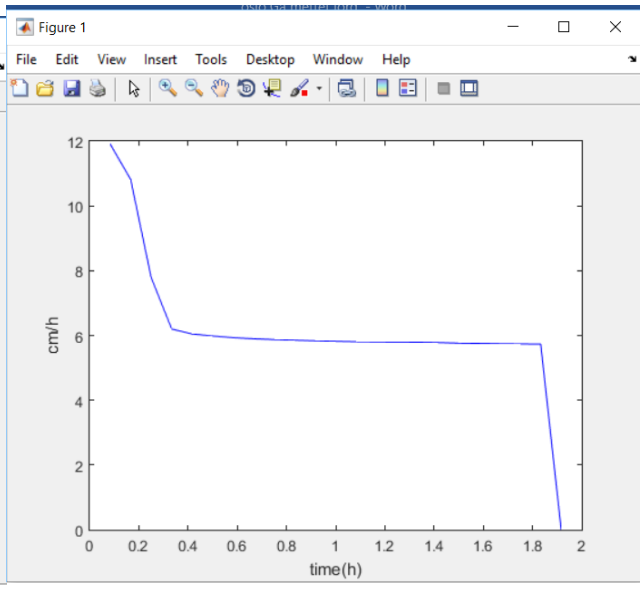

Site 3

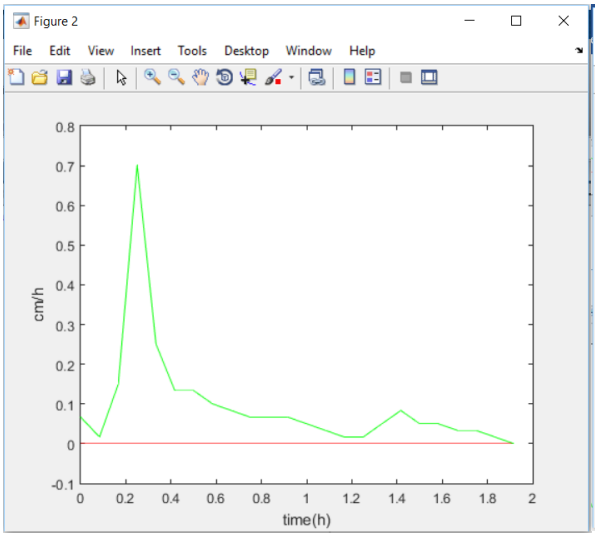

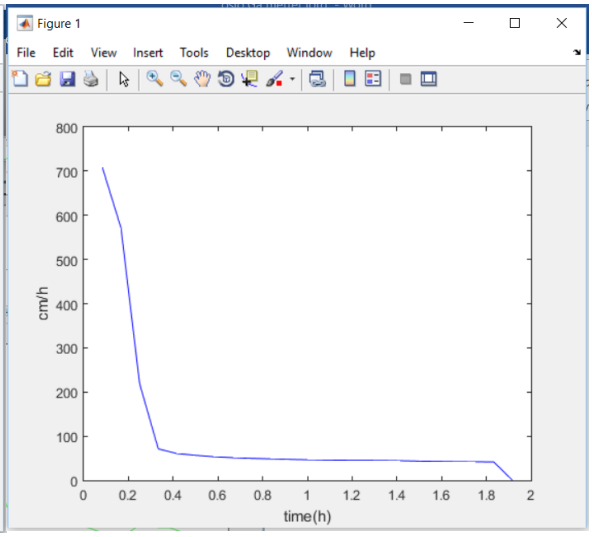

Results: Different K_{sat}- values

Computed by using Green-Ampt infiltration model

The different sites in Oslo

R5 ksat=0.059

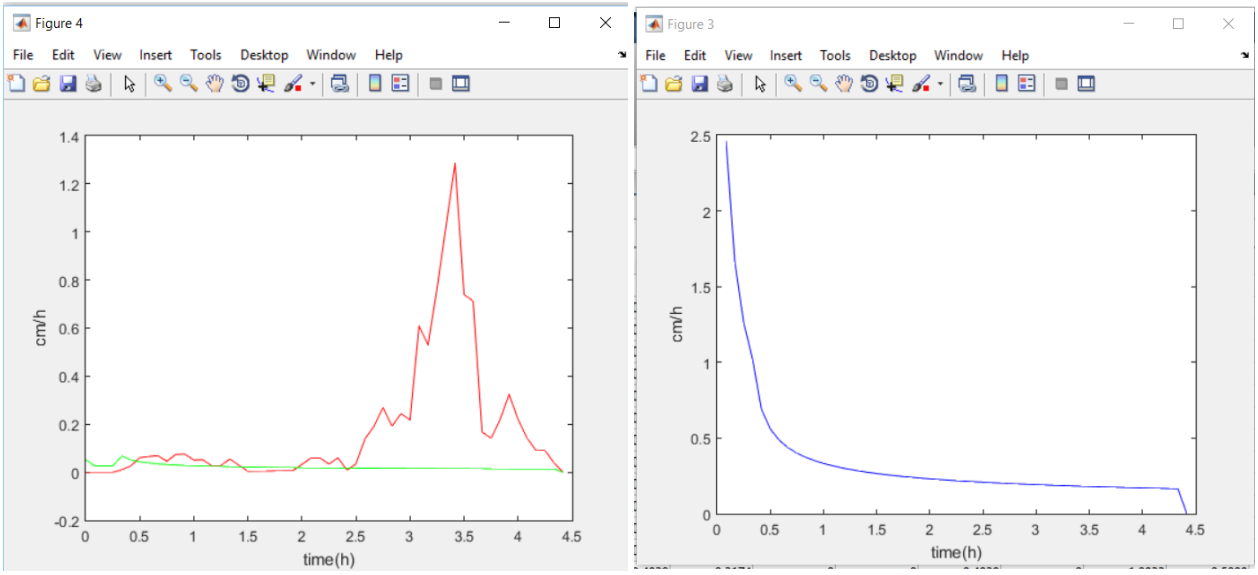

R 5 ksat= 20.021

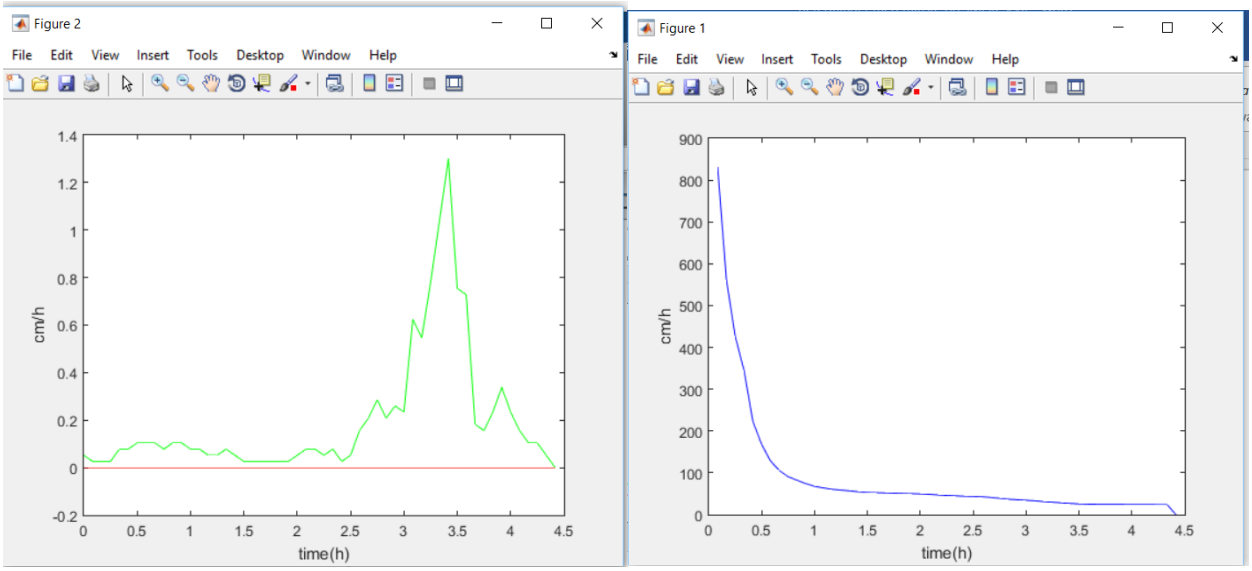

R44 ksat=12.939

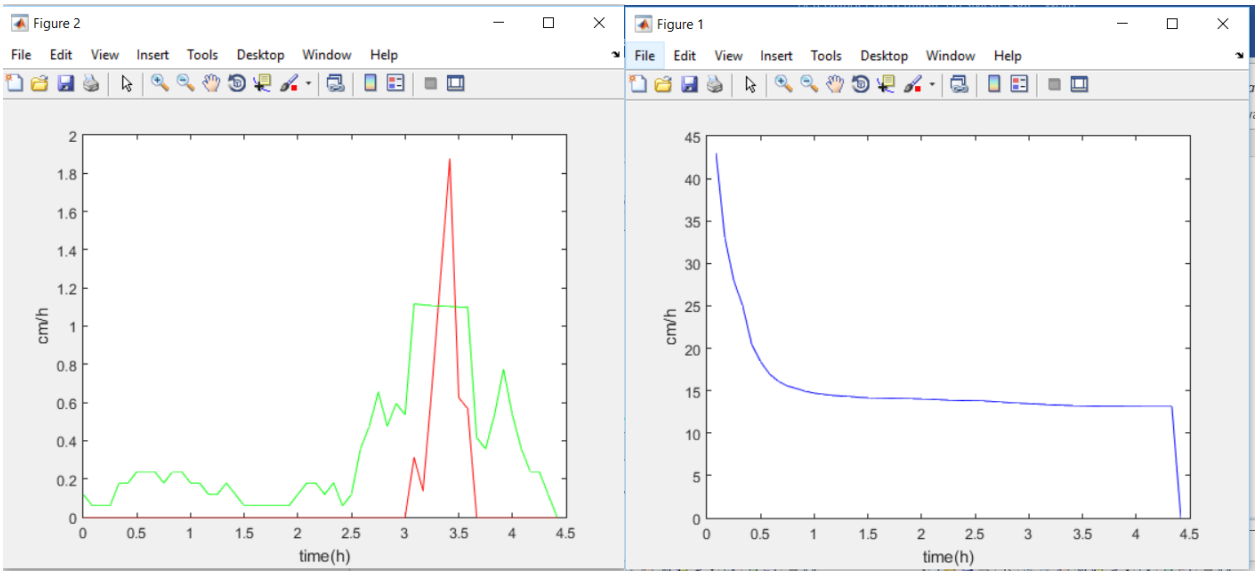

R44 ksat=88.82

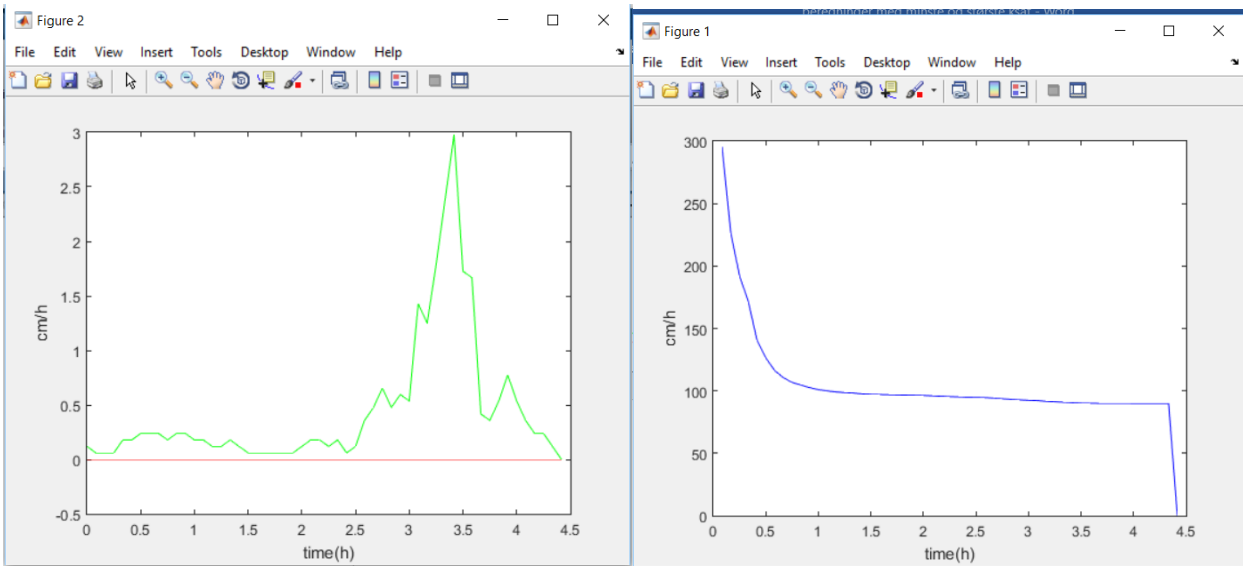

The different sites in Trondheim

Site ksat= 3.188 sandy loam

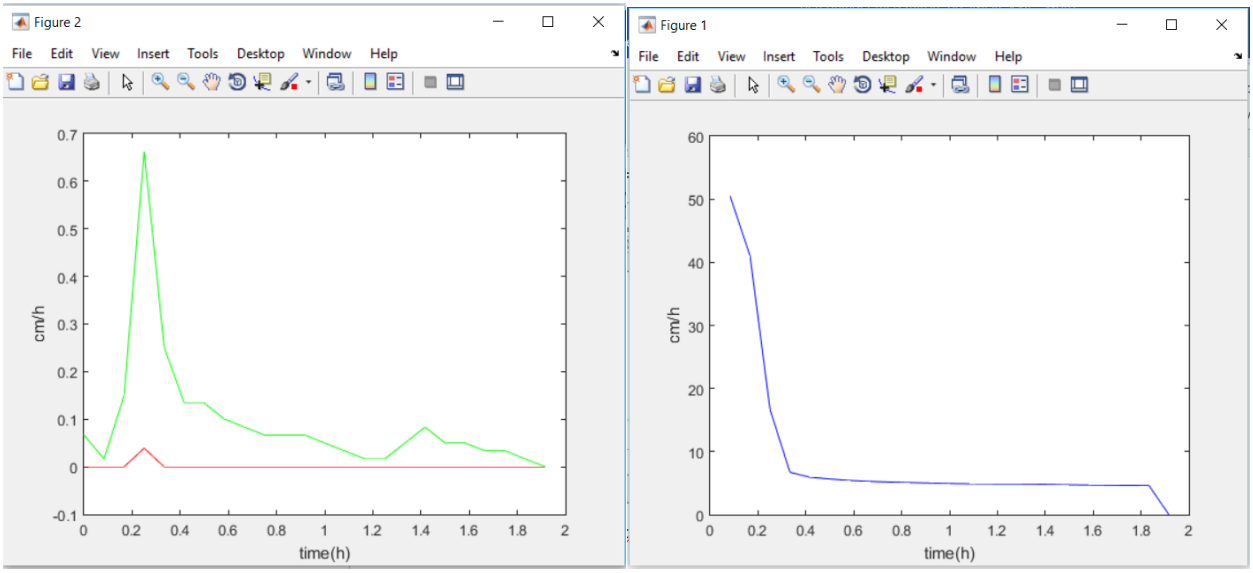

Site 3 ksat=3.188 loamy sand

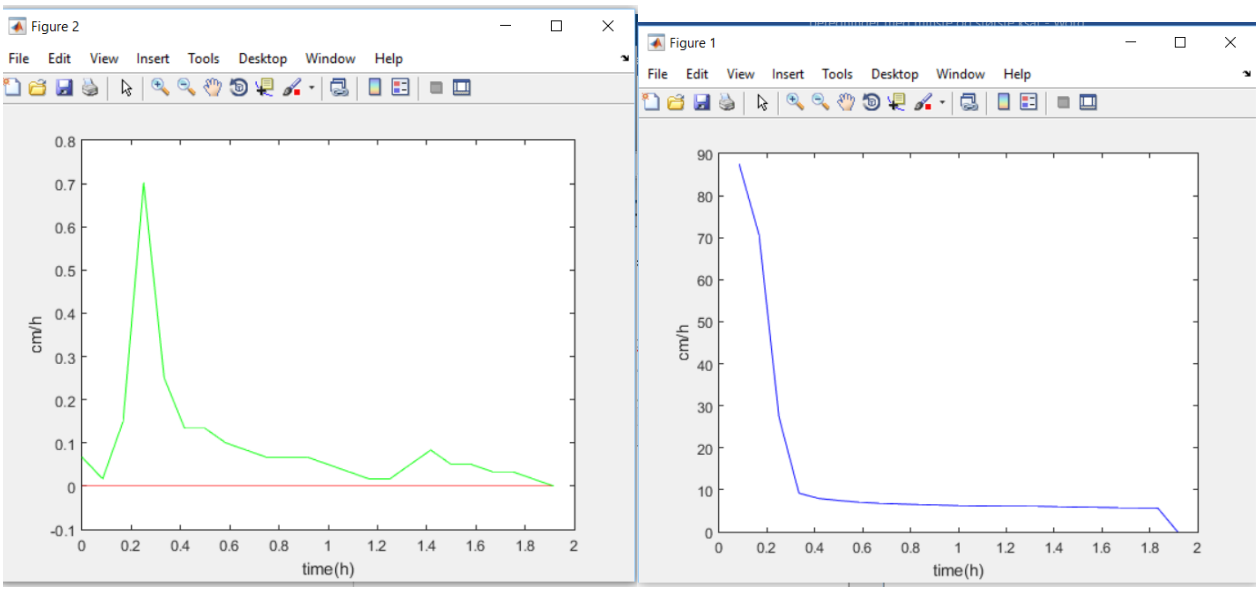

Computed by using Philip infiltration model

The different sites in Oslo:

R 5 ksat = 0.059

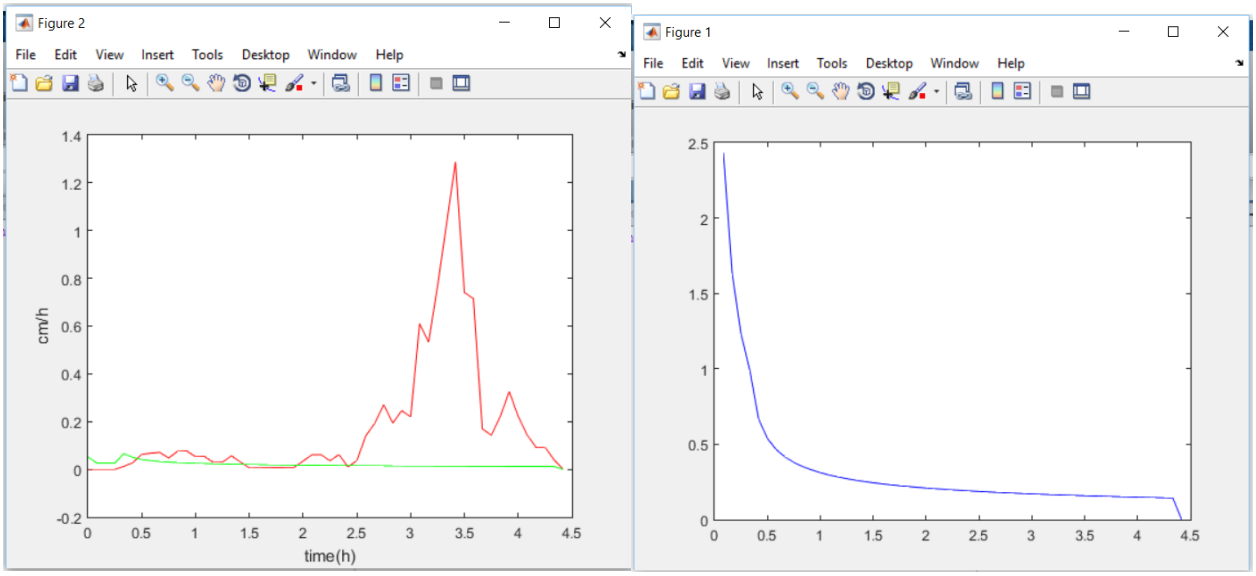

R 5 ksat= 20.021

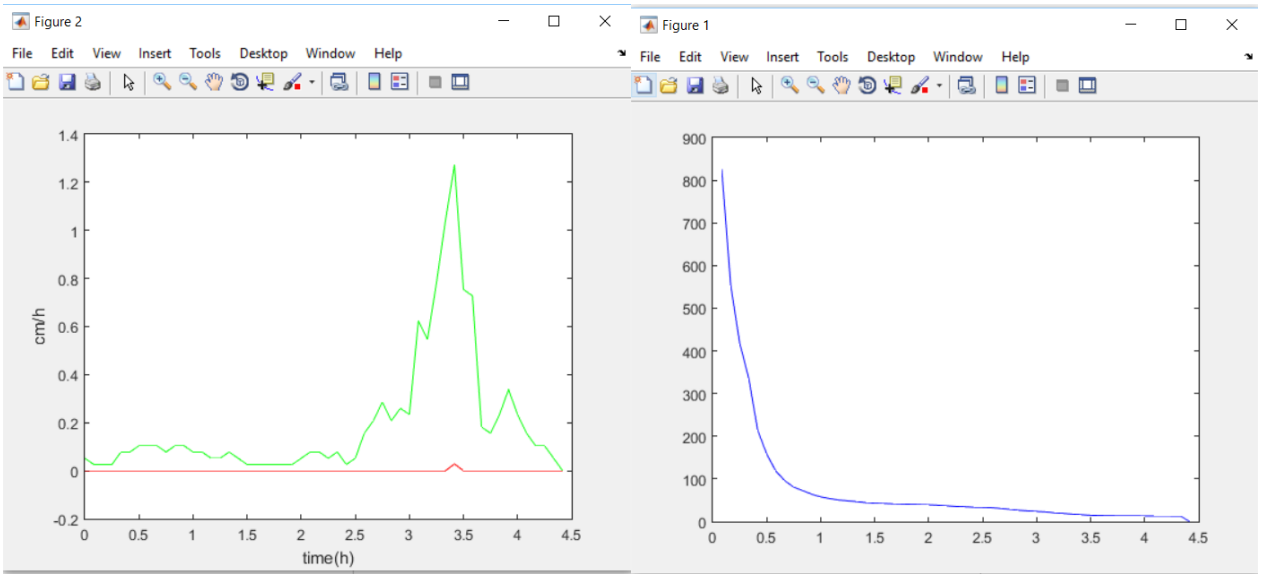

R44 ksat= 12.939

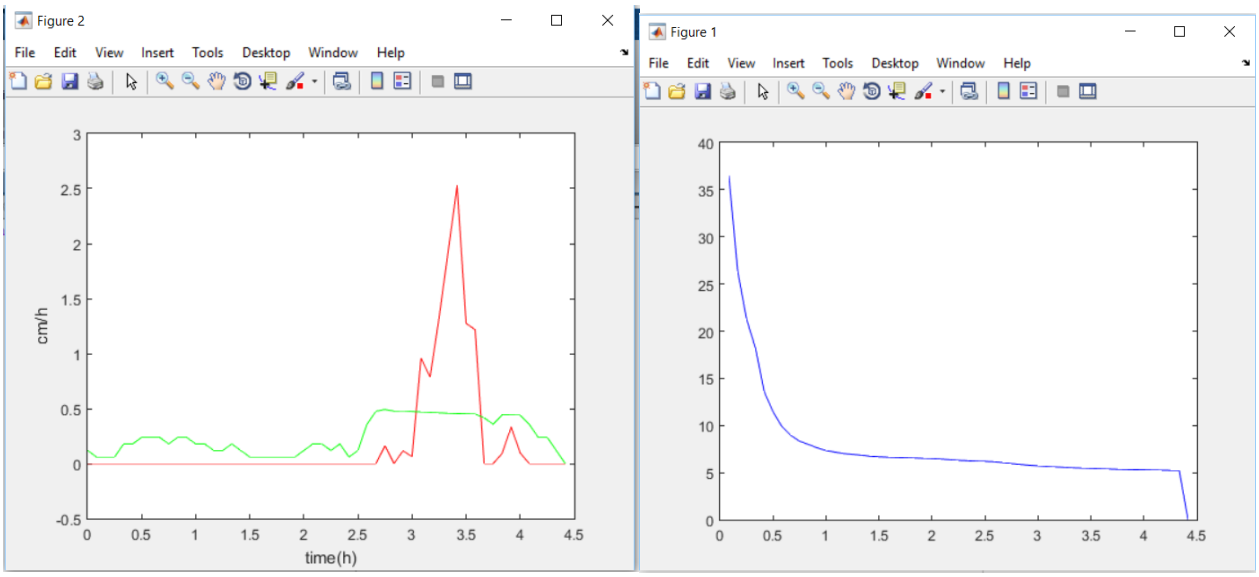

R 44 ksat= 88.82

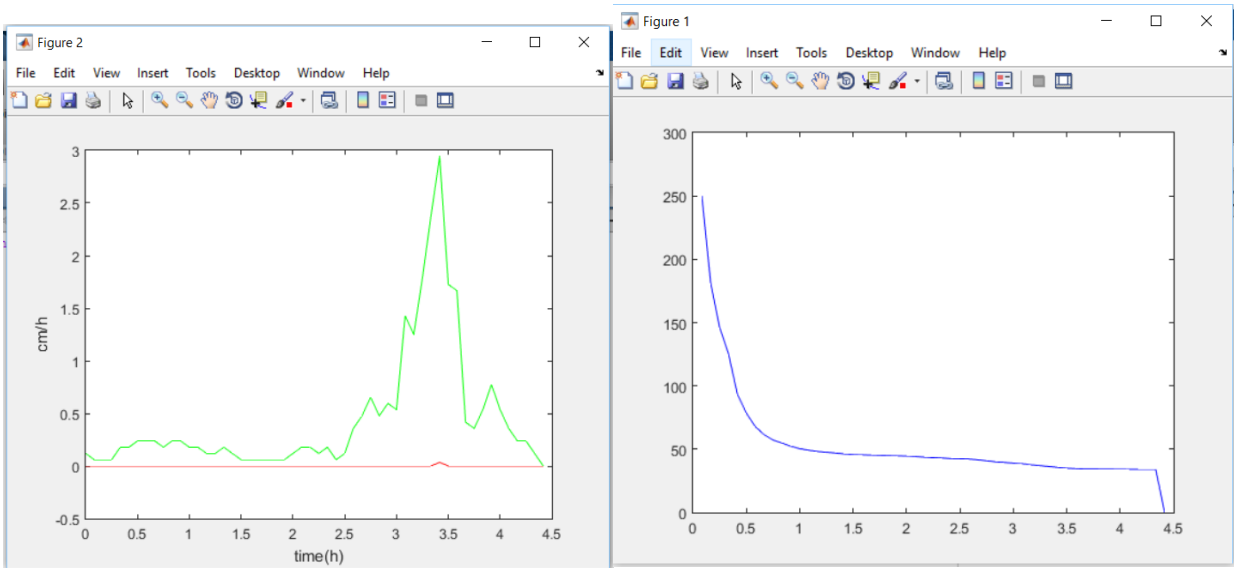

The different sites in Trondheim

Site 3 ksat=3.188 sandy loam

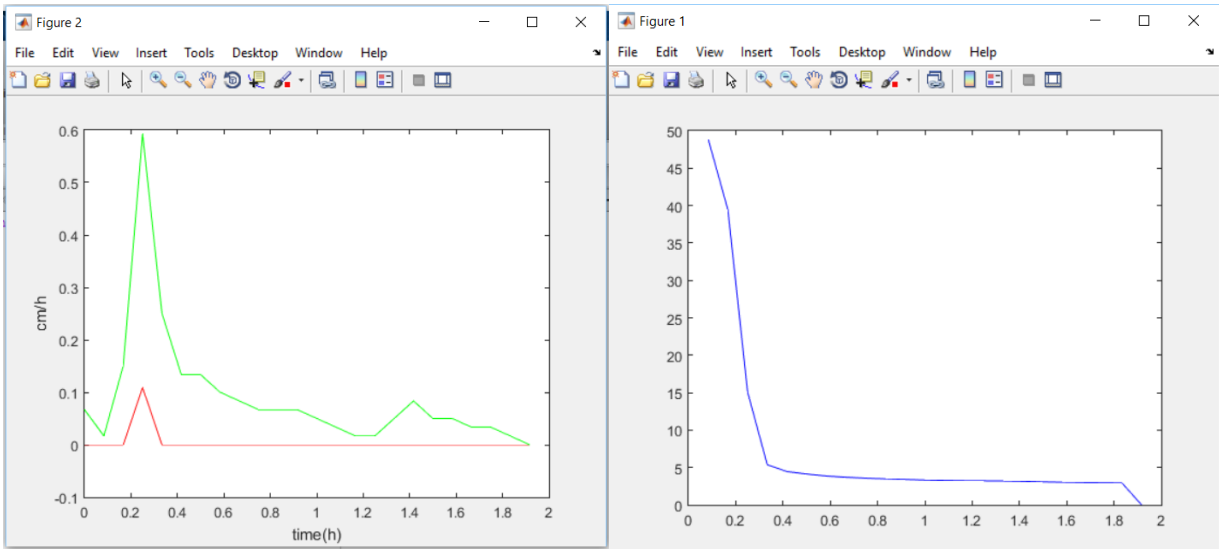

Site 3 ksat=3.188 loamy sand

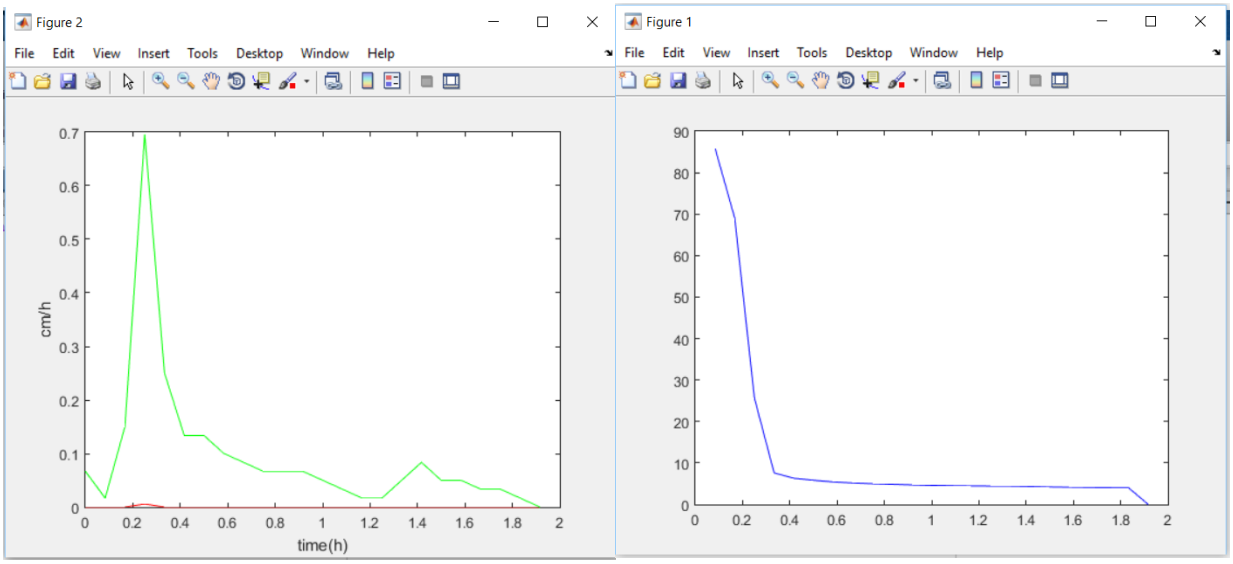

Results: Change in size of infiltration area

Calculated with Green- Ampt infiltration model

Site R5

Twice as big as the roof area (32m^2)

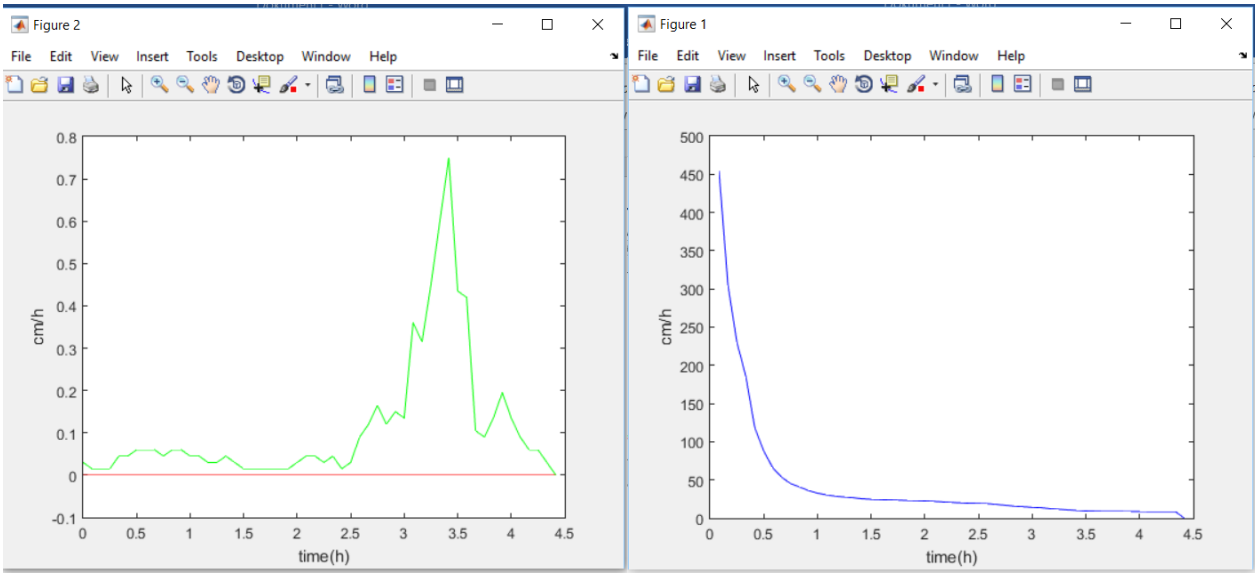

1.5 times bigger than the roof area (24m^2)

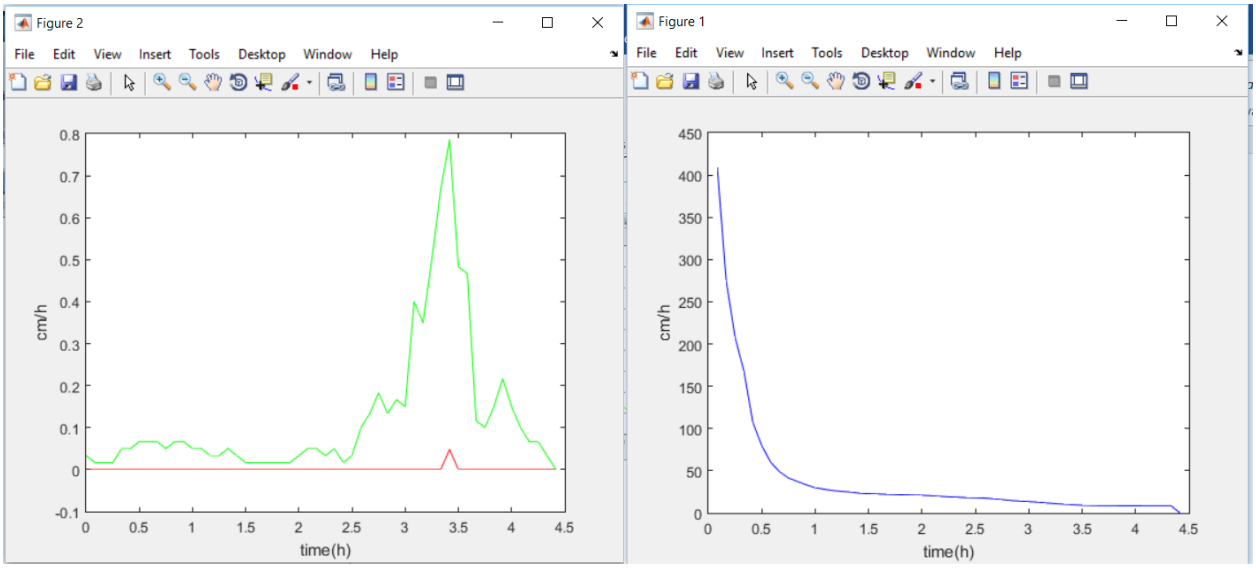

As big as the roof area (16m^2)

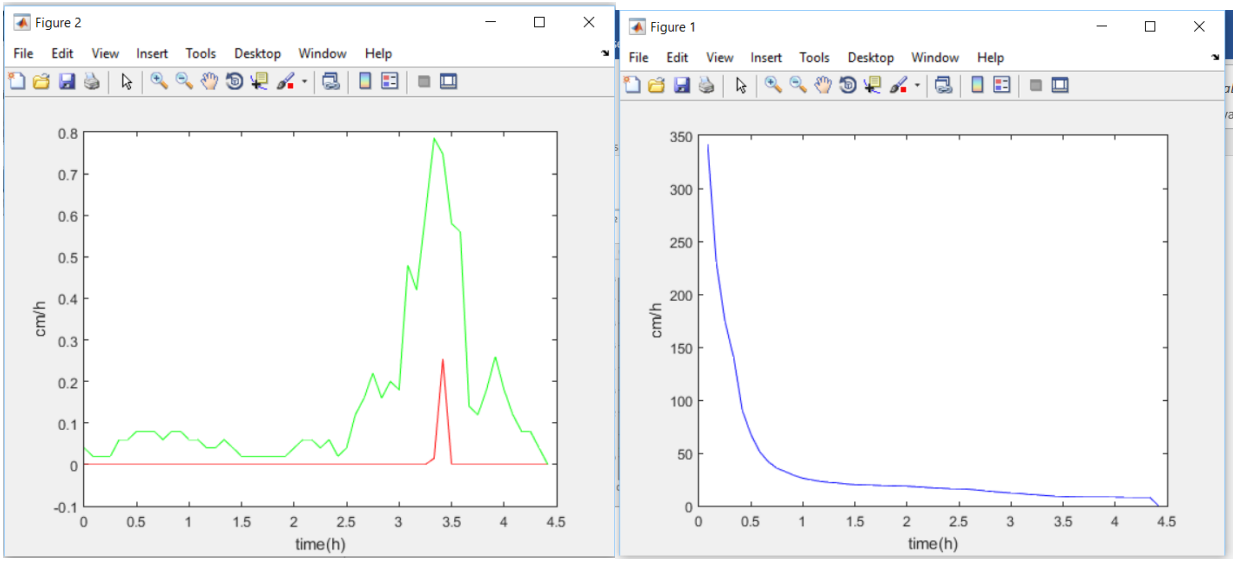

Calculated by using the Philip infiltration model

Twice as big as the roof area (32m^2)

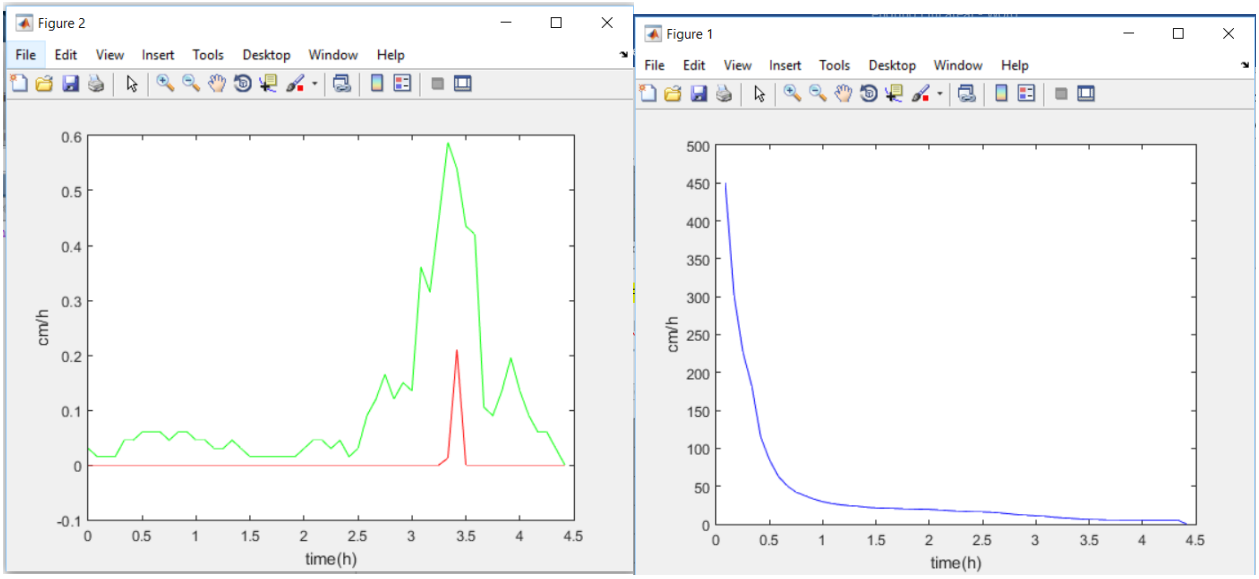

1.5 times bigger than the roof area (24m^2)

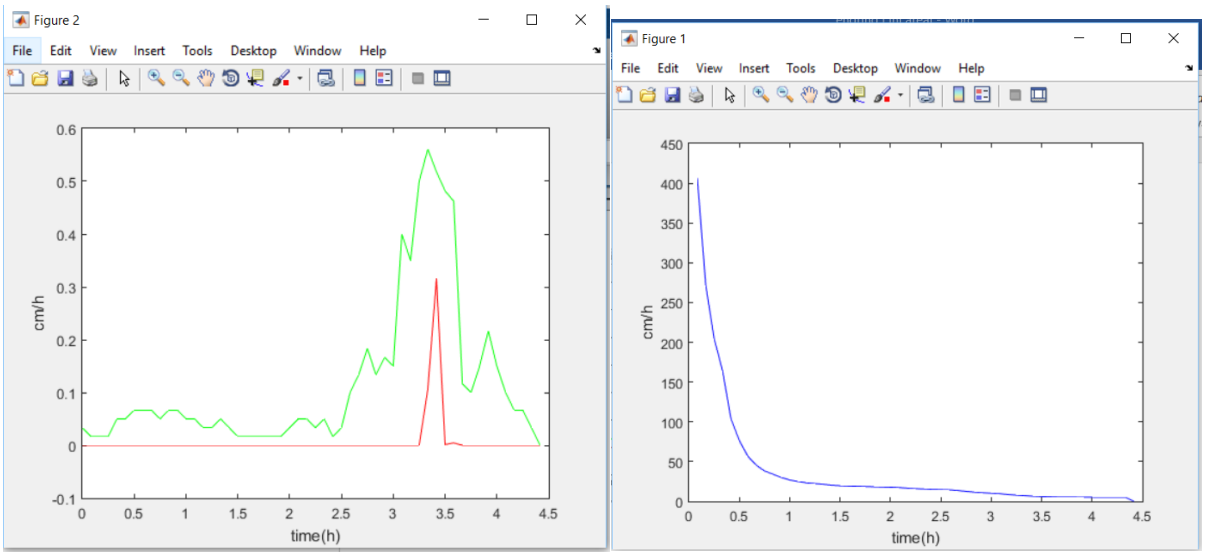

As big as the roof area (16 m^2)

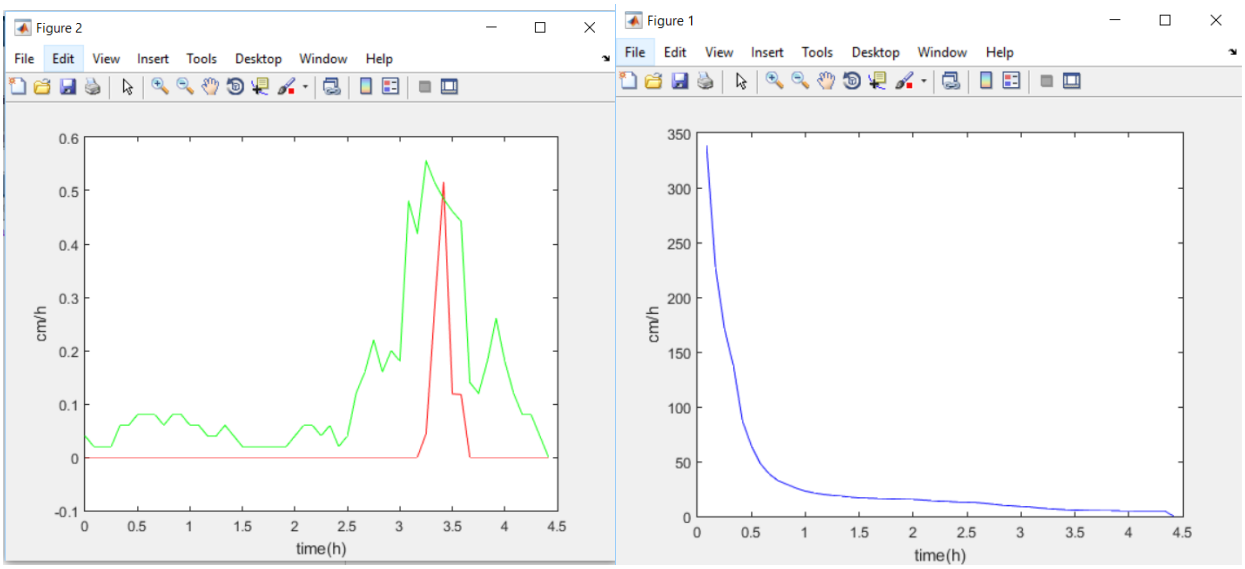

Appendix 4: Excel input sheet

	Input parameters						calculated input parameter		Input data		calculated Input data				input data				calculated Input data	
Name of sample	Saturated hydraulic conductivity ,ksat	Porosity, n	Wetting front capillary pressure head,yf	Bubbling - pressure, ya	Pore- size distribution index,b	Initial moisture content, ø0	Sorptivity, Sp	Kp	Time (min)	Incremental Rainfall, i (mm)	Time (h)	Incremental Rainfall, i (cm)	Rainfall Intensity, w (cm/h)	delta t	Roof Area (cm^2)	Number of downspouts	Length of infiltration area (cm)	Width of infiltration area (cm)	Water volume from roof (cm^3/h)	Adjusted Rainfall Intensity, w (cm/h)
Loam	6.34	0.4	23.55	30.93	0.3	0.31	5.184135415	2.113333333			0	0.02	0.24	0.083333333	640000	4	1600	100	38400	0.48
											0.083333333	0.01	0.12	0.083333333					19200	0.24
											0.166666667	0.01	0.12	0.083333333					19200	0.24
											0.25	0.01	0.12	0.083333333					19200	0.24
											0.333333333	0.03	0.36	0.083333333					57600	0.72
											0.416666667	0.03	0.36	0.083333333					57600	0.72
											0.5	0.04	0.48	0.083333333					76800	0.96
											0.583333333	0.04	0.48	0.083333333					76800	0.96
											0.666666667	0.04	0.48	0.083333333					76800	0.96
											0.75	0.03	0.36	0.083333333					57600	0.72
											0.833333333	0.04	0.48	0.083333333					76800	0.96
											0.916666667	0.04	0.48	0.083333333					76800	0.96
											1	0.03	0.36	0.083333333					57600	0.72
											1.083333333	0.03	0.36	0.083333333					57600	0.72
											1.166666667	0.02	0.24	0.083333333					38400	0.48
											1.25	0.02	0.24	0.083333333					38400	0.48
											1.333333333	0.03	0.36	0.083333333					57600	0.72
											1.416666667	0.02	0.24	0.083333333					38400	0.48
											1.5	0.01	0.12	0.083333333					19200	0.24
											1.583333333	0.01	0.12	0.083333333					19200	0.24
											1.666666667	0.01	0.12	0.083333333					19200	0.24
											1.75	0.01	0.12	0.083333333					19200	0.24
											1.833333333	0.01	0.12	0.083333333					19200	0.24
											1.916666667	0.01	0.12	0.083333333					19200	0.24
											2	0.02	0.24	0.083333333					38400	0.48
											2.083333333	0.03	0.36	0.083333333					57600	0.72
											2.166666667	0.03	0.36	0.083333333					57600	0.72

Appendix 5: Example m-table

Time (h)	Incremental rainfall (cm)	Adjusted Rainfall intensity (cm/h)	Δt	Ft (cm)	fc (cm)	F' (cm)	fc' (cm)	Fp (cm)	dt' (h)	ts (h)	t0	Ft+Δt (cm)	Infiltration (cm)	Runoff (cm)
0	0.02	0.624	0.08333333	0	Inf	0.052	261.581676		0	0	0	0.052	0.052	0
0.08333333	0.01	0.312	0.08333333	0.052	261.581676	0.078	175.440905		0	0	0	0.078	0.026	-3.47E-18
0.16666667	0.01	0.312	0.08333333	0.078	175.440905	0.104	132.369478		0	0	0	0.104	0.026	3.47E-18
0.25	0.01	0.312	0.08333333	0.104	132.369478	0.13	106.525798		0	0	0	0.13	0.026	-1.04E-17
0.33333333	0.03	0.936	0.08333333	0.13	106.525798	0.208	67.7572507		0	0	0	0.208	0.078	0
0.41666667	0.03	0.936	0.08333333	0.208	67.7572507	0.286	50.1319686		0	0	0	0.286	0.078	0
0.5	0.04	1.248	0.08333333	0.286	50.1319686	0.39	37.5949033		0	0	0	0.39	0.104	1.39E-17
0.58333333	0.04	1.248	0.08333333	0.39	37.5949033	0.494	30.3335427		0	0	0	0.494	0.104	1.39E-17
0.66666667	0.04	1.248	0.08333333	0.494	30.3335427	0.598	25.595452		0	0	0	0.598	0.104	-4.16E-17
0.75	0.03	0.936	0.08333333	0.598	25.595452	0.676	22.9972615		0	0	0	0.676	0.078	2.78E-17
0.83333333	0.04	1.248	0.08333333	0.676	22.9972615	0.78	20.3398282		0	0	0	0.78	0.104	1.39E-17
0.91666667	0.04	1.248	0.08333333	0.78	20.3398282	0.884	18.30621		0	0	0	0.884	0.104	1.39E-17
1	0.03	0.936	0.08333333	0.884	18.30621	0.962	17.0686988		0	0	0	0.962	0.078	2.78E-17
1.08333333	0.03	0.936	0.08333333	0.962	17.0686988	1.04	16.0161602		0	0	0	1.04	0.078	2.78E-17
1.16666667	0.02	0.624	0.08333333	1.04	16.0161602	1.092	15.3976652		0	0	0	1.092	0.052	-4.86E-17
1.25	0.02	0.624	0.08333333	1.092	15.3976652	1.144	14.8351447		0	0	0	1.144	0.052	-4.86E-17
1.33333333	0.03	0.936	0.08333333	1.144	14.8351447	1.222	14.0806943		0	0	0	1.222	0.078	-8.33E-17
1.41666667	0.02	0.624	0.08333333	1.222	14.0806943	1.274	13.6287791		0	0	0	1.274	0.052	-4.86E-17
1.5	0.01	0.312	0.08333333	1.274	13.6287791	1.3	13.4163005		0	0	0	1.3	0.026	-2.43E-17

Appendix 6: Values for Bulk density

Critical bulk density values

Urban designs succeed only when the tops of trees grow and create shade. This can only happen when roots grow vigorously. Soil bulk density must be below the critical value in order for roots to grow. The chart below shows the bulk density that limits root growth for various soil types. Soil should have a value below that indicated in order to support root growth.

Critical bulk density values for difference soil textures

SOIL TEXTURE	Critical bulk density range (g/cc)
clay, silt loam	1.4-1.55
silty clay, silty clay loam, silt	1.4-1.45
clay loam	1.45-1.55
loam	1.45-1.6
sandy clay	1.55-1.65
sandy clay loam	1.55-1.75
sandy loam	1.55-1.75
loamy sand, sand	>1.75
Based on Harris 1990 and Morris and Lowery 1988	

hort.ifas.ufl.edu/woody/critical-value.shtml. Downloaded 29.10.2015 kl. 19.13

Appendix 7: Soil samples

Soil samples taken in Trondheim:

Prøvenavn	% Leire	% Silt	% Sand	% Grus	Betegnelse
S1 nr.1	0	20	70	10	Siltig sand
S1 nr.2	0	16	69	15	Siltig sand
S1 nr.3	0	14	69	17	Sand
S1 nr.4	0	20	64	16	Siltig sand
S1 nr.5	0	17	67	16	Siltig sand
S2 nr.1	0	25	65	10	Siltig sand
S2 nr.2	0	19	57	24	Sandig, grusig, siltig materiale
S2 nr.3	0	20	65	15	Siltig sand
S2 nr.4	0	34	52	14	Sandig, siltig, grusig materiale
S2 nr.5	0	26	61	13	Siltig sand
S3 nr.1	0	24	49	27	Sandig, grusig, siltig materiale
S3 nr.2	0	24	49	27	Sandig, grusig, siltig materiale
S3 nr.3	0	26	48	26	Sandig, grusig, siltig materiale
S3 nr.4	0	30	53	17	Sandig, siltig, grusig materiale
S3 nr.5	0	23	56	21	Sandig, siltig, grusig materiale
S4 nr.1	0	14	66	20	Sand
S4 nr.2	0	14	70	16	Sand
S4 nr.3	0	17	66	17	Siltig sand
S4 nr.4	0	20	61	19	Siltig sand
S4 nr.5	0	14	61	25	Sand

Soil samples taken in Oslo:

Prøvenavn	% Leire	% Silt	% Sand	% Grus	Betegnelse
B20 A	23.5	35.3	41.2	0	Lettleire
B28 A+B	29.3	51.2	19.4	0	Siltig mellomleire
B30	12.7	27.6	59.7	0	Lettleire
B65B prøve2	23.3	45.7	31.1	0	Lettleire
B65B prøve 3	17.9	33.9	48.2	0	Lettleire
E14	20.1	48.8	31.1	0	Lettleire
L34	10.7	21.7	67.6	0	Sandig lettleire
R5	22	33.5	44.5	0	Lettleire
R29	12.8	28	59.2	0	Lettleire
R44	7.55	15.85	76.6	0	Siltig sand
S10	20.5	32.55	47	0	Lettleire
S75A	9.65	18.7	71.7	0	Siltig sand
S75 BCDG	20.6	47.7	31.7	0	Lettleire